2018

Air entrainment and variation of air void system in fresh concrete

Xin Wang
Iowa State University

Air entrainment and variation of air void system in fresh concrete

by

Xin Wang

A dissertation submitted to the graduate faculty

in partial fulfillment of the requirements for the degree of

DOCTOR OF PHILOSOPHY

Major: Civil Engineering (Civil Engineering Materials)

Program of Study Committee:

Peter C. Taylor, Co-major Professor
Kejin Wang, Co-major Professor
Fatih Bektas
Franciszek Hasiuk
James Alleman

The student author, whose presentation of the scholarship herein was approved by the program of study committee, is solely responsible for the content of this dissertation. The Graduate College will ensure this dissertation is globally accessible and will not permit alterations after a degree is conferred.

Iowa State University

Ames, Iowa

2018

TABLE OF CONTENTS

Page

LIST OF FIGURES

LIST OF TABLES

ACKNOWLEDGEMENTS

I would like to take this opportunity to thank my co-major professor Dr. Peter Taylor and Dr. Kejin Wang. Dr. Taylor, thank you for your support on my wild ideas and my dry humor, and being so patient with my writing. Dr. Wang, thank you for your confidence in me at the very beginning of my academia life, and thank you for opportunities over the years.

I want to express my gratitude to my committee members for their kindness and time. Dr. Alleman, your comments on my work are always right on spot. Dr. Hasiuk, thank you for that coffee, and thank you for finding time for me on your last day in Ames. Dr. Bektas, thank you for willing to fill on such short notice.

I also want to express my gratitude towards my mentors, Dr. Gilson Lomboy, Dr. Xuhao Wang, and Dr. Seyedhamed Sadati. Gilson, thank you for your mentoring and model of a good researcher. Xuhao, thank you for having a son with the almost the same birthday as me. I know you tried your best, and he will be as cool as I am. Hamed, the main reason I graduate on time is your forward thinking which has kept me out of trouble.

I would send special thanks to Robert Steffes. Thank you for putting up with my undergraduates so long Bob, and of course, thank you for putting up with me so long. You ROCK! Special thanks to Paul Jeramefor your special humor.

Thank you my undergraduate helpers (Ming, Mo, Dokota, Chengning, Yifan, Guangfan). Though you guys got me into trouble so many times, I still love you.

Finally yet importantly, I want to thank my parents, they let me believe that I can be whoever I want, and that makes me who I am: a reckless child with a Ph.D.

I could not do this without all of you.

Jerry

ABSTRACT

An adequate air void system in concrete is critical to its freeze-thaw (F-T) durability. With an effective air void system, concrete can survive longer in a wet climate with F-T cycles. Over the years, researchers have focused on fresh air content and the hardened air void system, but little attention has been paid to changes in the air void system between those two states. Stability of air void system and its changes during handling, finishing, and even testing can influence the concrete performance.

This dissertation focuses on the air void system between when fresh air content is tested in practice and when the concrete is hardened. Three stages were investigated: 1). the stage after mixing and during transport/handling (at rest and not disturbed); 2). during pressure meter testing; 3) after internal vibration.

To study air voids during handling and transport, the first objective was to study the compatibility of the admixtures and cement that would be used in concrete mixing, and modified a method to evaluate compatibility to address critical details of the test procedure. Then 60 combinations of admixtures and cementitious binders were tested using this method to develop a pass/fail limit for compatibility of the materials. Using this limit, eight selected concrete mixtures were evaluated for air void system stability. The data indicated a good correlation between stability of air void system in concrete and compatibility of mixture ingredients.

The second topic reported in this dissertation is the variation of air void system in a Super Air Meter (SAM). The SAM uses cycles of pressure to assess the air-void spacing factor in fresh concrete. However, the mechanism behind this prediction and the changes in air volume inside the device under different pressures is not well understood. By comparing hardened air void

analysis results of mortar and concrete subjected to different pressure stages, the tendency for air to dissolve under pressure in concrete and mortar was studied. Moreover, by analyzing fresh concrete pressure results and the hardened concrete air void system, correlation between results from SAM and spacing factor was found.

The third topic was the variation in an air void system within a concrete sample consolidated by internal vibration. This topic was divided into two parts: understanding the mechanism for air void system variation; and distribution of aggregate and air voids in such concrete. It was noted that there was an increase in air content in part of the samples excessively consolidated by internal vibration. Work was conducted to understand the factors that may affect this type of variation in an air void system. For aggregate and air void distribution, digital image processing was used to evaluate aggregate distribution in vibrated concrete. It was found that excessive vibration will affect aggregate distribution and cause segregation in the system. In terms of air content and air void distribution, it was found that the air increase after vibration regardless of the types of admixtures.

CHAPTER 1. GENERAL INTRODUCTION

1.1. Background

It is well established that an adequate air void system is essential for concrete durability in an environment prone to freeze-thaw (F-T) Concrete with a proper air void system is better able to resist the action of F-T cycles, particularly in wet climates. Over the years, researchers have made efforts to test and evaluate characteristics of air void system, generally focusing on the total air volume and the spacing factor. Total air content is defined as the ratio of total volume of air voids to the bulk volume of concrete, including all the constituents of concrete. For concrete with ¾-in. maximum size aggregate, air content needs to be about 6% for effective F-T resistance (Klieger 1956). Spacing factor is a parameter related to maximum distance anywhere in the cement paste from to edge of an air void, and should be less than about 0.20 mm to ensure good F-T durability (Power 1956).

Stability of air void system is an often overlooked paramters, and it is critical to consistency of each construction project. Air content of a fresh concrete mixture is normally measured before concrete is placed into its final position and consolidated, which is acceptable if the air void system is generally stable. However, if the air void system of placed concrete is not stable, an acceptable fresh air content tested before placing will not guarantee the F-T durability. While There is no formal definition of air void system stability, it can be described as the percentage of air content lost from fresh concrete to hardened (or any other period of time after placement). On the other hand, it has been reported in some cases that air can increase with handling.

A test method called Super Air Meter (SAM) was introduced in 2014 that is similar in approach to a pressure meter (ASTM C231). However, unlike the pressure meter which uses pressure (~100 kPa) to compress fresh concrete, the SAM uses two more pressure stages (207 kpa and 310 kpa) over two rounds to further compress the sample. A so-called "SAM number" is the result obtained from this test based on changes in air volume. The SAM number reportedly correlate with spacing factor from hardened air void system analysis and durability factor from the ASTM C666 F-T durability test. SAM number is the difference between equilibrium pressure reading (after opening the valve) between upper and bottom chamber at 310 kpa of round 2 and round . However, the physical/chemical meaning behind SAM number is unclear.

A factor that can significantly influence an air void system during handling and placement to is vibration. Vibration is used to facilitate placing and consolidating concrete into complex forms. It will cause air bubbles to float to the surface, with larger bubbles moving faster than the smaller. Entrapped air voids are defined as those that are 1 mm or larger in width and irregular in shape, and are generally considered undesirable because they compromise strength while not providing significant freeze thaw protection to the mixture. On the other hand smaller bubbles are desirable to provide F-T protection as discussed above. Excessive vibration may also compromise the smaller bubbles in the air void system.

The focus of this dissertation is understanding the condition of an air void system after mixing, placing and finishing.

1.2. Objectives

This aim of the work 1) discussed in this dissertation is to investigate the quality of air void systems in concrete after mixing but before hardening, and 2) evaluate test methods used to

measure air void properties under such conditions. Four steps have been taken to achieve this goal:

1. Modify an existing test method to predict the stability of air void system in concrete by evaluating the compatibility of admixtures and cement system, then use this method to set up a pass/fail limit for compatibility.
2. Study the volume change of air bubbles in fresh concrete under multiple pressure stages, and find the relationship between this volume change and air void system characteristics in hardened concrete.
3. Investigate changes in the air void system under internal vibration, and study the factors that may affect this behavior.
4. Study the influence of different air entraining agents on air stability under vibration. Investigate the influence of internal vibration on aggregate distribution using a digital image processing method.

1.3. Dissertation organization

This dissertation contains seven chapters.

Chapter 1 provides background, objectives, and the organization of this dissertation.

Chapter 2 provides a literature review on four aspects of air void system in concrete including constituent materials, formation of air void system, characteristics of air void structure, and effects of air void system on mechanical properties of concrete.

Chapter 3 to Chapter 6 present four separate papers as described above. All of these papers are ready for peer-review. These papers are presented as follows:

- Chapter 3 (Paper 1)

Chapter 3 presents a paper investigating the compatibility of admixtures and stability of air void system in concrete using admixtures. This work modified an existing method (Cross et al. 2000) and establish a pass/fail limit for compatibility using the modified method. The investigation also looked at the correlation between the compatibility measured by the modified method and the stability of air void system in concrete using a conventional air void analysis method.

- Chapter 4 (Paper 2)

Chapter 4 presents a paper studying volume changes of air bubbles in mortar under multiple pressure stages. Using the volume change and fresh multiple pressure stage results, correlation between fresh results and hardened air void analysis was found.

- Chapter 5 (Paper 3)

Chapter 5 presents a paper investigating the mechanism of air changes in concrete that has been consolidated by an internal vibrator. The mechanism and source of air increases were studied, and then factors that may affect this behavior were also tested including vibration speed and vibration duration.

- Chapter 6 (Paper 4)

Chapter 6 presents a paper studying the influence of internal vibration on both air void system and aggregate distribution. Different chemical-based, air-entraining agents were used to study the variation in air void system, and digital image processing was used to evaluate the

aggregate distribution in three different parameters: including inter-particle spacing, mortar thickness index, and fabric tensor.

Chapter 7 provides a general summary for this dissertation, as well as conclusions and future research recommendations.

CHAPTER 2. LITERATURE REVIEW

This chapter reviews the four subjects that are relevant to air void system in concrete: constituent materials, mechanisms of air entrainment, air void structural characteristics, and variation in air void system at the fresh stage. The first three subjects introduce the current state of knowledge on air void system of concrete, and last subject is dedicated to reviewing changes in the air void system before and after concrete is handled.

2.1. Constituent materials and air void system

Air entrainment is required for concrete subjected to an F-T environment. This air entraining process is affected by the amount and composition of each ingredient in a concrete mix as well as the interactions among them. The characteristics of portland cement paste including fly ash, slag cement, and silica fume, determine the pore structure and permeability of concrete, which in turn determines its potential durability. Porous coarse aggregates may affect concrete durability as well because they will affect the water transport properties of concrete. Air entraining agents are used to stabilize entrained air voids, although the stability of these voids is also impacted by the presence of supplemental cementitious materials (SCMs) and other admixtures. This section reviews the influence of each concrete component to air void system.

2.1.1. Cement and supplementary cementitious materials

2.1.1.1. Portland cement

Portland cement is produced by heating limestone and clay minerals, which contains lime, silica, iron and alumina. The hydration between cement and water is affected by both physical and chemical characteristics of portland cement, and hydration determines the porosity,

connectivity between pores in cement paste, and the distribution of hydration products in pores. These factors could all affect F-T resistance (1).

Porosity is affected grain size of cement. Pigeon and Pleau reported that finer cement particles tend to subdivide the space between particles into smaller pores. As result, there will be less freezable water since the freezing point in smaller pores is lower than in larger ones due to surface tension. Connectivity of pores is affected by the amount of hydration products formed within them (1) (3). Hydration rate, which is controlled by the cement chemical composition, affects both pore connectivity and hydration products inside of pores. Faster hydrating systems have been reported to ultimately result in a coarser microstructure (4).

Cement would affect stability of air void system. Cement composition, for instance alkali level of cement, may also affect stability of an air void system. Higher alkali content cement is reported to cause more air entraining agent to remain in solution, depending on the chemical base of admixtures used in individual mixture (5) (6).

2.1.1.2. Fly ash and slag

Both fly ash and slag cement are used as supplementary cementitious materials (SCMs) in concrete. Percolation of pores will reduce with decreasing water content in a mixture containing fly ash (7). Bilodeau and Malhotra (8) concluded that concrete containing up to 60% fly ash by weight will have a good F-T resistance with proper air entrainment. One the other hand the presence of carbon in fly ash may cause air void stabilization problems therefore causing a negative impact on F-T resistance (9). Boyd and Hooton (10) found that a high dosage of slag might decrease the amount of entrained air, but improve the air void system, at the same time.

2.1.1.3. Silica fume

Silica fume is a byproduct of producing silicon metal or ferrosilicon alloys, and it is often used in high strength concrete. Silica fume is very reactive as a pozzolan, largely due to its small particle size around 0.1 μm. Silica fume refines the pores (11), and increases the density of the interfacial transition zone between cement paste and aggregate. Concrete containing silica fume was found to have good F-T resistance (12) (13). Silica fume may not alter the stability or air content of concrete, but higher dosage of AEA is needed due to the high surface area of silica fume (14).

2.1.2. Aggregate

The process of air entrainment is affected by concrete aggregates during mixing. Parameters include shape, pore structure, absorption, gradation, and texture all contribute to formation of air void system in different ways (Verbeck and Landgren (15), Waugh (16), Gaynor (17), Powers (18), Kaneuji et al. (19), Hudec (20), and Page and Page (1))

2.1.2.1. Coarse aggregate

Using the same dosage of AEA and cement content, increasing maximum size of aggregate will lower the air content, but this phenomenon is negligible when maximum size reaches 3.81 cm (1 ½ in.) (21).

The type of coarse aggregate also has an effect on the amount and size of air voids in concrete, depending on if it is gravel or crushed limestone. Crushed limestone will generate smaller bubbles due to the higher shear action during mixing (22). Dodson (23) found that concrete containing aggregates with rounded shape (such as gravel) can have more air bubbles than concrete with angular aggregates like crushed limestone.

2.1.2.2. Fine aggregate

Fine aggregate provides a screen that holds air bubbles during mixing, and it also provides a space for paste and bubbles to stay during mixing due to wall-effect (24). There are two ways that fine aggregate can change the air entraining process, one is the amount of fine aggregate, and the other is the gradation of fine aggregate (21). Increasing fine aggregate tends to increase air content (25). Fine aggregate particles in the middle sizes results in more air bubbles than finer or coarser sizes, and a large amount of very fine particles (<150 μm) will result in reduction of entrained air (21). There is a good correlation between fineness modulus and amount of air entrained (26) (26) and higher fineness modulus will lead to a lower air content.

2.1.3. Admixtures

The most commonly used admixtures in concrete pavements are AEA and WRA. Influence of AEA and other types of admixture (supplemental cementitious materials included) on air void system is discussed below.

2.1.3.1. Air entraining agents

Air entraining agents were discovered in the late 1930's by accident. It was observed that concrete blended with portland and natural cement that contained 'crushed oil' is more resistant to surface scaling. Later it was observed that concrete pavement using certain types of cement was more durable than other cements. And these durable cements were manufactured with grinding aids including beef fat, calcium stearate, and fish oil, all of which act as AEAs(27).

There are several ways to categorize(23) (28). Two typical methods will be reviewed. In 1954, U.S. Bureau of Public Roads (29) conducted an evaluation program on 27 commercial admixtures and classified them into seven categories (27) :

- **Salts of wood resins (pine wood stumps)**

This used to be the most used type. Vinsol is the insoluble residue from distillation and extraction of pine stumps to obtain other materials. It is a mixture of carboxylic acid, phenol, and other substances.

- **Synthetic detergents**

Synthetic detergents refer to alkyl aryl sulfonates, a common class of surfactants. The alkyl groups are complex petroleum residues that are condensed with benzene, then the product is sulfonated and neutralized to obtain the soluble salt.

- **Salts of sulfonated lignin**

These salts are by-products from paper industry. It's not a good one but often used Salts of petroleum acids

- **Salts of proteinaceous materials**

These salts are by-products of petroleum refining. The left-over sludge from petroleum treatment with sulfuric acid contains water-soluble sulfonates.

- **Salts of proteinaceous materials**

They are products of the animal processing industries, which consist of salts of a complex mixture of carboxylic and amino acids.

- **Fatty and resinous acids and their salts**

These are produced from various materials, and soap, vegetable oils, and tall oil, can be used as surfactants.

- **Organic salts of sulfonated hydrocarbons**

If the neutralization of petroleum refining is done with triethanolamine, then it fits into this category.

On the other hand, based on practice and raw materials, Rixom and Mailvaganam (28) divided air entraining agents in five categories:

- **Neutralized wood resins**

Wood-derived tall oil rosins and pine stump extracts consist of complicated mixtures with abietic acid together with pimaric acid and phenolic compounds are categories.

- **Fatty-acid salts**

Fatty-acid salts are present in a distribution of chain lengths in naturally occurring fats and oils, for instance tall oil and coconut oil.

- **Alkyl-aryl sulfonates**

Alkyl-aryl sulfonates are used in lightweight concrete and freeze-thaw resistant concrete

- **Alkyl sulfates**

Alkyl sulfates are can be used as air-entraining water-reducing agents, which often contains sodium sulfate

- **Phenol ethoxylates**

Phenol ethoxylates are nonionic materials. They are often used in low dosage but perform well. The most common material is nonylphenol ethoxylate.

Effects of AEA on concrete influence both fresh and hardened concrete. For fresh concrete, air-entrained concrete improves workability and increases plasticity, which as a result may reduce the water needed for the mixture (30). The inter-particle friction between cement and aggregate grains will be reduced by entrained air bubbles, so less water will be needed to achieve the same slump (31). For hardened concrete, the principle objective of using air entraining agent in concrete is to protect concrete from the potential deterioration brought by F-T cycles. Cordon (30) believed that the presence of a large number of air bubbles in concrete will improve concrete durability by increasing uniformity, and decreasing absorption and permeability. To achieve the improvement of F-T durability, air void system must have certain characteristics. Many researchers have proposed their own theory regarding these characteristics (34) (35) (36). Most of them relate to spacing of air voids and their size distributions. The spacing and size distribution of the air voids must be able to provide efficient protection to the paste (37) (38). Researchers also found that internal surface area of air entrained concrete can be important to sound absorption (32), and alkali-silica reaction can be mitigated by air-entrainment (33).

The stability of air entrainment and air void system can be influenced by either the handling of the concrete or concrete mixture itself. After the removal of concrete from the mixer, transport, handling and placing techniques can cause reductions in air content and air system parameters. Measurement of air content usually is after these operations, during which air voids could be lost (28). Taylor et al. (39) found that excess vibration will impact the spacing factor of the concrete, with concomitant impacts on durability of concrete.

2.1.3.2. Other admixtures and SCMs

Oher types of admixtures may also be used in air-entrained concrete to modify concrete properties such as setting time and workability. The interaction between these admixtures and

AEA may alter the stability of the air void system. Certain combinations of WRA and AEA can be incompatible and create a non-stable air void system.

Klieger called attention to the effect of supplementary cementitious materials (SCMs) on air entrainment (42) (43). There is carbon in fly ash that can attract and absorb surfactants used in AEA (42) (44). Silica fume and slag has some impacts on air entrainment (45) (46). More AEA is needed when slag particle size is fine, and silica fume will always need more AEA due to its fineness.

Cross et al. (47) reviewed a simple test method to measure the potential stability of entrained air bubbles in a paste called the foam drainage test. Taylor et al. (48) reviewed several test methods to evaluate their potential to predict the compatibility between admixtures at early age. This study included tests such as the foam index and foam drainage test to detect potential unexpected effects on air void systems. A protocol was then developed to allow product manufacturers, concrete producers, contractors, and owners to monitor materials and concrete systems and reduce the risk of incompatibilities. The foam drainage test evaluates the performance of AEA before their application in concrete, determined in terms of the stability of the air-entraining system resulting from use in cementitious systems. Mixtures are prepared with the AEA alone, mixed with cement, and, if required, mixed with other chemical admixtures and supplementary cementitious materials.

2.2. Formation of air void system in concrete and variations

This section discusses the formation of air void system in concrete and the changes of air void system from fresh concrete to hardened, then this section discusses the variations caused by construction activities.

2.2.1. Development of air void system in fresh concrete

There are two mechanisms in the literature on how the air void system forms during mixing. One mechanism is that air layers are trapped between the in-folding surfaces (cement grains and fine aggregates) to entrap air bubbles (27). Power (49) described another mechanism that there was a vortex formed during mixing, providing the energy to build a interface between air and liquid to form large air voids, and then split them into small voids. AEA's prevent coalescence of small air bubbles after they are formed. Coalesce of small bubbles will increase the possibility of bubbles escaping from concrete since larger bubbles exert higher buoyance force (50).

2.2.1.1. Mechanism of air entraining agent

The principal objective of using AEAs in concrete is to provide and stabilize an air void structure that is able to protect concrete from the potential deterioration brought on by freezing and thawing. AEAs are surfactants that are adsorbed strongly at air-water or solid-water interfaces. Surfactant molecules segregate from the solution phase and concentrate at surfaces, hence, serving as bubble stabilizers (Figure 1). AEAs are commonly combination of different surfactants. Their chemical structure is a two-tail unit in which the hydrophobic end repels water while the hydrophilic head has a tendency to adsorb water molecules. Two functions of AEAs have been suggested. One is the stabilizing action, which is the result of its adsorption at the bubble surface. The adsorbed molecules are oriented with their anion polar heads in the water phase that help to separate two bubbles due to electrostatic repulsion. The other action is the formation of a layer of water around the bubbles that can also serve as a stabilizer and separate the bubbles (27) (23) (14).

2.2.1.2. Surfactants at the air/water interface

Surfactant molecules are randomly oriented in the system when mixing starts, but they have a tendency to orient themselves to minimize the interaction between the liquid phase and surfactant molecules. In order to decrease the total free energy of the system, the hydrophobic tails of surfactant molecules stay away from water molecules and so force the bubbles into a spherical shape. Ionic surfactants have a greater influence on the surface tension than other types of surfactants due to the electrostatic component of the repulsive force (51).

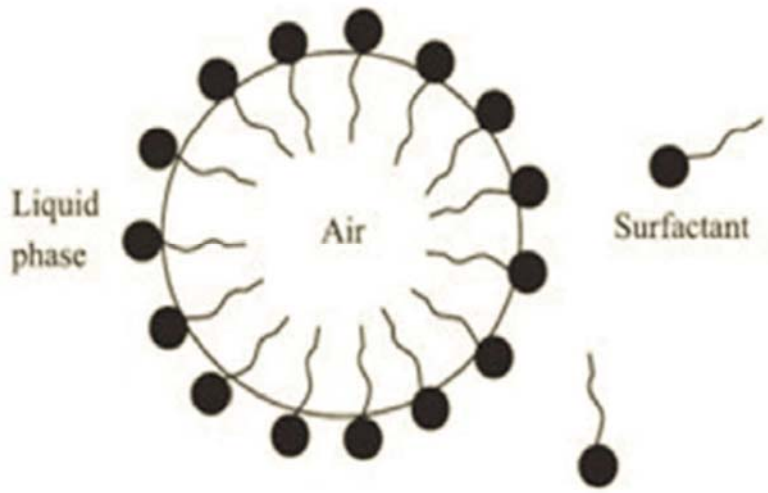

Figure 2.1. Stable air bubble by air entraining agent (51)

2.2.2. Conversion from fresh to hardened concrete

During the hydration process, air voids are gradually surrounded with a shell that plays an important role in the ability of air voids to resist coalescence and diffusion of air into paste. Mielenz et al. (36) proposed that diffusion of air between bubbles and their surrounding fluid will affect the size of bubbles. However, Power (52) showed that this change is limited due to

restriction from cement paste. Mielenz et al. (53) showed that air voids are initially covered by an early hydration shell, which in some cases is either a precipitated solid or gelatinous, membrane from the AEA calcium salts, or metal ions from the hydrating cement paste. The formation of this shell involves calcium salts of AEA precipitated once concentrated around the interface between air and water. During initial hydration, Ley et al. (54) found that the amount of $CaCO_3$ around air void shell is higher than the bulk cement, and increases with time up to 30 minutes. After 60 days of hydration, they observed a very dense hydration produced a shell around air voids with ~1 μm thickness, and there is a disjunction of phases between the shell and cement paste, which agrees with the results from other literature (55) (56) (47). Ettringite crystals on the surface of the voids and calcium silicate hydrate gel (C-S-H) in the air void have been seen using visual petrography and the energy-dispersive X-ray spectroscopy analyses.

Pigeon and Plante (57), Diamond (58) and Ley et al. (54) have shown that the calcium/ silicon ratio for the C-S-H of the bulk cement paste is 1.5, while according to Ley et al. (54) the ratio of the air-void shell is 1.1. They also found that the air-void hydration shell seemed to be denser than the C-S-H found in the bulk paste, which confirms results from Corr et al. (47) about thickness and presence of a “transition zone” around bubbles.

2.2.3. Factors that may alter air void system

2.2.3.1. Mixing

Mixing is the primary process that entrains the air bubbles into concrete. During concrete mixing, the movement of the aggregates affects the amount of air entrainment as well as the size of bubbles because large air bubbles can be split into smaller ones due to the motion of aggregates in the mixer. Stirring raw materials will create a vortex, and the air is drawn into it

and the shearing action will disperse and break up the air into smaller bubbles. In drum mixers this vortex exists at the end of shelves where the mass tumbles down, while in pan mixers it is created by the passage of the mixing blades. Mixer type, mixing time, and rotation rate can all affect the number and size of the air bubbles (59).

2.2.3.2. Temperature

With higher temperature, a higher dosage of AEA is needed to maintain the same level of air content (31). Increasing the temperature will accelerate hydration of cement which will lead to a higher absorption of AEA from the liquid phase of the concrete, and this will make it more difficult for concrete mixtures to develop and stabilize air bubbles (60) (61). Some AEAs can cause accumulation of bubbles on the surface of concrete leading to lower strength on top layers in hot weather (47).

2.2.3.3. Vibration

The internal concrete vibrator was introduced in the early 1930s to consolidate reinforced concrete structures, allowing stiffer mixtures with less water be placed (62) (63). Extensive research on vibration and concrete properties has been conducted over the past 90 years. The benefits of vibration include removing entrapped air bubbles and producing a dense and more durable concrete (64). Vibration can enhance the air void system by removing entrapped bubbles, and those bubbles with 1 mm or larger in width and irregular in shape (65). Entrapped air voids provide no benefit on concrete hardened properties like F-T durability and may decrease concrete strength (66). Stability of air void system is mainly depending on AEA. Excessive vibration would remove entrained air from the system, and may cause bleeding in fresh concrete.

During their work, Taylor et al. (48) reviewed a test method called the foam drainage test. It is a method proposed by Gutmann (67) to measure the potential stability of entrained air bubbles in a paste. The test comprises agitating a mixture of paste ingredients, and agitating in a blender to create 1000 mL of foam. This foam is poured into a graduated cylinder, and the rate at which liquid collects at the bottom of the cylinder is then monitored over 60 minutes.

Concrete internal vibrators are mostly rotary, meaning that oscillations are caused by imbalanced rotation, usually achieved by off-setting weights from the vibrator's and center of rotation (68) (69). This rotation creates harmonic waves which eventually cause compression waves and shear wave in fresh concrete. Banfill and his colleagues (74) also confirmed that flow inside the radius of action is controlled by a shear waveform, while outside of this radius motion of materials is governed by a compression waveform. The rotation of vibrator and liquefied zone within the radius of action makes it possible to form a vortex in concreteat the surface (70). Most vortex research has been conducted with rotation on the surface (71) (72). Increasing rotation speed leads to a deeper vortex. An observation made by Plowman (73) was that a vortex in the concrete may suck air into the system under the influence of a rotary vibration.

2.3. Air void structure characteristics and testing methods

Concrete is a porous material by nature. Its pore structure affects both its mechanical and durability properties. During concrete placing, as described above, constituent materials and construction procedures may alter the air void system in concrete, therefore the air void system needs to be characterized and properly monitored during construction to ensure a high quality. This section will focus on discussing these characteristics and testing methods.

2.3.1. Pore type and size

The quantity and types of pores is critical to most concrete properties. Pores in concrete are distinguished by size, shape, pore solution, and origin. Cordon (1966) proposed that there are three types of pores in cement paste: gel pores, capillary cavities (pores), and entrained air bubbles. Aligizaki (74) subdivided them into the five classes: voids in the cement paste matrix (gel pores, capillary pores, air voids, and hollow-shell pores); pores in aggregates; pores associated with interfacial transition zone; water voids; internal discontinuities in the cement paste. Various types of air voids and their influence on freeze/thaw behavior will be discussed in the following sections. Voids in aggregate will not be discussed since it is beyond the objective of the dissertation.

2.3.1.1. Gel pores

The calcium silicate hydrate gel, known as C-S-H gel, is the principle product of cement hydration. Powers et al. (75) recognized the formerly known as tobermorite gel as C-S-H gel, and showed that this gel would determine strength and porosity of cement paste. When C-S-H gel has filled all available space, the porosity of gel is about 25%, and it contains pores a few nanometers in size (30). Powers and Brownyard (76) calculated the minimum volume fraction of gel pores in hydration productions 28%, and this could be used to distinguish gel and capillary pores. Gel pore in the Powers-Brownyard model contain different kinds of pores. The *inter-gel* pores are believed to locate within gel, while *inter-hydrate* pores are located in spaces between C-S-H gels and Calcium Hydroxide (CH) (77).

The formation of ice within a pore is dependent on the size. Nucleation of ice crystals becomes more difficult as pore size decreases. The freezing point depression of pore water is

related to the pore radius by the Gibbs-Thomson equation (78). Due to their small size, it is impossible for water to freeze inside of gel pores at normal temperatures. At the same time, ice crystals cannot form since not enough water molecules can occupy the gel pore, so the water in gel pores will be cold but not freeze (75).

2.3.1.2. Capillary pores

During hydration, solid products of the reaction have more volume than the initial ingredient, so these products will replace part of the water-filled space. The space between cement grains that are not filled with solid products are called *capillary pores* (79). Size ranges from ~ 5 nm to 10 μm and can be divided into large and small capillary pores. The volume of capillary pores depends on both the degree of hydration and original water/cement ratio (80) (81) (82). Capillary pore size of capillary pores will decreases with an increasing degree of hydration, while the number of large capillary pores will reduce as water-to-cement ratio (w/c ratio) is decreasing. Capillary pores contain water, and this water is almost completely evaporable at humidities below ~ 40% (80). Water in capillaries is an ionic solution that is in equilibrium with surrounding hydrated paste (74). Water can freeze in capillary pores since there is sufficient space to accommodate ice crystals, and this could cause damage inside the concrete (30). Figure 2 shows the composition of cement paste with both gel pores and capillary pores.

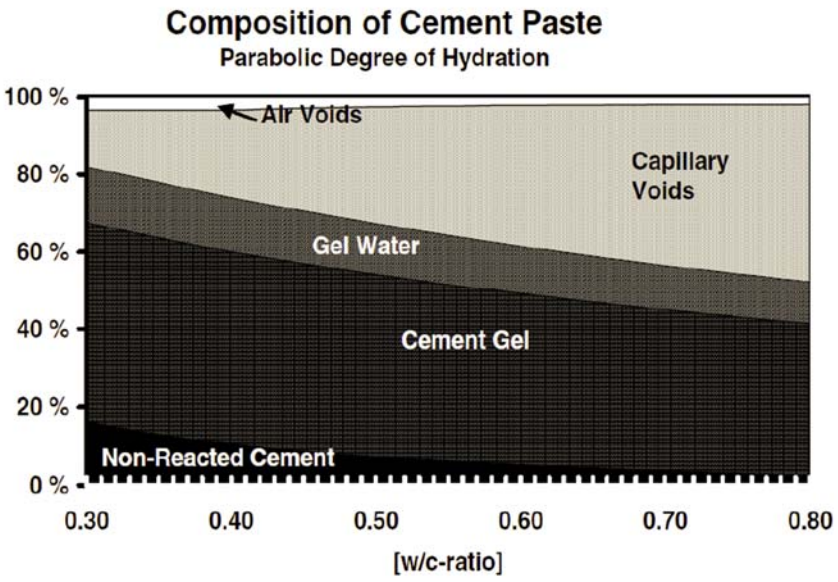

Figure 2.2. The structural components of cement paste in concrete (83)

2.3.1.3. Hollow-shell pores

In early stages of hydration, cement grains produce hydration products, and these products will grow outward, into capillary pore space. A void may develop inside the original cement grains as cement recedes with continued hydration. Smaller grains leave a completely hollow shell after about 1 day, while larger grains will leave a hollow shells with remnant anhydrous cores (84) (74). Hollow-shell pores usually have a diameter of approximately 15 μm, and seem to largely remain saturated within pore fluid, due to the connectivity of the pore system. In mature systems, hollow-shell pores are embedded in cement gel and are connected to capillary pores by gel pores. Therefore hollow-shell pores may not drain until the neighboring gel pores are drained (84).

2.3.1.4. Air voids

Air voids in hardened cement paste can be either entrapped or entrained. Entrapped air voids occur due to insufficient mixing, or consolidation. Entrapped air voids are defined as 1 mm

or larger in width and irregular in shape (86), and are typically isolated from other entrapped air voids. Typically they do not enhance hardened properties such as F-T durability or permeability (66). Entrained air voids are typically 10 to 1000 μm in diameter and spherical or nearly so. They are entrained intentionally by using air-entraining agent. Entrained air voids are distributed uniformly in concrete and are not interconnected with each other, therefore have no effect on concrete permeability. Entrained air voids provide concrete with boundaries for water to escape from capillary pores during ice formation and so limit the hydraulic pressure during the initial stages of freezing (1) (60) (74).

A comparison of pore sizes and their effects is presented in Table 1.

2.3.2. Geometry of pores

Pore shape in concrete is usually assumed to be cylindrical or spherical, but concrete has a multitude of internal pores with a various cross-sectional shapes (87). A shape factor is applied if the cross section is assumed to be irregular. Shape factor is the total pore volume divided by product of the pore area and average pore radius. Other researchers also have used different ways to define shape factor. Mason and Morrow (87) defined it as the hydraulic radius of one pore divided by perimeter of the pore, making shape factor a dimensionless factor that is appropriate for capillary behavior. Other researchers also proposed different formulas for the shape factor:

$$G=\frac{rd}{P} \quad \text{or} \quad G=\frac{Ap}{Pp^2} \tag{1}$$

where *G* is the shape factor, rd is the hydraulic radius, and P_p is the perimeter of the pore cross section. Ap is the cross-sectional area of a pore. Roundness (Eq.2) and circularity (Eq.3) are defined from Eq.1 and also used to determine the impaction from shape of the pores (74).

Table 2.1. Pore properties and location in air void system

Pore Type	Diameter	Location	Effects on F-T
Gel Pore	Intra-gel: <0.6nm	Inside of C-S-H gel (Intra)	Water in gel pore will travel into capillary pores to reduce solution concentration due to osmotic pressure
	Inter-hydrate:0.1-100 nm	Space between C-S-H gels and CH	
Capillary pore	small: 2-50 nm	Between cement grains and products of hydration	Ice crystals form in capillary pores and may generate tension then damage the paste
	large: 1 μm to 10 μm		
Hollow-Shell pore	10 μm	cement grains	Connected to capillary pores by gel pores, and stay saturated within pore fluid
Air voids	Entrained: 10 μm-1000 μm	Between cement grains and products of hydration	Providing boundaries for water to be forced out in capillary pores due to ice formation, and also limit hydraulic pressure
	Entrapped: 1mm		No effect

$$R=\frac{Pp^2}{4\pi A_p} \quad (2)$$

$$C=\frac{4\pi A_p}{Pp^2} \quad (3)$$

It can be seen that a circle has a circularity of 1, and the value will decrease when the irregularity of the cross section increases. A possible reason why circularity is often used as the shape factor for image analysis (88).

Other parameters are employed when irregular pores are characterized. Aligizaki also reviewed these parameters and presented a figure regarding these parameters (Figure 3). These parameters could be useful when microscope and image analysis are used, and pore size and pore shape of an irregular pore needs to be defined. The void shape becomes irregular when the pore size increases (89).

2.3.3. Total air volume

Total air content is defined as the proportion of the total volume of air voids to the bulk volume of concrete including all the constituents of concrete and the total volume of air (86). Klieger suggested that it would be more appropriate to express the air content in mortar or cement paste, since air voids contribute to frost resistance only in cement paste. So when calculating spacing factor, the air content should be the fraction of the "air free" paste, by dividing the total air volume by the volume of cementitious materials and water only. Another

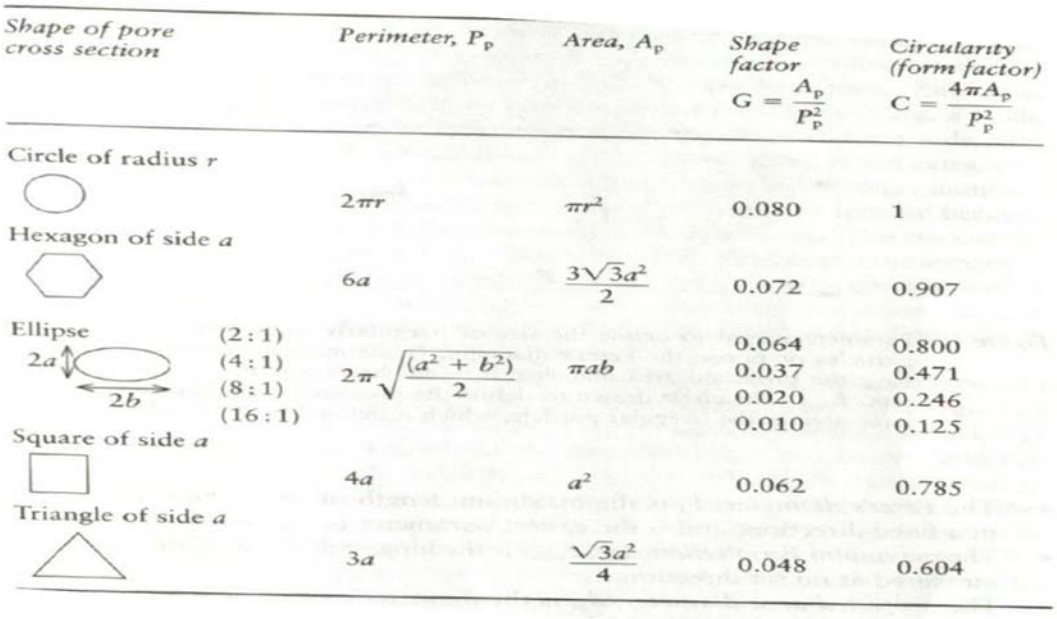

Shape of pore cross section		Perimeter, P_p	Area, A_p	Shape factor $G = \frac{A_p}{P_p^2}$	Circularity (form factor) $C = \frac{4\pi A_p}{P_p^2}$
Circle of radius r		$2\pi r$	πr^2	0.080	1
Hexagon of side a		$6a$	$\frac{3\sqrt{3}a^2}{2}$	0.072	0.907
Ellipse	(2 : 1)	$2\pi\sqrt{\frac{(a^2+b^2)}{2}}$	πab	0.064	0.800
	(4 : 1)			0.037	0.471
	(8 : 1)			0.020	0.246
	(16 : 1)			0.010	0.125
Square of side a		$4a$	a^2	0.062	0.785
Triangle of side a		$3a$	$\frac{\sqrt{3}a^2}{4}$	0.048	0.604

Figure 2.3. Example of values of factor and circularity of various shapes of cross section of pores

similar parameter is pore volume. When stereology is employed in volume analysis application on materials, volume fraction is used to describe pore volume. Point counting and linear analysis, are two commonly used methods for pore structure analysis. When a point is placed within a volume, the probability that it will fall within a given constituent is equal to the volume fraction of that constituent. In point counting method, the expected value P_p is given in Equation 4.

$$P_p=V_v, \quad P_p=A_A, P_p=L_L \tag{4}$$

Where P_p is the fraction of points falling in the point of interest, V_v is the volume fraction of the point of interest, A_A is the areal point of the area of interest, and L_L is the line fraction of the point of interest.

For linear analysis, Rosiwal (90) and Delesse (91) stated that volume fraction could be determined by a linear analysis approach. Brown and Pierson (91) then developed the analysis method linear transverse method. They proposed that the length of segments or chords intercepted could be summed together of each constituent. The proportion of any constituent in the volume is the summation of all segments for that constituent divided by the summation of the chords of all constituents (Equation 5) (92)).

$$V_v = V_v/V = L_L, \text{ where } L_L = l/L \tag{5}$$

Where Vv is the volume fraction of a phase in the solid volume, Vp is the total volume of the particles in the solid, V is the volume of the solid, LL is the length fraction of a line within the volume of the solid is the total length of the segments falling in a constituent, and L is the total length of the line.

2.3.4. Pore spacing, distribution, and connectivity

2.3.4.1. Pore spacing

Powers (49) believed that voids perform two functions in concrete: they limit the hydraulic pressure in the paste during the early stage of freezing and they limit the formation of ice bodies. The efficiency of these functions depends on the thickness of the paste between them. Air voids provide enough space for water to expand if the voids are sufficiently close together, while wider spacing will not provide enough space for water to escape. Multiple researchers

have offered different methods to determine this spacing factor, which is defined as the mean half distance between the outer boundaries of two adjacent air voids in (86). Powers gave a simpler model by calculating the relative proportion of the hardened cement paste within the beneficial zone of influence of one or more air voids. Lamond and Pielert (93) provided a schematic layout of Powers' spacing factor model based on the assumption that all air voids have the same size and are arranged in a simple cubic lattice (Figure 4). Based on the assumption above, Powers provided equations to calculate spacing factor, which is calculated from the total volume of air voids, paste content, and specific surface of air voids (Equation 6, Equation 7).

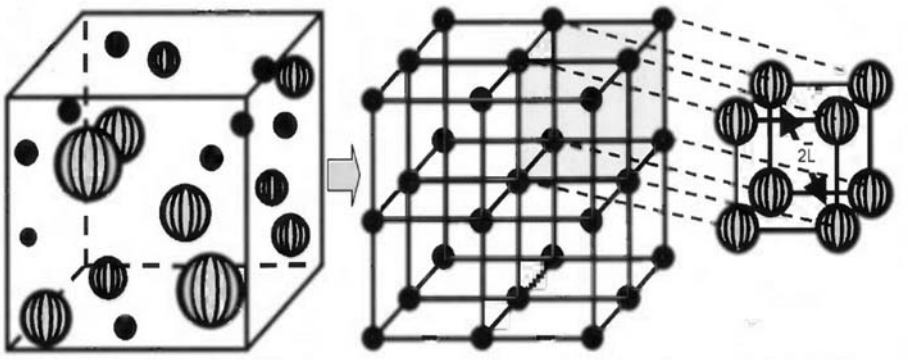

Figure 2.4. Air voids arranged in a simple cubic lattice (Lamond and Pielert 2006)

$$\bar{L}=\frac{Pcem}{\alpha Aa}, \text{ if} = \frac{Pcem}{\alpha Aa} < 4.342 \quad (6)$$

$$\bar{L}=\frac{3}{\alpha}[1.4(\frac{Pcem}{\alpha Aa}+1)^{1/3}-1], \text{ if} = \frac{Pcem}{\alpha Aa} \geq 4.342 \quad (7)$$

In equations, $\bar{L}$ is the spacing factor, P_{cem} is the cement paste content (%), Aa is total air content (%), and α is the specific surface of air voids (mm-1). Equations 6 and 7 do not take into consideration the actual shapes of the paste-filled spaces between the spheroidal voids. In most of air-entrained concretes, P_{cem}/Aa is greater than 4.342, so Equation 7 is used in most cases. ASTM C 457 (94) required a spacing factor of 0.10 mm to 0.20 mm to ensure the frost durability of concrete, based on Powers' equations.

Through the years, the validity of these equations has been questioned (74) (95). For instance, they cannot explain why porous materials can be damaged by F-T when they are saturated with organic liquids that do not expand upon freezing (96)(97). Some limitations of these equations were proposed by these researchers: (1) They are only applicable to concretes with similar void size distributions since spacing factor is calculated from total void volume and specific surface; (2) the spacing factor is calculated based on the assumption that all air voids have the same size.

Philleo (95) proposed a new method using Lord and Willis method to calculate air bubbles per unit volume called Philleo factor. It indicates the distance around an air void up to which hardened cement paste is protected from the effects of F-T. This method provides a more realistic appraisal of the internal geometry of air-entrained paste than the spacing factor. Pleau and Pigeon proposed a similar idea (99) called flow length, which provides a better estimate of the real spacing of air voids. The flow length is defined as the distance between any given point of the volume and the perimeter of the nearest air void, representing the distance that water must travel to reach a relief zone.

2.3.4.2. Pore size distribution

Pore size distribution is the fraction of the pore volume in which the pores lie within a certain size range. The pore size distribution can be presented in two ways, cumulative pore size distribution and differential pore size distribution. These can be presented wither either as a continuous function or as a histogram, and mathematical method is applied since the number of pores in sample is large enough to use statistical method. Gaussian (normal) distribution and the log-normal distribution are two methods normally used by researchers. Log-normal distribution is more commonly used in hardened cement paste. An equation proposed by Diamond and Dolch

(100), presented a pore size distribution with a single log-normal distribution that was continuous over the range from gel to capillary pores:

$$f(M) = \frac{1}{\sqrt{2\pi} ln\sigma} \exp[-\frac{1}{2} (\frac{\ln M - Ln\bar{M}}{ln\sigma})^2] \quad (8)$$

where $\bar{M}$ is the geometric mean diameter of the distribution, m is the radius of a give pore, f(M) is the probability density.

Pore size distribution is mainly determined by mercury intrusion porosimetry (throat size of bubbles). It varies with the age and w/c ratio of paste, and impacts the permeability and frost durability of concrete (98) (99). Zhang et al. (101) examined porosity of paste samples and found that paste samples with an intermediate pore size (between 0.04 and 0.2 μm) exhibited the least F-T resistance, lower resistance than both samples with finer pores (finer than 0.04 μm) and samples with coarser pores (coarser than 0.2 μm). Cook et al. (98) found that longer curing time or lower w/c ratio lowered the threshold pore width values. Recent studies have found that much smaller air voids and spacing also play a significant role in F-T deterioration (101) (102).

2.3.4.3. Connectivity

Connectivity of pores affects the transport properties of concrete, determining permeability (103). During hydration, a network of capillary pores is created that act as a kind of infrastructure, via which chemicals can be transferred and so damage the microstructure (104). It was concluded that connectivity is impacted by those parameters that influence the formation of capillary pore network. Connectivity of pores in concrete will affect both the ingress from the environment and fluid transfer internally, both of which are related with F-T durability.

2.3.5. Test method for air void systems

The most commonly used parameters for expressing characteristics of an air void system in concrete are the total volume of air, specific surface (SS), and spacing factor (SF). Conventionally the average chord length of voids is used to calculate the specific surface and spacing factor. Although related to pore sizes, these SS and SF values do not directly reflect pore size distribution. Research has revealed that some admixtures may induce clusters of air voids in concrete, significantly affecting pore connectivity, fluid movement, and pressure alleviation in concrete. More recent technologies, such as use of flatbed scanners with Bubble Counter analysis software (105) and x-ray imaging (96), allow analysis of air void connectivity and clustering.

2.3.5.1. Test methods for fresh concrete

A list of existing technologies that are being used in the analysis of the air void system of concrete, either fresh or hardened states is presented in Table 2. In any measurement system, the main challenges are the timeliness of results, resolution and precision of size measurement, ease of sample preparation, comparison between methods, and relating the results to F-T durability. Although it is widely known that the structure of an air void system is primarily responsible for concrete F-T durability, the pressure and volumetric test methods that measure only the total air content are still commonly used in fresh concrete because of their speed and simplicity.

Volumetric method uses a unit weight of concrete and specific gravity of each ingredient in concrete to calculate air content. Another gravimetric method also needs unit weight of the concrete and displacement in water of a weighed sample of concrete. An air indicator determines the air content for fresh concrete by displacing the air with alcohol and recording the change of liquid. Air void analyzer (AVA) is an efficient fresh air void system test that can present both air

content and spacing factor of fresh concrete. The downside to AVA is that due to the test, it is very sensitive to test environment, even shaking of the table or changing of room temperature may cause errors, which makes it difficult to use in the field. Acoustic bubble spectrometer is can provide bubble size distribution in fresh concrete by measuring sound speed and attenuation at various frequencies. Pressure method is commonly used in practice. Fresh air content can be tested using pressure method without information of the mix proportion or unit weight.

The Super Air Meter (SAM) is a relatively new fresh air test method. Ley and Tabb (106) first introduced SAM in 2014, then updated the test procedure in 2017. Unlike pressure meter which used 1 atmospheric pressure (14.5 psi.) to compress fresh concrete, SAM used two more pressure stages (30 psi. 45 psi) to further compress the sample and as a result, a more accurate air content is obtained. A so-called SAM number also can be obtained from this test. SAM number is reported to correlate with spacing factor from hardened air void system analysis and durability factor from ASTM C666 F-T durability tests. SAM number is the difference between equilibrium number (the pressure reading after open the valve between upper and bottom chamber) at 45 psi. of round 2 and round 1. The physical/chemical mechanisms behind SAM number reminas unclear.

2.3.5.2. Test methods for air voids system in hardened concrete

This section discusses sample preparation including water removal and polishing methods before testing, then the section will introduce current available methods for hardened concrete air voids system analysis.

- Water removal

Aligizaki (74) conducted a throughout review of water removal procedures from concrete. Water removal is required for most methods for testing air void systems, and evacuation prior to testing is usually used for water removal. Unfortunately Water removal may collapse the microstructure of cement paste. Water in gel pores and interlayer spaces can be removed by heating, evacuation, or a combination of these two. As for water that is part of the hydration products sequestered in pores, removal is challenging.

Even empty pores would have walls that are covered with an adsorbed layer of water vapor. Pore water removal would generate a temporary capillary pressure, which could cause shrinkage. Pore volume would decrease if such shrinkage happens in fine pores. Drying techniques and solvent replacement techniques are two general methods of water removal.

Drying techniques include oven-drying, vacuum-drying, D-drying, desiccant drying, and freeze-drying. Oven-drying at 105℃ is the most convenient and is sufficient for most purposes. The specimen would be placed in to an oven set at 105℃ and the drying process is considered completed when the mass difference is less than 0.1% between weighing 24-hours apart. Contraction and thermal expansion may occur during the drying cycle.

For vacuum drying, the sample is placed in a sealed container, and then a vacuum-generating mechanical pump will generate and remove the pore water from concrete paste. This method is quite slow and more suitable for concrete older than 28 days because it may cause micro cracking.

Table 2.2. Test methods for air void system for fresh concrete

Test method specifications							Air void parameter					Evaluation	
Method	**AASHTO/ASTM**	**Direct (D) /Calculate (C)**	**Extraneous information**	**Accuracy**	**Concrete (Conc), Mortar (Mor), or Paste (Pa)**	**Equipment**	**Total Volume**	**Size, chord length, SS**	**Spacing Factor, SF**	**Size distribution, frequency**	**Benefits**	**Limitations**	**References**
Gravimetric	T 121/C138	C	SpG from materials	0.1%	Conc	Container, balance, Rob, Strike-off plate, Mallet	×				Concrete tested can be used for other tests	Rely on SpG from other materials, not applicable in the field, not appropriate for lightweight aggregate	ASTM C138
Pressure Meter	T 125/C231	D	-	0.1%	Conc	Air meter, Measuring bowl, Cover assembly, Calibration vessel, Spring, tube, Trowel, Rob, Mallet, Strike-off plate, Funnel	×				No knowledge of SpG is needed	Not applicable for lightweight aggregates or aggregate with high porosity	ASTM C231
Volumetric Method	T 196/C173	D	-	0.25%	Conc	Air meter, others the same as C231, Isopropyl alcohol is needed	×				Can determine LW agg, slag, and high porosity agg	May have problem at high air content concrete	ASTM C173
Chance Air Indicator	T 199	C	Mortar content	-	Mor	Vial, Sample cup, Squeeze bottle	×				Fast method	30% lower than pressure method, not an accurate method, mortar air content	Sprinkel 1981, AASHTO T 199

Table 2.2. (continued)

Test method specifications							Air void parameter					Evaluation	
Method	**AASHTO/ASTM**	**Direct (D) /Calculate (C)**	**Extraneous information**	**Accuracy**	**Concrete (Conc), Mortar (Mor), or Paste (Pa)**	**Equipment**	**Total Volume**	**Size, chord length, SS**	**Spacing Factor, SF**	**Size distribution, frequency**	**Benefits**	**Limitations**	**References**
Super Air Meter		D	-	-	Conc	Super Air meter	×	×	×		15 mins to determine SAM number, and it can be used to determine spacing factor SF	-	Ley and Tabb 2014,
Air Void Analyzer	TP 175	D	-		Mor from Conc	AVA, blue fluid, wire cage, vibrator, syringe	×	×	×	×	Quick determination of SF for fresh concrete	Cannot capture bubbles larger than 0.012 in., sensitive to environment (temp, balance)	Wang et al. 2008,
Fiber Optic Air Meter		C	-	-	Conc	Opto-electronic PC interface card for use with the fiber optic probe, operating software for testing operations and data logging, various fiber optic probes, and a hand held vibrator	×				Determination of air void characteristics for fresh concrete rapidly (in a matter of seconds)	-	Ansari 1994
Acoustic bubble spectrometer		D	-	-	Pa	Microporous tube, water shear, air/water mix tank, transducer, high speed video camera, ABS, Pump	×	×		×	Measure size distribution for fresh concrete	-	Wu et al. 2010, Hackley et al. 2007

D-drying (dry-ice drying) was mentioned by Power and Brownyard (76) and proposed by Coperland and Hayes (115). A sealed glass container with a mechanical vacuum pump through a cold trap that cooled by a mixture of solid CO_2 and alcohol is used. It can remove all of the physically adsorbed water in paste pores (gel and capillary pores) without damaging the microstructure of the specimen. This method can even remove the water from interlayer spacing of gel pores (116).

Freeze-drying is also known as vacuum freeze-drying, which is a fast drying technique and causes little damage to the microstructure of concrete. Samples are immersed directly in liquid nitrogen for 5 mins, and then transferred to a sealed container and a vacuum is applied. This method cause less damage than oven-drying (117).

The solvent replacement procedure is used as an alternate drying technique prior to porosity analysis. It is considered to be gentle to concrete microstructure (Hughes and Crossley 1994). During solvent replacement, the specimen is weighed then immersed in an organic liquid. The solvent penetrates into the pores and replaces the pore solution. This method is believed to reduce micro cracking since the removal of solvent may not cause as much as surface tension as the original pore water.

- Preparation for observation

Sample preparation for microscopic is critical since it impacts the examination and interpretation of microstructure features. A highly polished surface is required for scanning electron microscope (SEM) and Optical Microscopy to be used. Polished and fracture surfaces may be used for reflected light microscopy and thin sections are used for transmitted light microscopy.

A polished surface is a plane surface with efficient amount of observation points in the material. A low quality polish can produce pitting and scarring. Impregnating the concrete pores with low viscosity epoxy resin is a common method for sample preparation for microscopic analysis to reduce the effects of sample preparation, and it can also enhance contrast between the pores and paste/aggregate.

Fracture surfaces are analyzed by secondary electron imaging due to the high resolution and depth of field associated with the method. Compared with polished surfaces, fracture surfaces expose the microstructural features unaltered, at the same time, no further treatment is required. A downside of this method is that the size of the sample may be too small to be representative of the whole.

- Air void system test methods for hardened concrete

Existing test methods for assessing the air void system of hardened concrete are listed in Table 3. They are able to provide an accurate measure of the air void size, spacing, and spatial distribution. The microscopy method ASTM C457 has been a reference for hardened air void system testing for hardened concrete.

There are two methods described in ASTM C457, one is linear traverse method and the other is point count. When using the linear traverse method, the traverse lines randomly intercept a fraction of the depressions on the plane surface, and the number and length of these sections are recorded. These lines are likely not be the diameter of the circles (voids), instead their chord length. Average chord length is defined as the average length of the chords formed by the transection of the voids by the line of traverse (118). Chord length is the cumulative length of

chord sections divided by the number of chords intercepted produces the average chord intercepts $\bar{l}$

$$\bar{l} = \frac{\mathrm{Ta}}{N} \tag{9}$$

Chord length, or average chord intercept, is statistically related to specific surface of the air-void distribution according to ASTM C 457:

$$\alpha = \frac{4}{\bar{l}} \tag{10}$$

where α is estimate of specific surface of the voids with an average chord length $\bar{l}$.

Void Frequency is another parameter in ASTM C 457. It is the number of voids encountered in per length of transverse:

$$n = \frac{\mathrm{N}}{Tt} \tag{11}$$

The Greater the void frequency, more voids are encountered per unit length of traverse.

Care should be taken when considering it the reference for comparative testing since the methodology behind ASTM C457 is statistical. A Rapid Air device is an automated technique modified from ASTM C457. Using lapping and coloring to enhance contrast, a machine conducts an automatic analysis with shorter testing time and less operator error. The down side to the test is that sample preparation (polishing, coating and coloring) is critical to the test's connectivity (119) (120).

Several automated techniques that utilize digital image processing have been proposed (121) (122). In order to determine the size distribution and volume fraction of air voids, the contrast between the air voids with respect to background of aggregate and hardened cementitious paste has been a challenge. This has been done by treating a polished sample with black ink and voids filled with white pigment. The drawback to this method is that the proportion

of the tested concrete is still needed to calculate for spacing factor and specific surface. Peterson, et al. (2009) added a step of treating the polished sample with phenolphthalein and flatbed scanning, prior to black ink treatment and re-scanning to obtain a contrast between air voids, hardened paste and aggregates.

For smaller samples, scanning electron microscopy (SEM) and small angle scattering (SAXS) can be used. SEM is able to provide a high magnification and high resolution image of solid samples, and it can provide information on chemical composition and crystal orientation of specimens. SEM has the potential to test most characteristics of the air void system in paste and concrete, but due to the small size of sample (usually a few millimeters), care must be taken sample is representative of the whole. At the same time, sample preparation of SEM involves vacuum drying and coating, which may change the microstructure of the paste, and the operating cost of an SEM is high.

Other techniques are used to find pore size distribution of concrete. The most common is Mercury Intrusion Porosimetry (MIP) in which the pressure required to force mercury into paste is correlated to pore throat sizes. Some limitations are t m v vhat the assumptions are not necessarily accurate for pores in concrete and mercury is a hazardous substance, while the oven-trying process may affect the test results (118) (123). Another technique is helium pycnometer. It can determine total porosity including capillary pores, but does not report pore size distribution (124).

Table 2.3. Test method for air void system in hardened concrete

Testing method specifications					Air void parameter								Evaluation		
Test method	Typical sample size	Sample Preparation	Procedure	Equipment	Total Volume	Specific Surface	Spacing Factor	Frequency	Geometry	Connectivity	Pore size Distribution	Smallest pore size	Benefits	Limitations	References
Microscopical ASTM C457	Minimum area depends on NMSA, surface area at least 72 sq in. and 3 in. deep	Surface preparation, Polishing	A: Linear-Traverse; B: Point-Count	A: Linear-Traverse Device, Microscope Lamp, Sprint Level, Leveling Device; B: Point-Count Device, Stereoscopic Microscope, Microscope Lamp, Spirit Level, Leveling Device	✔	✔	✔	✔			✔	2 μm	Original model of Rapid Air and automated	Time consuming, judgment calls are involved, no distinction between entrapped air voids and other voids	ASTM C457, Hanson 2012, Simon 2005
Rapid Air 457	Same as above	Polishing, lapping, contrast enhancement (coloring)	Automatic	Rapid Air 457 Air Void Analyzer, Automatic analysis system	✔	✔	✔	✔			✔	2 μm	Proved accuracy, takes about 15 mins to prepare the sample	Sample preparation is critical, Threshold setting can affect spacing factor	Hanson 2012, Jakobsen et al. 2006

Table 2.3. **(continued)**

Testing method specifications					Air void parameter								Evaluation		
Test method	Typical sample size	Sample Preparation	Procedure	Equipment	Total Volume	Specific Surface	Spacing Factor	Frequency	Geometry	Connectivity	Pore size Distribution	Smallest pore size	Benefits	Limitations	References
Automated Microscopical	Same as above	Polishing, contrast enhancement (coloring)	Image Analysis		✔	✔	✔	✔			✔		Provding more reliable results, better assessment of the real spacing	Frame edge effects, surface finishing is critical, misclassification of aggregate as cement paste	Pleasu et al. 2001, Chatterji and Gudmudsson 1977
Flatbed scanner	100 x 100 x 20 mm slab	Four foil on the corners, then slab will be sprayed with phenolphthalein in isopropanol diluted to 50:50 with distilled water		High-resolution flatbed scanner	✔	✔	✔	✔			✔	10 µm	Inexpensive, easy to operate	Underestimates the spacing factor, overestimation of air content, determination of threshold	Peterson et al. 2001
Light Micrographs	Provide at least the minimum finished surface	Polishing	Image Analysis	Differential Interference Microscopy (DIM)	✔	✔	✔	✔					High contrast so that raw materials can be distinguished from one another	Polishing process is critical, but time consuming	Scott 1997

Table 2.3. **(continued)**

Testing method specifications					Air void parameter								Evaluation		
Test method	Typical sample size	Sample Preparation	Procedure	Equipment	Total Volume	Specific Surface	Spacing Factor	Frequency	Geometry	Connectivity	Pore size Distribution	Smallest pore size	Benefits	Limitations	References
SEM	fairly small, few millimeters	Specimen will be coated with conducting material, then high vacuum dried for SEM, but not for ESEM or low temperature observations	-	Scan generator, Display and recording, Video amplifier, Electron source, Vacuum system	✓	✓	✓	✓	✓	✓	✓	0.1 µm	Extended range of magnification, high-resolution images with sufficient contrast	Vacuum drying and coating may change the micro structure of paste sample (resolved by ESEM), high instrument cost, high test cost, sample preparation could be time consuming	Aligizaki 2006, Monterior et al. 1989
Small Angel Scattering (SAXS or SANS)	Small sample with 1 cm diameter and thin (<1 mm)	-	-	Small angle X-ray: X-ray sources, Monochromators, Slit and collimation, Focusing devices, Detector; Small-angle neutron: Neutron sources, Monochromator, Slits and collimation, Sample container, detectors	✓						✓	0.001 µm	No oven-drying required, which will not impact the state of saturation of the sample, can detect structure of porous materials on scale 1-100 nm	Expensive, signal limited, limited research on pore structures	Aligizaki 2006, Monterior et al. 1989

Table 2.3. **(continued)**

Testing method specifications					Air void parameter								Evaluation		
Test method	Typical sample size	Sample Preparation	Procedure	Equipment	Total Volume	Specific Surface	Spacing Factor	Frequency	Geometry	Connectivity	Pore size Distribution	Smallest pore size	Benefits	Limitations	References
Mercury Intrusion Porosimetry (MIP)	Small size (cores 5 mm diameter and 10 mm long)	Oven-drying 105-110°C	Dried sample will be weighted, then placed into mercury-filling device to be evacuated, then pressurization test (low and high)	Penetrometer, high pressure vessel, vacuum, pressure generator, hydraulic fluid	✔						✔	0.0067 µm	Simpler, faster testing method, which provides much wider range of pore sizes, and only takes short time (30-45 mins)	Oven dry may impact pore size distribution and total porosity, Dimensions of specimen limit the size, assumptions that voids are conical in shape and decrease in diameter from the surface to core, ink-bottle effect, contact angle is required, mercury is a hazardous substance	Aligizaki 2006, Kaneuji 1978, Kurmar and Bhattacharjee 2002, Lamond and Pielert 2006

Table 2.3. **(continued)**

Testing method specifications					Air void parameter								Evaluation		
Test method	Typical sample size	Sample Preparation	Procedure	Equipment	Total Volume	Specific Surface	Spacing Factor	Frequency	Geometry	Connectivity	Pore size Distribution	Smallest pore size	Benefits	Limitations	References
Helium pycnometry	5 mm wide and 30 mm long disc	D-drying (dry-icing drying)	Conditioned at 11% RH and then dried to the d-dried condition, then exposed sample to 11, 32, 42, 66, 84, and 100% RH, helium flow rate and solid volume will be measured	Helium generator, selector valve, sample cell, reference cell	✔							2-200 nm	Can determine capillary porosity	Only pore volume no pore size distribution, and not sensitive to pores less than 2nm	Aligizaki 2006, Feldman 1980
Capillary Flow	Depends on researchers	100°C for 24 hrs	Sample will be put under pressure to identify the pore size distribution	Capillary flow porometer	✔						✔	0.2 µm	Simple and fast test method		Jena et al. n.d. Leventis et al. 2000

Table 2.3. **(continued)**

Testing method specifications					Air void parameter								Evaluation		
Test method	Typical sample size	Sample Preparation	Procedure	Equipment	Total Volume	Specific Surface	Spacing Factor	Frequency	Geometry	Connectivity	Pore size Distribution	Smallest pore size	Benefits	Limitations	References
Thermo-porometry	Depends on researchers	Not required	Samples are immersed in water or benzene (frozen), as the temp increases, the amount of solid melting is measured, and the amount of frozen liquid will be measured	Varies by researchers	✔				✔	✔	✔	4 nm	No drying required, Effective in detecting capillary pores and crystallization in them, real size of the pores can be measured	Cannot go lower than 2 nm, hypothesis about the pore shape	Fontenay and Sellevold 1980, Aligizaki 2006
Nitrogen Gas Adsorption	1/2 in. diameter and 2 in. deep mold	-	Complex	Helium generator, nitrogen generator, clear vessel with liquid nitrogen, calibrated volume, vacuum pump	✔						✔	40 nm	Well-established testing procedure, no assumptions on pore shape	Small specimen, complex procedure, time consuming, not useful for large pores, ink-bottle effect	Aligizaki 2006

Table 2.3. **(continued)**

Testing method specifications					Air void parameter								Evaluation		
Test method	Typical sample size	Sample Preparation	Procedure	Equipment	Total Volume	Specific Surface	Spacing Factor	Frequency	Geometry	Connectivity	Pore size Distribution	Smallest pore size	Benefits	Limitations	References
Nuclear Magnetic Resonance	16 mm diameter and 80 mm long cylinder, paste or mortar or concrete	Vacuum-dried	Specimen is placed in a magnetic field and irradiated with intense radio frequency pulses; when the nuclei relax, the NMR probe receives a weak RF resonance response back from the sample		✔						✔		Fast, non-destructive technique, no limitation on sample size, no drying required, can be used to monitor pore structure during hydration	Complicated equipment, high cost and significant expertise in order to obtain reliable data	Leventis et al. 2000 Aligizaki 2006, Valckenborg et al. 2001
Water absorption	Depends on standard	Oven dry at 105°C, then vacuumed	Specimen is submerged in de-aired water, then water will be sucked into pores due to raised pressure		✔								Fast and indication of porosity using simple and inexpensive equipment	Not absolute values for porosity	Aligizaki 2006

2.4. Effects of air void system on mechanical properties

The mechanical properties of concrete are influenced by each component in the matrix. The major impact of air voids to concrete is on durability, especially frost resistance. But air voids content and pore distribution will also impact some mechanical properties like compressive strength and shrinkage resistance. This section will review the influence of air voids to mechanical properties of concrete.

2.4.1. Compression strength and elastic modulus

2.4.1.1. Compression strength

It is well-understood that increasing air content may cause a commensurate loss of strength, which, as a result impacts the durability of concrete 21) (96). One percentage point increase of air content increment may lead to a 2-6 percent loss of compressive strength (31). The reduction of strength due to air voids can be reduced when the void size istribution is reduced. Regarding air voids and compressive strength, two phenomena are used to explain the low compressive strength: interfacial transition zone and air void clustering.

Interfacial transition zone (ITZ) in concrete is a 10-50 μm thin zone between cement paste and aggregate particles. It is identified as the weakest region of concrete, which impacts both mechanical properties and durability of concrete (126). The existence of ITZ impacts permeability and strength of concrete

Formation of the IFZ is due to the influence of the wall effect (127). Spatial arrangement of anhydrous grains becomes looser in the vicinity of aggregate particles. As a result, the porosity and local w/c ratio increases from the bulk to the surface of aggregate particles. This wall effect has been confirmed by observing mortars using back-scattered electron imaging

(BSEM) (128). The other mechanism suggests that micro bleeding may be a contributor (129). In this mechanism, aggregate particles have a lower submerged weight than cement paste, so it settles at a slower rate than cement particles. The void between aggregate particles and paste will be filled by bleed water. During compaction, relative movement between aggregates and cement paste particles will encourage formation of a water-rich layer round aggregate particles. These mechanisms explained the tendency observed by Hover (130) that air bubbles tend to accumulate at the mortar/coarse aggregate interface, which reduces the paste/aggregate bond.

South Dakota DOT and Kansas DOT experienced loss of compressive strength reportedly caused by the weak bond between cement paste and coarse aggregate where air bubbles are clustered (47) (134) (118) (130). Researchers have reported that when vinsol resin admixtures are used, no air void clustering is observed (47) (135), while low-alkali cement and synthetic admixtures can cause air void clustering. Kozikowaski et al. (135) also proposed a method to evaluate clustering. Aggregate particles from concrete are observed under a microscope and assigned to a category represented with a number from 0- to 3 based on severity of void clustering. However recently Riding et al. (134) observed that it is not air clustering that has a significant impact on strength, instead, it is total air content and inhomogeneous microstructure of cement paste that caused the low strength.

2.4.1.2. Elastic modulus

Concrete elastic modulus is one of key components in pavement design since it influences stresses in the concrete and traffic and environmental loading. The characteristics affect the compressive strength will also impact elastic modulus (Rao et al. 2012). Pore size or continuity dose not impact elastic modulus significantly, but the increasing volume of the pores will lead to a reduction inelastic modulus (118) (136). At the same time, the bonding of the

interface between paste and aggregate impacts the mechanical properties of concrete (137). Modulus of elasticity decreases with increasing air at a rate of about 105,000 psi to 200,000 psi (3-6 percent reduction) per percentage point of air (30).

2.4.2. Creep

Creep is the time-dependent deformation or increase in strain that happens due to sustained load (131). It is a typical manifestation for viscoelastic materials. It can reduce stress caused by shrinkage or settlement, but it also leads to bigger deflections (138). Creep is recognized as a paste property due to its porous structure with a large internal surface area (139). Water movement in gel pores is the main cause of creep Disjoining pressure, which is a transverse compressive stress, is exerted by the hindered layers on the micropore walls (81) (141)). Jennings et al. (134) defined the disjoining pressure as a pressure between two closely-spaced solid surfaces, and it tries to push the solids apart. Tensile forces have to balance this pressure, and these forces are partially carried by solid framework of C-S-H and partially by bridges or bonds between the opposite walls. Meanwhile, due to this disjoining pressure, solid part of gel in hardened cement is in a pretensioned state, and this pretensioned state can be caused by hydration process or drying process as well (141). Due to the short distance for water diffusion inside of pore structure, Bazant and Chern believed that the hindered adsorbed water established a thermodynamic equilibrium with capillary water in a short period. Creep of cement gel occurs in the gel microstructure from shear slips driven by the shear stress and impacted by normal stresses across the slip planes. The bond or bridges between atomics which contains the adsorbed water are the slip planes causing creep. It is a result of multiple internal bond or bridges break occurring in multiple times at different creep sites in the hindered adsorbed layers (141). This microprestress of creep sites theory is not the only mechanism to explain creep. Many other

mechanisms were proposed to demonstrate creep. Bazant and Prasannan discussed solidification theory for short-term aging, comparing to long-term aging and Pickett effect he proposed at 1997. New models include rate-of-flow model, rate-of creep model, double power loaw and dog-double power law for basic creep, etc. Review of these models is beyond the objective of this project. Creep rate will decrease when relative humidity decreases, and Wittmann proposed that it will be not creep if RH value is less than 50%, which can be concluded that adsorbed water on C-S-H surface is necessary for creep. Weiss (139) also believed that though creep occurs in cement paste, aggregate can substantially decrease creep. There is no clear relationship between pore size/pore size distribution and creep. But it is clear that gel pore plays a significant role in creep.

2.4.3. Shrinkage

When a porous material is subjected to an outer relative humidity lower than its initial inner relative humidity, the vapor thermodynamic imbalance forces the porous material to exchange water vapor with the outer atmosphere, so that the outer relative humidity progressively takes hold within the material. In turn liquid water simultaneously evaporates in order to maintain the vapor-liquid equilibrium. This causes a decrease of the degree of liquid saturation. (143).The shrinkage of the porous material final results from the lowering in liquid pressure induced by the desaturation process at the gas-liquid water interface, while the kinetics of drying is governed by transport phenomena. When concrete is exposed to its service environment it tends to reach an equilibrium with that environment. If the environment is a dry atmosphere the exposed surface of the concrete loses water by evaporation. The first water to be lost is that held in the large capillary pores of the hardened concrete. The loss of this water does not cause significant volume change. As drying continues, loss of water from small capillaries

and later from gel pores takes place. Reduction in the vapor pressure in the capillary pores, tensile stress in the residual winter increases. Tensile stress in the capillary water are balanced by compressive stress in the surrounding concrete and as a result the concrete shrinks. It has been proposed that water meniscus in small capillaries (5-50 nm) applies a hydrostatic tension, and during drying process the water removal will induce a tensile stress on the walls of these capillary pores, and as a result cause contraction of the system, leading to shrinkage (144).

Autogenous shrinkage is defined as the volume change occurring with no moisture transferred to the exposure environment. It is a chemical contraction due to hydration and volume difference between hydration products and cement paste. During hydration, the unhydrated cement particles may absorb water from nano-pores and capillary pores for further hydration, especially in low water cement ratio concrete like high strength concrete, and self-desiccation and autogenous shrinkage would occur till hydration stops. Autogenous shrinkage comprises both chemical shrinkage and self-desiccation. Self-desiccation is due to the water movement from capillaries to fine voids created by hydration. Coarse capillary pores may be emptied by this during hydration progress without mass loss. Chemical shrinkage is caused by hydration of cement and water, which creates products that have less absolute volume than the reactants, and this would deification the solid phase of concrete (145). Chemical shrinkage is the key factor for autogenous shrinkage before concrete sets, and self-desiccation becomes dominant after concrete sets (146) (147). Hua et al. (148) demonstrated that autogenous shrinkage is caused by capillary forces due to the water consumption in capillary pores. It has been proposed that pores with diameter of 5 to 50 nm will impact the autogenous shrinkage the most, and more percentage of this range of capillary pores would lead to larger autogenous shrinkage (149).

2.5. References

1) Page, C.L., Page, M. M., *Durability of concrete and cement*, WOODHEAD PUBLISHING LIMITED, Cambridge, England, 2007

2) Power, T.C., Copeland L.E., and Mann, H.M., PCA Bulletin 10, 1959

3) Garboczi, E.J., Bentz, D.P., "Multi-scale picture of concrete and its transport properties: introduction for Non-cement researchers," NISTIR 5900, 1996

4) Klieger, P., "Air-Entraining Admixtures," *Significance of Tests and Properties of Concrete and Concrete Making Materials*, ASTM STP 169c. Eds. Paul Klieger and Joseph F. Lamond. West Con¬shohocken, PA: American Society for Testing and Material, 1994, pp. 484–490

5) Greening, N.R. "Some Causes for Variations in Required Amount of Air Entraining in Portland Cement Mortar," *PCA Journal*, Vol. 9, No. 2, 1967, pp. 22–36

6) Pistilli, M.F., "Air Void Parameters Developed by Air-Entraining Admixtures as Influenced by Soluble Alkalies from Fly Ash and Portland Cement," *ACI Journal*, Proceedings, Vol. 80, No. 3, 1983, pp. 217–222

7) American Coal Ash Association, *Fly Ash Facts for Highway Engineers*, FHWA-IF-01-019, 2003

8) Bilodeau, A., Malhotra, V.M., "Concrete incorporating high volumes of ASTM class F fly ashes: Mechanical properties and resistance to deicing salt scaling and to chloride-ion Penetration, in Fly Ash, Silica Fume, Slag & Natural Pozzolands in Concrete," *ACI Special Publication SP-132*, American Concrete Institute, 1992, pp.319-349

9) Karakurt, C., Bayazit, Y., "Freeze-Thaw REsistacne of Normal and High Strength Concrete Produced with Fly Ash and Silica Fume," *Advances in Materials Science and Engineering*, 2015

10) Boyd, A., and R. D. Hooton, "Long-Term Performance of Concretes Containing Supplementary Cementing Materials," *Journal of Materials in Civil Engineering*, Vol.19, 10, 2007, pp. 820–825

11) Perraton, D., Aitcin, P.C., Vezina, D., "Permeabilities of silica fume concretes," ACI Special Publications SP-108, 1988, pp. 63–84

12) Hooton, R.D., "Influence of silica fume replacement of cement on physical properties and resistance to sulfate attack freezing and thawing, and alkali-silica reactivity," *ACI Materials Journal*, 90(2), 1993, pp. 143–152

13) Cwirzen, A., Penttala, V., "Aggregate–cement paste transition zone properties affecting the salt–frost damage of high-performance concretes," *Cement and Concrete Research*, 35(4), 2005, pp.671–679

14) Nagi, M.A., Okamoto, P.A., Kozikowski, R.L., and Hover, K., "Evaluating Air-Entraining Admixtures for Highway Concrete," NCHRP Report 578, Transportation Research Board, 2007

15) Verbeck, G., Landgren, R. "Influence of Physical Characteristics of Aggregates on Frost Resistance of Concrete," Proceedings, Vol. 60. American Society for Testing and Materials. Conshohocken, PA, 1960, pp. 1063-1079

16) Waugh, W. R., "Selection and Use of Aggregates for Concrete," *Journal of the American Concrete Institute*, Vol. 58, No. 5, November, 1961, pp. 513-542

17) Gaynor, R. D., "Laboratory Freezing and Thawing Tests; A Method of Evaluating Aggregates," National Aggregates Association Circular No. 101, 1967

18) Powers, T.C., "Freezing effects in concrete, Durability of concrete," ACI SP-47, 1975

19) Kaneuji, M., Winslow, D.N., and Dolch, W.L., "The relationship between aggregate pore size distribution and its freeze-thaw durability in concrete," *Cement and Concrete Research*, 10(3), 433-441, 1978

20) Hudec, P., "Deterioration of rocks as a function of grain size, pore size, and rate ofcapillary absorption of water," *Journal of Materials in Civil Engineering*, 1(1), 1989

21) Kosmatka, K., Wilson, M.L., *Design and Control of Concrete of Mixtures*, 16th Ed, Portland Cement Association, Skokie, IL, USA, 2016

22) Du, L., Folliard, K.J., "Mechanisms of air entrainment in concrete," *Cement and Concrete Research*, 35, 2005, pp. 1463 – 1471

23) Dodson, V.H., *Concrete Admixtures*, Van Nostrand Reinhold, New York, 1990

24) Deno, D.W., "The influence of Fine Aggregate Gradation Characteristics on Air Entrainment in Portland Cement Mortar," Joint Highway Research Project, Purdue University, 1966

25) Portland Cement Association, Concrete Information, "Air Entrained Concrete, Structural," Structural Bureau ST 89, 1962

26) Walker, S., Delmar, L., "Studies of Concrete Containing Entrained Air," Journal of the American Concrete Institute, Vol.17, No.6, 1946

27) Dolch, W.L., "Air-Entraining Admixtures," *Concrete Admixtures Handbook*, Properties, Science, and Technology, Second Edition, 1995

28) Rixom, M.R., Mailvaganam, N.P., "Chemical Admixtures for Concrete,"3re ed., Wiley, New York, 1999

29) U.S. Bereau of Public Roads, "Evaluation of Air Entraining Admixtures for Concrete," Public Roads, Vol. 27, No.12, 1954, pp.259-267

30) Cordon, W., *Freezing and Thawing of Concrete Mechanisms and Control*, American Concrete Institute Monograph No.3, 1966

31) Whiting, D.A., Nagi, M.A., "Manual on Control of Air Content in Concrete," EB116, PCA, Skokie, IL, 1998

32) Fujiwara, H., Douzono, A., Maruoka, M., and Numanno, T., "Study on Relation Between Void Structure and Sound Absorption Characteristic of Porous Concrete," Semento, Konkurit, Ronbunshu, Vol. 56, 2002, pp. 291–297

33) Wang, H., Gillot, J. E., "Combined Effect of an Air-Entraining Agent and Silica Fume on Alkali-Silica Reaction," 9th International Conference on Alkali-Aggregate React. Concr., Vol. 2, 1992, pp. 1100–1106

34) Powers, T.C., "The Air Requirement of Frost-Resistance Concrete," *Research Bulletin 33*, Portland Cement Association, Chicago, IL, in Proceeding, Highway Research Board, Vol.29, 1949

35) Larson, T.D., Candy, P.D., and Mallow, J.J., "The Protected Paste Volume Concept using New Air Void Measurement and Distribution Techniques," *ASTM Journal of Materials*, Vol.2, No.1, March, 1967, pp.202

36) Mielenz, R.C., Wolkodoff, V.E., Backstrom, J.E., and Flack, H.L, "Origin, Evolution and Effects of the Air Void System in Concrete, Part I- Entrained Air in Unhardened Concrete," Proceeding, American Concrete Institute, Vol.55, 1958, pp.95-121

37) Klieger, P., "Air Entraining Admixtures," *Significance of Tests and Properties of Concrete and Concrete-making Materials*, 1966

38) Jeknavorian, A.A., "Air Entraining Admixtures," Significance of Tests and Properties of Concrete and Concrete-Making Materials, 2006

39) Taylor, P., Wang, X., Wang, X.H., "Concrete Pavement Mixture Design and Analysis (MDA): Evaluation of Foam Drainage Test to Measure Air Void Stability in Concrete," 2015

40) Plante, P., Foy, C., "The Influence of Water-Reducers on the Production and Stability of the Air Void System in Concrete," *Cement and Concrete Research*, Vol. 19, pp. 621–633, 1989.

41) Taylor, P. C., W. Morrison, and V. A. Jennings, "The Effect of Finishing Practices on Performance of Concrete Containing Slag and Fly Ash as Measured by ASTM C 672 Resistance to Deicer Scaling Tests, " *Cement, Concrete, and Aggregates*, Vol 26, 2004, pp.155-159

42) Klieger, P. and Perenchio, W.F., "Further Laboratory Studies of Portland-Pozzolan Cements," Research and Development Bulletin RD041.01T, PCA, Skokie, IL, 1976

43) Gebler, S. and Klieger, P., "Effect of Fly Ash on the Air-Void Stability of Concrete," Fly Ash, Silica Fume, Slag and Other Mineral By-Products in Concrete, SP-79, American Concrete Institute, Detroit, MI, 1983

44) Ramachandran,V.S., "Concrete Admixtures Handbook: Properties, Science and Technology," Ottawa, Canada: Noyes Publications, 1995

45) Whiting, D.A., Nagi, M.A., "Manual on Control of Air Content in Concrete," EB116, PCA, Skokie, IL, 1998

46) Nagi, M.A., Okamoto, P.A., Kozikowski, R.L., and Hover, K., “Evaluating Air-Entraining Admixtures for Highway Concrete,” NCHRP Report 578, Transportation Research Board, 2007

47) Cross, W., Duke, E., Kellar, J. and Johnston, D., “Investigation of Low Compressive Strengths of Concrete Paving, Precast and Structural Concrete,” Report SD98-03-F. South Dakota Department of Transportation. Pierre, SD, 2000

48) Taylor, P. C., Johansen, V. C., Graf, L. A., Kozikowski, R. L., Zemajtis, J. Z., and Ferraris, C. F, “Identifying incompatible combinations of concrete materials: Volume II-test protocol,” FHWA-HRT-06-080, 2006

49) Powers, T. C., "The thermodynamics of volume change and creep." Mat. and Struct., Paris, France, 1(6), 1968, pp. 487 -507

50) Torrans, P.H., Ivey, D.L., “Review of Literature on Air-Entrained Concrete,” Air Entrainment in Concrete, Research Study Number 2-5-66-193, the Texas Highway Department, 1968

51) Du, L., Folliard, K.J., “Mechanisms of air entrainment in concrete,” *Cement and Concrete Research*, 35, 2005, pp. 1463 – 1471

52) Powers, T. C., "The thermodynamics of volume change and creep." Mat. and Struct., Paris, France, 1(6), 1968, pp. 487 -507

53) Backstrom, J., Burrows, R., Mielenz, R., Wolkodoff, V.E., “Origin, Evolution, and Effects of the Air Void System in Concrete, Part 2-Influcen of Type and Amount of Air-Entraining Agent,” *Journal of the American Concrete Institute*, Title No.55-16, 1958

54) Ley, M.T, Chancey, R., Juenger, M., and Folliard, K.J., “The physical and chemical characteristics of the shell of air-entrained bubbles in cement paste,” *Cement Concrete Research,* 2009

55) Rashed, A.I., Williamson, R.B., “Microstructure of entrained air voids in concrete: Part I,” *J. Mater. Res.* 6 (9), 1991, pp. 2004-2012

56) Rashed, A.I., Williamson, R.B., “Microstructure of entrained air voids in concrete: Part II,” *J. Mater. Res.* 6 (11), 1991B, pp. 2474-2483

57) Pigeon, M., Plante, P., "Study of Cement Paste Microstructure around Air Voids: Influence and Distribution of Soluble Alkalies," *Cement and Concrete Research* 20, 1990, pp. 803-814

58) Diamond, S., "Cement Paste Microstructure – An Overview at Several Levels, Hydraulic Cement Pastes: Their Structure and Properties," *Cem and Concr Assoc*, Slough U.K., 1976, pp. 2-30

59) Barbee, J.F., "Effect of Mixing Time and Overloading on Concrete Produced by Stationary Mixers," Highway Research Board Bulletin 295, HRB, Washington, DC, 1961, pp. 26–37

60) Powers, T.C., "Topics in Concrete Technology. 3-Mixtures Containing Intentionally Entrained Air," J. PCA Research and Development Laboratories, Vol. 7, No. 1, 1965, pp. 23–41

61) Myers, D., *Surfaces, Interfaces, and Colloids: Principles and Applications*, 2nd ed., Wiley-VCH, New York, 1999

62) Abrams, D.A., "Effect of vibration, Jigging, and pressure on fresh concrete," *Bulletin 3*, Structural Materials Research Laboratory, Lewis Institute, Chicago, IL

63) ACI 309-1R-09, "Report on behavior of fresh concrete during vibration," American Concrete Institute, 2008

64) Banfill, P.F.G; Teixeira, M.A.O.M; Craik, R.J.M.; "Rheology and vibration of fresh concrete: Predicting the radius of action of poker vibrators from wave propagation", Cement and Concrete Research, 2011

65) ASTM C125-18, "Standard Terminology Relating to Concrete and Concrete Aggregates," ASTM International, West Conshohocken, PA, 2018

66) Power, T.C., "Void Spacing as a Basis for Producing Air-entrained concrete," *Research Bulletin,* 49, Portland Cement Association, Journal of the American Concrete Institute, 1954, pp. 741-760

67) Gutmann, P. F., Bubble Characteristics as they Pertain to Compressive Strength and Freeze-thaw Durability. ACI Materials Journal, 1988, pp. 361-366

68) Ghadban, A.A.; PhD Dissertation, Kansas State University, 2016

69) Anderson, R.A., Fundamentals of Vibrations, New York: The Macmillan Company, 1967

70) Hayduk, W., Neale, G., T, Vortex Formation in Stirred Draining Vessels, The Canadian Journal of Chemical Engineering, Vol. 56, 1978

71) Gowda, B.H.L., Akhuli, S., Anudeep, B.R., Kishore, K., Influence of Base Inclination on Vortex Formation during Draining from Cylindrical Tanks, Indian Journal of Engineering & Materials Sciences, Vol. 20, 2013

72) Torre, J.P., Fletcher, D.F., Lasuye, T., Xuereb, C., An Experimental and Computational Study of the Vortex Shape in a Partially Baffled Agitated Vessel, Chemical Engineering Science, 62, 2007

73) Plowman, J.M. The Influence of Variables in the Vibration of Concrete, Concrete Building Construction Products, 28, 1953

74) Aligizaki, K., *Pore Structure of Cement-based Materials*, Taylor & Francis, 2006

75) Powers, T. C. and Steinour, H., "An Interpretation of Published Researches on the Alkali-Aggregate Reaction," *Journal, American Concrete Institute*, Proceedings, Vol. 51, 1955, pp. 497–516

76) Powers, T.C., and Brownyard, T.L., "Studies of the Physical Properties of Hardened Portland Cement Paste," Research Bulletin 22, Portland Cement Association, Chicago, IL, Reprinted from the Journal of the American Concrete Institute, in Proceedings Vol 43, 1948, pp. 101

77) Maekawa, K., Ishida, T., and Kishi, T., *Multi-Scale Modeling of Structural Concrete*, Taylor & Francis Group, 2009

78) Beddoe, R.E., Setzer, M.J., A low-temperature DSC Investigation of Hardened Cement Paste Subjected to Chloride Action, Cement and Concrete Research, Vol.18, Issue 2, 1988

79) Jennings, H.M., Bullard, J.W., Thomas, J.J., and Andrade, J.E., "Characterization and Modeling of Pores and Surfaces in Cement Paste: Correlations to Processing and Properties," *Journal of Advance Concrete Technology*, Vol.6, No. 1, 5-29, 2008, pp. 5-29

80) Verbeck, G., "Pore Structure," *in Significance of Tests and Properties of Concrete and Concrete Aggregates*, STP 160A, American Society for Testing and Materials, 1966, pp. 211-219

81) Power, T.C., "Physical Properties of Cement paste," *in Proceeding of the Fourth International symposium on the Chemistry of Cement*, Washington, DC, 1960, pp. 577-613

82) Jennings, H.M., Bullard, J.W., Thomas, J.J., and Andrade, J.E., "Characterization and Modeling of Pores and Surfaces in Cement Paste: Correlations to Processing and Properties," *Journal of Advance Concrete Technology*, Vol.6, No. 1, 5-29, 2008, pp. 5-29

83) Herholdt, A. G., Justesen, C. F. P., Nepper Christensen, P., and Nielsen, A., Editors, Beton Bogen [in Danish], Aalborg, Denmark, Aalborg, Portland, 1979

84) Kjellsen, K.O., Atlassi, E.H., "Pore Structure of Cement Silica Fume Systems Presence of Hollow-Shell Pores," *Cement and Concrete Research 29*, 1999, pp.133-142

85) Kjellsen, K.O., Wallevik, O.H., and Fjallberg L., "Microstructure and microchemistry of the paste-aggregate interfacial transition zone of high performance concrete," *Advances in Cement Research*, 10, 1998, pp 33-40

86) ASTM C125-03 *Standard Terminology Relating to Concrete and Concrete Aggregates*, American Society for Testing and Materials, 2003

87) Collins, F.G., Sanjayan, J.G., "Capillary Shape: Influence on Water Transport within Unsaturated Alkali Activated Slag Concrete," *Journal of Materials in Civil Engineering*, 2010.22(3), 2010, pp. 260-266

88) Russ, J.C., *The Image Processing Handbook*, CRC Press, Boca Raton, Fl, 4th Edition, 2002

89) Clift, R., Grace, J.R., and Weber, M.E., *Bubbles, Drops, and Particles,* Prentice Hall, Academic Press, New York, 1985

90) Rosiwa, A., "Uber geometrische gesteinsanalysen. Ein einfacher weg zur ziffemassigen festellung des quantitatsverhaltnisses des mineralbestandteile gemengter gesteine," 1898, pp.143-175

91) Delesse, A., Procede mecanique pour determiner la composition des roches," *Annales des Mines*, Vol.13, 1848

92) Hilliard, J.E., Cahn, J.W., "An evaluation of procedures in quantitative metallography for volume-fraction analysis," *Transactions of the Metallurgical Society of AIME*, Vol.221, 1961, pp.334-352

93) Lamond, J.F., Pielert, J.H., *Significance of Tests and Properties of Concrete and Concrete-Making Materials*, ASTM International, 2006

94) ASTM C457 / C457M – 12 *Standard Test Method for Microscopical Determination of Parameters of the Air-Void System in Hardened Concrete*, American Society for Testing and Materials, West Conshohocken, Pennsylvania, 2013

95) Philleo, R.E., "A method for analyzing void distribution in air-entrained concrete," *Cement, Concrete, and Aggregates*, Vol.18, No.1, 1006, 1983, pp.19-29

96) Sutter L.L., "Evaluation of Methods for Characterizing Air Void Systems in Wisconsin Paving Concrete," SPR# 0092-03-16, Wisconsin Highway Research Program, June 2007

97) Marchand, J., Sellevold E. J., and Pigeon M., "The Deicer Salt Scaling Deterioration of Concrete - An Overview. Durability of Concrete," Third International Conference, Nice, France. V.M. Malhotra. ACI SP-145. 1994, pp. 1-46

98) Cook,, R.A. Hover, K.C. "Mercury porosimetry of hardened cement pastes," *Cem Concr Res* 29 (6), 1999, pp.933-944

99) Pigeon, M., Pleau, R., *Durability of Concrete in Cold Climates*, E& FN SPON, London, UK

100) Diamond, S., Dolch, W.L., "Generalized log-normal distribution of pore sizes in hydrated cement paste," *Journal of Colloid and interface science,* Vol.38, No.1, 1972, pp. 234-244

101) Zhang Y., Cai J., Xu S., and Hu Z., "Experimental Analysis of Relationship between Pore-structure and Frost-resistance of Concrete," Applied Mechanics and Materials, vol. 174-177, 2014, pp. 117-120

102)Liu L., Shen D., Chen H., Sun W., Qian Z., Zhao H., and Jiang J., “Analysis of damage development in cement paste due to ice nucleation at different temperatures," Cement & Concrete Composites 53, 2014, pp.1-9

103)Mehta, P.K., Monteriro, P.J.M., *Concrete, Microstructure, Properties, and Materials*, Fourth Edition, Mc Graw Hill Education, 2014

104)Koenders, E.A.B., Ukrainczyk, N., and Hansen, W., “Micro-Hydration, Pore Connectivity, and Durability of Cementitious Materials,”Second International Conference on Microstructural Durability of Cementitious Composites, Amsterdam, the Netherlands, 2012

105)Anzalone G., BubbleCounter, Michigan Tech's Open Sustainability Technology Lab, https://github.com/mtu-most/bubblecounter

106)Ley M.T., Frazier R.M., and Tabb B.M., “System And Method For Rapid Measurement of The Air Void Distribution Of Fresh Concrete,” United States Patent Application Publication Us 2014/0096593 A1, April 10, 2014

107)ASTM C231 / C231M-14, *Standard Test Method for Air Content of Freshly Mixed Concrete by the Pressure Method*, ASTM International, West Conshohocken, PA, 2014

108)ASTM C173 / C173M-14, *Standard Test Method for Air Content of Freshly Mixed Concrete by the Volumetric Method*, ASTM International, West Conshohocken, PA, 2014

109)ASTM C138 / C138M-14, *Standard Test Method for Density (Unit Weight), Yield, and Air Content (Gravimetric) of Concrete*, ASTM International, West Conshohocken, PA, 2014

110)Sprinkel, M.M., Lee, B., "The Chace Air Indicator," Virginaia Highway & Transportation Research Concil, VHTRC 81-R37, 1981

111)AASHTO T199-00, *Standard Method of Test for Air Content of Freshly Mixed Concrete by the Chace Indicator*, American Association of State Highway and Transportation Official, 2011

112)Ansari F., “Fiber-Optic Airmeter,” *SHRP-C-677*, Strategic Highway Research Program, National Research Council, Washington, DC 1994

113) Wu. X., and Chahine, G.L., “Development of an acoustic instrument for bubble size distribution measurement,” Journal of Hydrodynamics, Ser. B, Volume 22, Issue 5, Supplement 1, October 2010, pp. 330-336

114) Hackley, A.V., Lum, L., and Ferraris, C.F., "Acoustic Sensing of Hydrating Cement Suspensions: An Exploratory Study," NIST Technical Note 1492, National Institue of Standards and Technology, 2007

115) Coperland, L.E., Hayes, J.C., “Determination of non-evaporable water in hardened Portland-cement paste,” ASTM Bulletin, Vol.194, 1953, pp.70-74

116) Thomas, J.J., Jennings, HM., and Allen, A.J., “The surface area of cement paste as measured by neutron scattering: Evidence for two C-S-H morphologies,” Cement And Concrete Research, 28(6), 1998, pp. 897-905

117) Day, R.L., Marsh, B.K., “Measurement of porosity in blended cement pastes,” *Cement and Concrete Research*, Vol.16, No. 1, 1986, pp.71-78

118) Lamond, J.F., Pielert, J.H., Significance of Tests and Properties of Concrete and Concrete-Making Materials, ASTM International, 2006

119) Hanson, T.D., "Evaluation of the RapidAir 457 Air Void Analyzer," Final Report for MLR-12-01, 2012

120) Jakobsen U.H., Pade C., Thaulow N., Brown D., Sahu S., Magnusson O., De Buck S., and De Schutter G., “Automated air void analysis of hardened concrete — a Round Robin study,” *Cement and Concrete Research*, Volume 36, Issue 8, August 2006, pp. 1444-1452

121) Dewey, G.R., and Darwin D, “Image Analysis of Air Voids in Air-Entrained Concrete,” Structural Engineering and Engineering Materials SM Report No. 29, University of Kansas Center for Research, August 1991

122) Chatterji, S., and Gudmundsson, H., "Characterization of Entrained Air Bubble Systems in Concrete by Means of an Image Analyzing Microscope," *Cement and Concrete Research*, Vol. 7., No. 4, 1977, pp. 423-428

123) Kaneuji, M., Winslow, D.N., and Dolch, W.L., “The relationship between aggregate pore size distribution and its freeze-thaw durability in concrete,” *Cement and Concrete Research*, 10(3), 433-441, 1978

124)Feldman, R.F., “Application of Helium inflow Technique for Measuring Surface Area and Hydraulic Radius of Hydrated Portland Cement,” Cement and Concrete Research, 10(5), 1980, pp. 657-664

125)Valckenborg, R.M.E., Pel, L., Hazrati, K., Kopinga, K., and Marchand, J., “Pore water distribution in mortar during drying as determined by NMR,” Materials and Structures, 34(244), 2001, pp. 599-604

126)Tasong, W.A., Cripps, J.C., and Lynsdale, C.J. “Aggregate-Cement Chemical Interactions”, Cement and Concrete Research,” Vol. 28, 1998, pp. 1037-1048

127)Scrivener, K., Pratt, P.L. “Characterisation of interfacial microstructure,” In RILEM TC 108 State of the Art Report, 1994, pp. 1-16

128)Escadeillas, G., Maso, J.C., *In Advances in Cementitious Materials*. Mindess. S., Ed., 1991, pp 169-184

129)Chatterji, S., Jensen, A. D., "Formation and Development of Interfacial Zones Between Aggregates and Portland Cement Pastes in Cement-Based Materials," *Interfaces in Cementitious Composites*, Proceedings of the RILEM International Conference, October, 1992, pp. 3-12

130)Hover, K. C., “Some Recent Problems with Air Entrained Concrete,” Cement, Concrete, and Aggregates, Vol. 11, No. 1, 1989, pp. 67–72

131)Mehta, P.K., Monteriro, P.J.M., *Concrete, Microstructure, Properties, and Materials*, Fourth Edition, Mc Graw Hill Education, 2014

132)Ollivier, J.P, Maso, J.C., Bounrdette, B., “Interfacial Transition Zone in Concrete,” Advn Cem Bas Mat, 1995

133)Yuan, C.Z., Odler, I., “The Interracial Zone between Marble and Tricalcium Silicate Paste, “Cen & Concr. Res 17, 1987, pp. 784-792

134)Riding, K.A., Esmaeily, A., and Vosahlik J., “Air Void Clustering, Air void Clustering,” K-TRAN:KSU-13-6, Kansas Department of Transpiration, 2015

135)Kozikowski, R. L., Jr., Vollmer, D.B., Taylor, P.C., and Gebler, S.H., "Factors affecting the origin of air-void clustering," PCA R&D Serial No. 2789, Skokie, IL: Portland Cement Association, 2005

136)Rao C., Titus-Glover, L., Bhattachary, B., Darter, M.I., Stanley, M., and Von Quintus, H.L., "Estimation of Key PCC,Base, Subbase, and Pavement Engineering Properties from Routine Tests and Physical Characteristics," FHWA-HRT-12-030, 2012

137)Guinea, G.V., El-Sayed, K., Rocco, C.G., Elices, M., Planas, J., "The effect of the bond between the matrix and the aggregates on the cracking mechanism and fracture parameters of concrete," *Cement and Concrete Research* 32, 2002, pp. 1961-1970

138)Havlasek, I.P., "Creep and Shrinkage of Concrete subjected to Variable Environmental Conditions," Doctoral Thesis, 2014

139)Weiss, J., "Elastic Properties, Creep, and Relaxation," *Significance of Tests and Properties of Concrete and Concrete-Making Materials*, ASTM International, 2006

140)Mullen, W. G. and Dolch, W. L., "Creep of Portland Cement Paste," Proceedings, Vol. 64, 1964, pp. 1146–1171

141)Bazant, Z.P., Hauggaard, A.B., Baweja, S., and Ulm, F., "Microprestress-Solidification theory for Concrete Creep. I: Aging and Drying Effects," *Journal of Engineering Mechanics*, 1997

142)Feldman, R. F., and Sereda, P. J., "A model for hydrated Portland cement paste as deduced from sorption-length change and mechanical properties," Mat. and Struct., Paris, France, I, 1968, pp.509-520

143)Coussy, O.P., Brisard, S., "Prediction of Drying Shrinkage beyong the pore is isodeformation assumption," *Journal of Mechanics of Materials and structures*, Vol.4, No.2, 2009

144)Goodwin, F., "Volume change, *Significance of Tests and Properties of Concrete and Concrete-Making Materials*," ASTM International, 2006

145)Bissonnette, B., Marchand, J., Charron, J. P., Delagrave, A., and Barcelo, L., "Early Age Behavior of Cement-Based Materials," *Materials Science of Concrete VI*, American Ceramic Society, Westerville, OH, 2002, pp. 243–262

146)Hua, C., Ehrlacher, A., and Acker, P., “Retrait d’Autodessiccation du Ciment: Analyse et Modelisation,” Bulletin Liaison Laboratoire des Ponts et Chaussees, Vol. 196, 1999, pp. 35–41

147)Takashi, T., Nakata, H., Yoshida, K., and Goto, S., “Autogeneous Shrinkage of Cement Paste During Hydration,” Proceedings of the 10th International Congress on the Chemistry of Cement, Gothenburg, Sweden, Vol. II, Paper 2ii070, 1997

148)Hua, C., Acker, P., and Ehrlacher, A., “Analyses and models of the autogenous shrinkage of hardening cement paste (II Modeling at scale of hydrating grains),” *Cement Concrete Res*, 1997, pp.245–58

149)Li, Y., Bao, J., and Guo, Y., “The Relationship between Autogenous Shrinkage and Pore Structure of Cement Paste with Mineral Admixtures,” Construction and Building Materials, Vol: 24, 2010, pp. 1855-186

CHAPTER 3. A MODIFIED FOAM DRAINAGE TEST PROTOCOL FOR ASSESSING INCOMPATIBILITY OF ADMIXTURE COMBINATIONS AND STABILITY OF AIR STRUCTURE IN CEMENTITIOUS SYSTEMS

Xin Wang[1], Xuhao Wang[2], Seyedhamed Sadati[3], Peter Taylor[4], Kejin Wang[5]

1. Ph.D. candidate, Civil, Construction and Environmental Engineering, Town Engineering Building, Iowa State University, Ames, Iowa, 50014, U.S.A
2. Associate Professor, School of Highway Chang'an University, Xi'an, China; Associate Research Scientist, Qinghai University-Tsinghua University Sanjiangyuan University Sanjiangyuan Research Institute, Qinghai University, Xinning, China
3. Postdoctoral Research Associate, Concrete Pavement Technology Center, Iowa State University, Ames, Iowa, 50014, U.S.A.
4. Director, National Concrete Pavement Technology Center, Ames, Iowa, 50014, U.S.A
5. Professor, Civil, Construction and Environmental Engineering , Town Engineering Building, Iowa State University, Ames, Iowa, 50014, U.S.A

Corresponding should be address to Xin Wang: xin@iastate.edu

Abstract

Unexpected interactions between chemical admixtures and other ingredients in a cementitious systems may occur as cementitious systems become more complex and demands on the systems are more rigorous. Incidents related to use of chemical admixtures in highway concrete have been reported in some states. A common problem was instability of the air void system with air contents changing significantly during handling and placing. The stability of an entrained air void system in fresh concrete can have a profound influence on the potential durability such as freeze / thaw resistance.

A technique known as the foam drainage test has been in use to assess the potential stability of air void system in fresh paste samples in the laboratory. However, there has been little reported work on the correlation between the test results and air void system in hardened

concrete. In addition, the method, as published, is not rigorous with respect to some factors such as test temperature, and there is no pass/fail limit to evaluate testing results.

The work presented here sought to evaluate the effects of variables such as environmental conditions, testing procedures, and admixture dosages on the data obtained. Multiple cementitious combinations with various chemical admixtures, such as air entraining and water reducing agents, were used to propose a pass/fail limit for admixture combinations. In addition, selected combinations were used to prepare concrete specimens and the air void system was evaluated after handling activities were mimicked in the lab.

Keywords: Incompatibility - Stability—Air Void System—Admixtures—Foam Drainage Test

Highlights

- Evaluated effects of testing variables on foam drainage test
- Proposed modifications to the foam drainage test with more specific details and data analysis methods
- Proposed a pass/fail limit for foam drainage test results
- Found a good correlation between results from modified foam drainage test and air void system stability in concrete mixtures

3.1. Introduction

It is well established that an adequate air void system is essential for concrete durability in a freeze-thaw (F-T) environment. Concrete with a proper air void system is better able to resist the action of freezing and thawing cycles, particularly in wet climates. Over the years researchers

have made efforts to test and evaluate characteristics of the air void system, generally focusing on the total air volume and the spacing factor. Total air content is defined as the ratio of total volume of air voids to the bulk volume of concrete, including all the constituents of concrete (1) . Kosmatka and Wilson (2) reported that for concrete with ¾-in. maximum size aggregate, air content needs to be about 6% for effective freeze-thaw resistance. Spacing factor is a parameter related to maximum distance in the cement paste from the edge of an air void, and should be less than about 0.20 mm to ensure a good F-T durability (3)

Besides spacing factor and total amount of air voids, the stability of the air void system is also critical to concrete durability because it is the air-void system in the final position that matters. Air content of a fresh concrete mixture is normally measured before concrete is placed into its final position and consolidated, which is acceptable if the air void system is generally stable. However, changes in chemistry of the paste system and admixtures have been leading to reported variability in the concrete during handling. There is no standard definition for air void system stability. Researchers have attempted to study stability by tracking air void characteristics up to 2 hours after mixing (4)(5). In the field, concrete measured to contain 5 to 6% air at the truck has been observed to contain anywhere between 3 and 13% in situ, leading to potential poor F-T durability or loss of strength, respectively (6). Compositions of concrete and compatibility of the ingredients can determine both characteristics of air void system and stability of the system. Taylor et al. (7) evaluated this compatibility issue using a method called foam drainage method (8).

Air entraining admixtures (AEA) are used to stabilize small air bubbles in concrete (2). During concrete mixing, air layers are trapped between the folding surfaces of paste. Normally the bubbles will coalesce and float out of the mixture during mixing without AEA (9). There are

two functions of AEA during concrete mixing. One is to stabilize small bubbles and prevent them from coalescing with others, by means of the adsorbed chemical on the surface of the bubble. The adsorbed molecules are oriented with their polar heads in the water setting up a charge on the outside of the bubble that causes electrostatic repulsion between bubbles (10) (5). The other action is the creation of a layer of hydration products around the bubbles, that can also serve as a stabilizer and separate bubbles.

As for other admixtures, certain combinations of water reducing agent (WRA) and air entraining agent can be incompatible and create a non-stable air void system. Plante et al. (4) indicated that increasing the dosage of water reducer will impact the air system. Taylor reported these incompatible combinations in different papers (6) (7). In multiple publications Klieger called attention to the effect of supplementary cementitious materials (SCMs) on air entrainment (11) (12). Some high-range water reducers (HRWR) may alter the air void system, and concrete with such products may have higher spacing factors. Polycarboxylate-based water reducing agents have been reported to affect air-entrainment (6) (13) (14).

3.2. Theory of foam drainage test and current knowledge

In 2000, Cross et al. (8) reviewed a simple test method from to measure the potential stability of entrained air bubbles in a paste called the foam drainage test. The foam drainage test comprises preparing a mixture of paste ingredients, and agitating in a blender to create 1,000 mL of foam. This foam is poured into a graduated cylinder, and the rate at which fluid collects at the bottom of the cylinder is then monitored over 60 minutes. The volume of fluid (V_d) is plotted against the inverse of time (1/t). The data are modeled to estimate the needs an adjective here volume (V_0) of fluid collected (Equation 1). This equation was proposed as an exponential kinetic function for final drainage stage for gravitational foam drainage (opposed to high

pressure drop foam drainage). Decreasing V_0 indicates systems that may be considered more stable and less likely to collapse in the field.

$$V_d = V_0 - 1/(k \times t) \quad \text{Equation 1}$$

Where

V_d = Volume of water at time t

V_0 = estimated initial liquid volume in the foam at t=0 (before drainage started)

t = time

k = slope of the V_d vs 1/t plot

Multiple researchers have attempted to use the foam drainage test to evaluate the stability of air void systems. Findings of these projects are listed in Table 1. It can be seen that little research has been focused on finding a correlation between foam drainage test results and stability of concrete air void system. There has been some work to identify whether paste systems are stable or unstable. However, the stability of air void system in concrete is quite different, therefore it is desirable to understand the relationship between V_0 in paste and air void system stability in concrete.

Although a method was described by Taylor et al. (7), there are some critical testing parameters that need to be specified, including temperature of water, mixing speed, and dosage of admixtures, because it is possible that these parameters may affect the foam drainage rate. High temperatures will make it difficult to entrain air into concrete, and evaporating moisture may affect the stability of the system. Speed of blending will determine the potential energy in the mixture and so may affect both stability and the volume of foam produced. Each type of

AEA has its own recommended dosage, meaning that the concentration of these AEAs are different, so testing properties of AEA at a fixed dosage is not representative. To validate these testing conditions, various temperatures, admixture dosages, mixing speed and testing duration were assessed in a sensitivity study of this method.

The work presented here sought to evaluate the effects of variables such as environmental conditions, testing procedures, and admixture dosages on the data obtained. Multiple cementitious combinations with various chemical admixtures, such as air entraining and water reducing agents, were used. In addition, selected combinations were used to prepare concrete specimens and the air void system was evaluated after field handing activities were mimicked in the lab.

3.3. Materials and methods

This research was conducted in three steps. The objective of Step I was to investigate and select parameters that should be controlled to reduce variability of the test method. Step II used the modified method to select suitable admixture combinations for Step III concrete mixtures. In Step III, two admixture combinations selected from Step II were used in concrete mixtures with four types of cement. Both fresh and hardened air void systems of these concrete mixtures were tested.

3.3.1. Step I: modification of foam drainage test method

Test conditions were varied in a controlled program to assess the properties that need to be controlled to reduce variability of the method. The parameters adjusted included: temperature of the liquid, admixture dosage, rotation speed and spin durations. Each test condition was tested using the draft test method (7) with one condition modified at a time.

Table 3.1. **Previous research on foam drainage test**

Author	Year	Method	Findings
Bruere (16)	1950s	Evaluate stability of foams generated by multiple AEA using cylindrical flotation test	-
Gutmann (15)	1988	Tested 10 admixtures mixing with water using kitchen blender, poured the produced foam into a graduated cylinder and measure the water drained (%) and bubble density. Only use admixtures and water, no cement/SCMs	Bubble wall structure could produce a more stable air system
Cross et al. (8)	2000	Standardized the test by using 300 ml (10oz) of water and 10 ml (0.3 oz) of AEA and 5 g (0.18) oz of cement, creating a 1000 ml foam and poured into a 1000 ml graduated cylinder. Use equation kinetic equation for data analysis. Mix cement with water and AEA	The thickness of bubble wall was greater for vinsol resin based AEA
Taylor et al. (7)	2006	Tested 50 combinations of 10 admixtures with water, cement, and fly ash (Class F and Class C) using foam drainage test in 60 minutes	Results from AEA+water could be different with the same AEA mixing with water and cementitious materials. Lower drainage rate indicates a more stable air void system. Little correlation between foam drainage test and fresh air content or hardened air void system
Nagi et al.(5)	2007	Tested various chemical based AEA using foam drainage test, and also tested pH, specific gravity, solid content of sample solution	Foam drainage test can be used as a screen/ selection process to select suitable admixtures
Taylor et al. (6)	2016	Tested various combination of AEA and WRA using foam drainage test, then select two combination to mix concrete to evaluate the correlation between result from foam drainage test and concrete air void system stability	Foam drainage test has the potential to evaluate stability of AEA and WRA combination, and it is possible to use foam drainage to evaluate the stability of concrete air void system using foam drainage test

Cement used in this Step was Type I low alkali cement (Table 2). Two admixture combinations were used: AEA 1+WRA 1 and AEA5+WRA3 (Table 3). Unless stated otherwise, dosage of admixtures followed the draft test method (i.e. 300 ml of fluid (water and 50 ml of chemical admixtures if necessary), 10 ml air-entraining admixture, and 5-gram cementitious materials.

The base-line version of the test procedure was:

- Water, admixtures, and cementitious materials (if any) were added to the blender
- Turned the blender on at a medium setting for 10 s.
- Immediately filled a 1,000 ml graduated cylinder with foam
- Recorded the volume of fluid at the bottom of the cylinder as function of time, for up to 60 min.

Testing conditions were varied to determine their influence results. Conditions included: liquid temperature (10°C, 21°C, 32°C), admixture dosage (recommended dosage from the draft test method, manufacture recommended dosage (median), manufacture recommended dosage (high), rotation speed (2000, 3000, 5000 RPM), and spin duration (10, 30, 60s).

3.3.2. Step II: data analysis and limits

Based on the findings of the work in Step 1, a modified procedure was adopted. Using this modified method, Step II was conducted to develop a method to analyze the test data, . Moreover, Step II was also aimed at proposing pass /fail limits. To achieve these objectives, 60 combinations of different cement, AEA, and WRA were tested.

Four types of cement were mixed with the admixture combinations, Type I low alkali, Type I high alkali, Type I high C_3A, and Type III cement. The chemical analysis of each cement is presented in Table 2. Five types of AEA with various chemical bases were used as shown in Table 3. Three polycarboxylate based water reducing agents (WRA) were used. Dosages of each admixture were selected based on the average of high and low limits of recommended dosages provided by the manufacturers (Table 4).

Table 3.2. **Chemical analysis of cements**

Description	Unit	Type I	High C_3A (HCA)	High Alkali	Type III
SiO_2	%	20.1	19.8	18.8	21.3
Al_2O_3	%	4.4	4.9	5.2	3.9
Fe_2O_3	%	3.1	2.4	2.1	3.6
CaO	%	64.3	63.4	62.0	63.9
MgO	%	3.4	2.8	3.2	1.9
SO_3	%	2.8	30.0	4.1	2.8
LOI	%	2.8	2.6	2.7	1.3
Na_2O	%	0.1	0.0	1.0	0.4
K_2O	%	0.6	0.7		-
CO_2	%	1.9	1.5	1.3	1.4
Limestone	%	-	3.7	3.0	-

Table 3.3. **Chemical composition and physical properties for admixtures**

No. of admixtures	Chemical base	pH-Value	Density g/ml
AEA			
1	Aqueous soap	8.0 (20° C)	1.00
2	Vinsol-Rosin	11.5-13.5 (25° C)	1.03
3	Rosin	10.0 (20° C)	1.00
4	Vinsol+Amine+Fatty acid	11.0 (20° C)	1.00
5	Fatty Acid Salts	10.7-12.3 (25° C)	1.01
WRA			
1	polycarboxylate	4.0 (20° C)	1.00
2	polycarboxylate	4.6 (22° C)	1.05
3	polycarboxylate	6.0 (temperature not specified)	1.07

Table 3.4. **Dosage selection for AEA**

AEA #	Low limit ml/100 kg cement (Manufacturer recommended)	High limit ml/100 kg cement (Manufacturer recommended)	Median ml/100 kg cement
1	25	62	43
2	2	25	13
3	3	19	11
4	2	19	10
5	1	9	5
WRA #	Low ml/100 kg cement	High ml/100 kg cement	Median ml/100 kg cement
1	12	61	36
2	12	121	67
3	12	91	52

*Assuming 335 kg/m3

Following is the modified foam drainage procedure used in this step:

- Water at room temperature (21°C)
- Admixtures used at median of manufacturer recommendation
- Materials were added to the blender
- Turned the blender on at a 3000 RPM for 10 s.
- Immediately poured the resulting foam (must be at least 1000 ml of foam) into a 1,000 ml graduated cylinder
- Recorded the volume of fluid at the bottom of the cylinder as function of time, for up to 60 min

3.3.3. Step III: analysis of stability and compatibility on concrete samples

Based on the results from Step II, two combinations of admixtures were selected for each type of cement. One combination was considered stable and the other was unstable. Eight concrete mixtures were cast to investigate the correlation between results from modified foam drainage test and concrete mixture performance.

For Step III concrete mixtures, coarse aggregate was 25.4-mm crushed limestone with 0.29% absorption and specific gravity (SpG) of 2.68. Fine aggregate was river sand with 2.2% absorption and SPG of 2.65. The cements used in Step II were also used in Step III (Table 2). Each mix used different chemical admixture combinations selected from Step I.

Compatible and Incompatible admixture combinations were selected from Step II, and mixed with each of the cements (Table 5). Two concrete mixtures from each type of cement were cast using the proportions in Table 6. Eight mixtures were cast in total. A high target air

content and slump were selected to investigate the air and slump loss during handling and mixing.

Table 3.5. **Selected admixture combination for each type of cement**

Cement Type	Admixture Combinations	
	Compatible (Stable)	Incompatible (Unstable)
Type I	AEA2+WRA1	AEA4+WRA3
Type III	AEA1+WRA1	AEA2+WRA2
High C_3A	AEA2+WRA1	AEA4+WRA3
High Alkali	AEA2+WRA1	AEA4+WRA2

Table 3.6. **Mix proportions for concrete mixtures**

Mix proportions	Type	Source	Amount kg/m^3
Cement	-	-	335
Coarse Aggregate	Iowa DOT D57 25.4 mm. crushed limestone		1023
Fine Aggregate	River sand		837
Water	141 kg/m^3		
w/c ratio	0.42		
Target Air (initial)	6%		
Target Slump (initial)	13 to 18 cm		

Test methods included:

- Air content of fresh concrete was determined by pressure method (ASTM 231) (17). Air loss was tracked using pressure method at 0, 30 (30 min.) and 60 minutes (with 1 minute vibration using vibration table) after mixing.
- Hardened air void system characteristics were determined by ASTM C 457 (18) linear traverse method using Rapid Air

3.4. Results and discussion

3.4.1. Step I: modification of foam drainage test method

The admixtures tested in this step were selected to be stable or unstable based on previous work by the authors (6) Combination with V_0<100 ml is considered compatible, andcombination with V_0>300 ml is considered incompatible.

3.4.1.1. Effect of temperature on foam ability

Fixed parameters were:

- Admixture dosage recommended by draft method (Taylor et al. 2006) (250 ml water, 50 ml WRA, 10 ml AEA, 5g cement).
- 3000 rpm rotation speed.
- Two admixture combinations - AEA1+WRA1 (compatible) and AEA5+WRA3 (incompatible). Compatibility was assessed by earlier testing of the products available in the laboratory. Compatibility was defined as a system that did not exhibit excessive foam decay over time.

Each system was tested at three different temperatures; 10, 21 and 32 °C. Temperature was adjusted by controlling the temperature of the mix water. The results are illustrated in Figure 1.

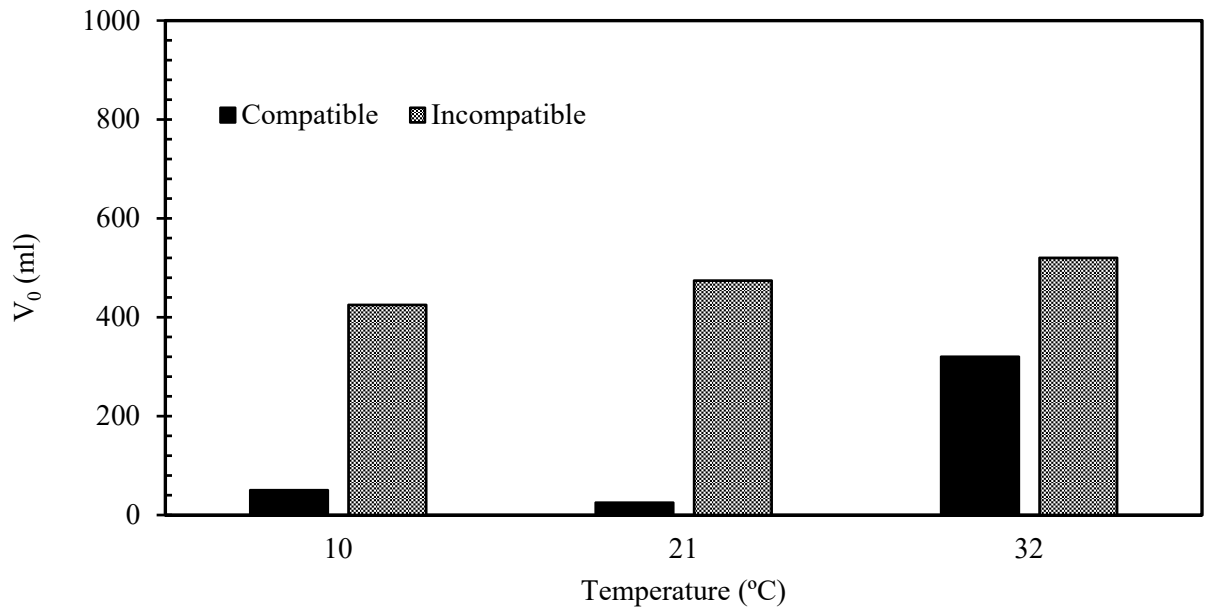

Figure 3.1. Relationship of stability of paste-admixture system and mixing temperature

It can be observed that for both systems, that increasing temperature generally decreased the stability of the foam, more markedly for the nominally compatible admixture combination. This suggests that a system that appears to be stable in the laboratory, may be unstable on a hot day in the field. This result is consistent with Miles et al (19) who reported that flow rate of liquid foam decreases as temperature drops, which will decrease rate of foam drainage. A Possible explanation for this could be that reactivity of admixtures would increase with increasing temperature. For this paper, testing temperature is recommended to be 21°C, while low temperature and high temperature testing would be recommended if construction conditions warrant it.

3.4.1.2. AEA dosage

Five AEA admixtures with three dosages were investigated:

- Foam drainage method dosage: 10 ml air-entraining admixture with 300 ml of fluid (50 ml of admixture if necessary) and 5 g cementitious material
- Recommended dosage range to simulate a the median of manufacturer recommended dosages)
- High dosage to simulate a high dosage application (Maximum of manufacturer recommended dosage)

Each mixture was prepared with type I cement, compatible WRA, and 21°C distilled water at 3000 RPM. Test results are presented in Figure 2.

The results show that the stability of the mixtures is sensitive to admixture dosage. It is noted that the highest V_0 is obeserved at the mid-point dosage for most of the systems tested. The dosages recommended by manufacture of AEAs are also different from each other, depending on the concentration. Using the same dosage (10 ml) as required in the current foam drainage method is not representative for most of AEAs, therefore the mid-point of the manufacturer recommended dosage was selected for the modified method.

3.4.1.3. Mixing speed and time

The speed of a kitchen blender varies from 1600 to 28500 RPM depending on the manufacturer and model. Three speeds were selected that can be achieved by most blenders, 2000, 3000, and 5000 RPM. Time of mixing was also considered since this would also affect the

potential energy in the foam created. Testing durations of 10s, 30s, and 60s were selected at 3000 RPM. Values of V_0 for all scenarios are shown in Figure 3.

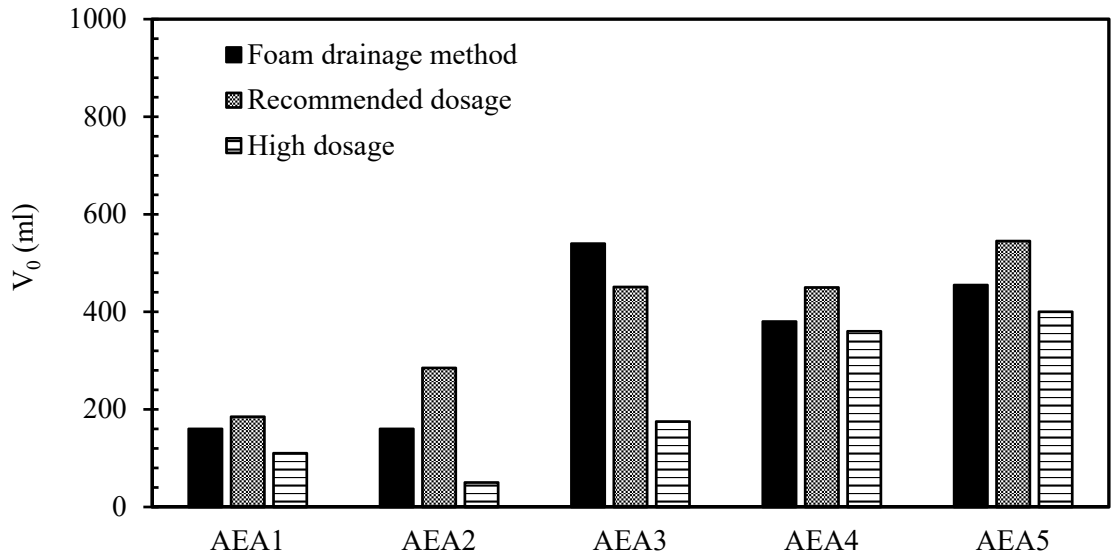

Figure 3.2. Stability of foam with AEA dosage

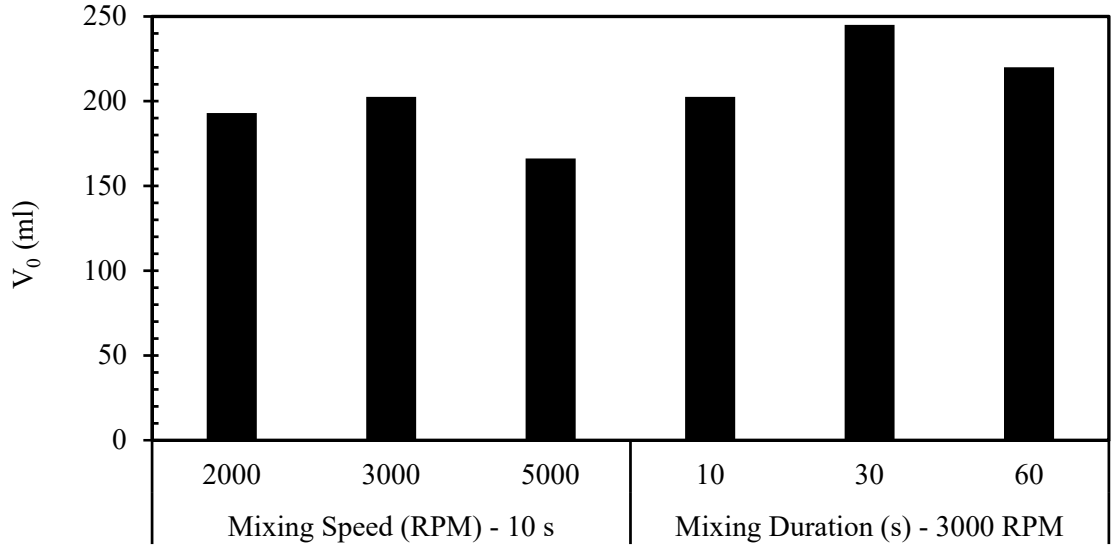

Figure 3.3. V_0 by various speed (RPM) and duration (seconds)

The greatest sensitivity was observed to be at 3000 PRM for 30 seconds, which are recommended for adoption as requirements in the test method.

Table 3.7. **Test conditions for foam drainage test and modified foam drainage test**

Parameter	Foam Drainage method	Modified Foam Drainage method
Temperature of water	Unspecified	21°C
Dosage	10 ml for 300 ml of liquid (50 ml WRA if necessary), 5 g cementitious material	Average of recommended dosages for AEA and WRA, 300 ml water, 5 g cementitious material
Speed	Unspecified	3000 RPM
Test duration	10 s	30s

3.4.2. Step II data analysis and limits

When Cross et al. (8) proposed the foam drainage test, both V_0 and slope -1/k were reported as outputs. Researchers have used either -1/ k or V_0 as an indicator of the stability of mixtures, but have never used both. Taylor et al. (7) compared slope, V_0, and percentage of foam drained to evaluate the relative stability of different admixture combinations and other mixture variables. Such an approach is only valid for a large test matrix. It is necessary to set a limit based on test data to determine the stability of a paste system.

In previous work, the authors had noted that foam drainage rates of certain paste combination are not represented by either V_0 or -1/k. In order to address this concern, 60 foam drainage tests were conducted to investigate appropriate limits for a suitable test output.

For example, in AEA4+WRA3 with Type I cement, most of the bubbles disappeared within the first 5 minutes, and the level of liquid stayed the same for the rest of test, since there was no foam left to drain. In comparison, AEA3+WRA2 with drained constantly over the test period and yet yielded a similar V_0. Results of these two tests are presented in Figure 4. It can be seen that V_0 from both combination are high, but it is not possible to detect the rapid drainage/collapse of bubbles observed during test of AEA4+WRA3.

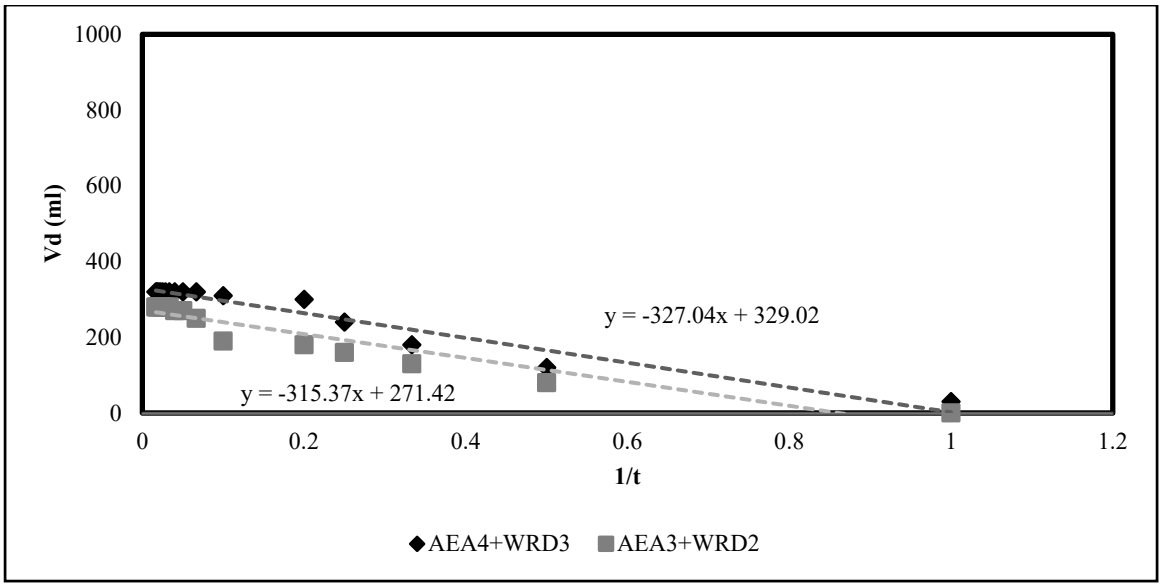

Figure 3.4. Selected results of V vs. 1/t

The same two combinations are presented in Figure 5 using V vs. √t, where V is liquid in the cylinder (ml), and t is testing time. S5 min is the slope of V vs. √t for the first 5 minutes. S5 from AEA4+WRA3 is clearly higher than AEA3+WRA2, which is consistent with the observed behavior.

In plotting data from the 60 combinations as V vs. $\sqrt{t}$ for the different types of AEA in Figure 6, it was found that there is a pattern for each type of AEA, and most of combinations would follow the same pattern regardless WRA or cement type. The changes usually happen in the first 5 minutes ($\sqrt{t}$ = 2.23), especially for those AEA with a less linear pattern for Vd vs $\sqrt{t}$. Another new parameter introduced in these figures is V60, the final liquid volume in test cylinder, which is the last reading of the test. S5 is a useful factor to indicate foam drainage rate in the first 5 minues, but in some cases longer observation is required to determine the compatibility of the tested system, hence there is a necessity to use V60 to indicate later age performance

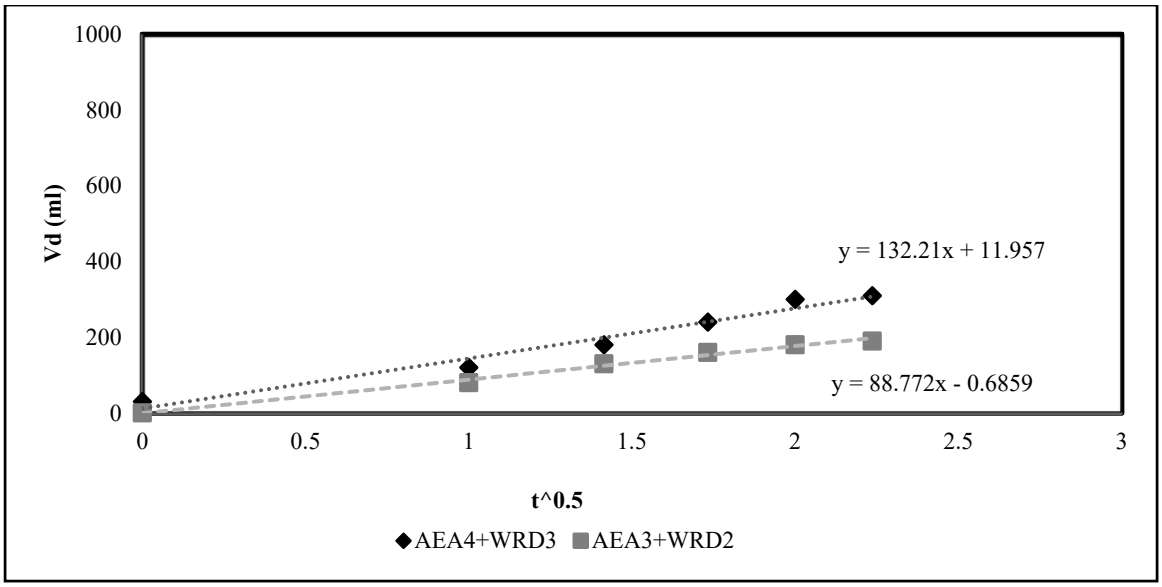

Figure 3.5. Selected results of V_0 vs. $\sqrt{t}$

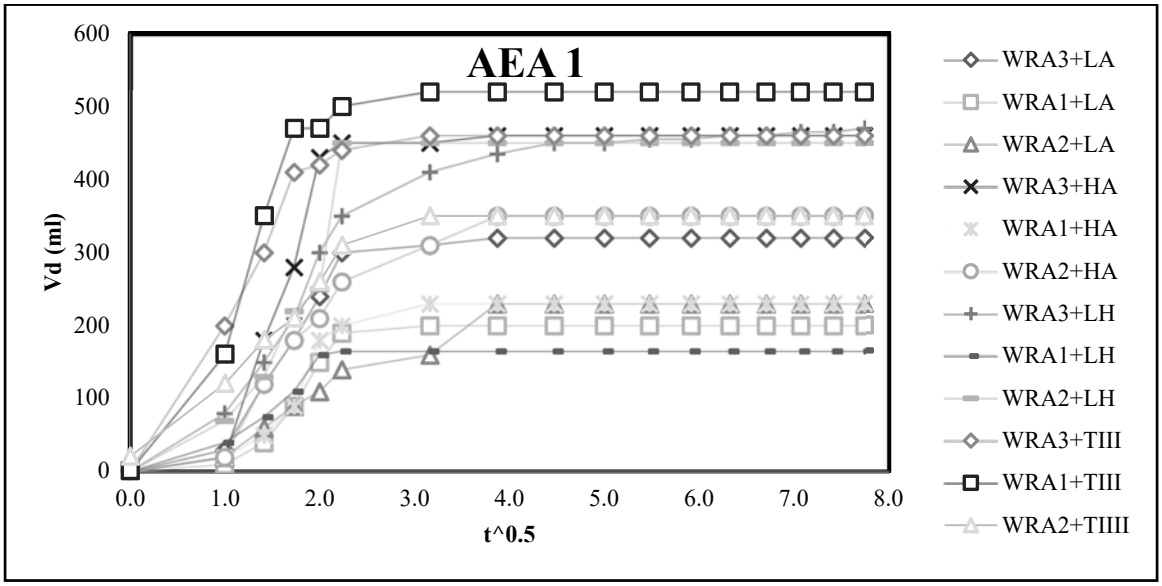

Figure 3.6. Liquid drained (Vd) vs $\sqrt{t}$ for AEA1

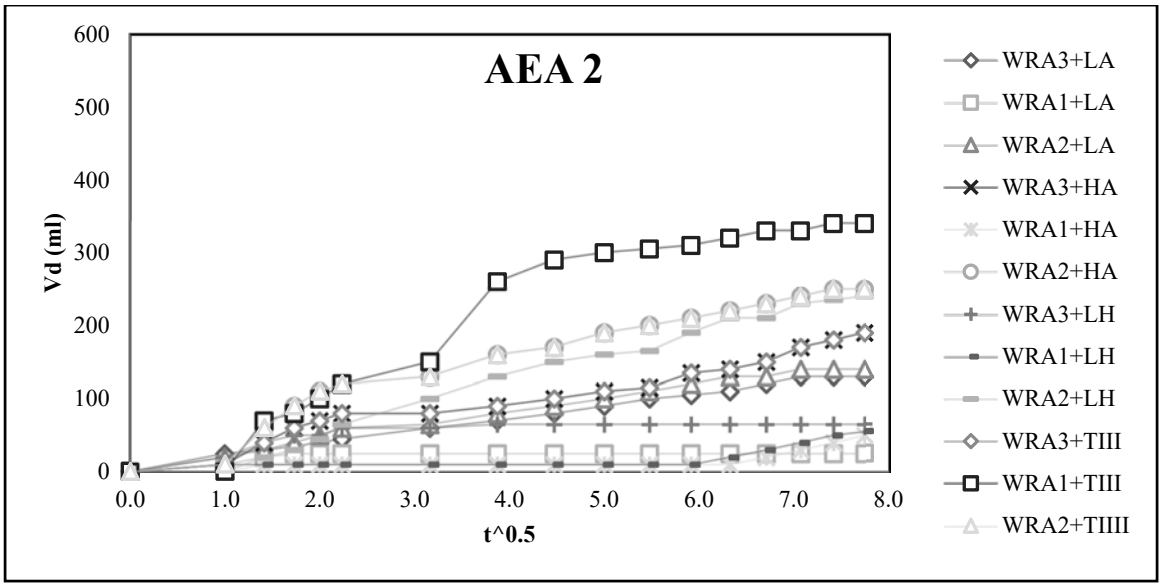

Figure 3.7. Liquid drained (Vd) vs $\sqrt{t}$ for AEA2

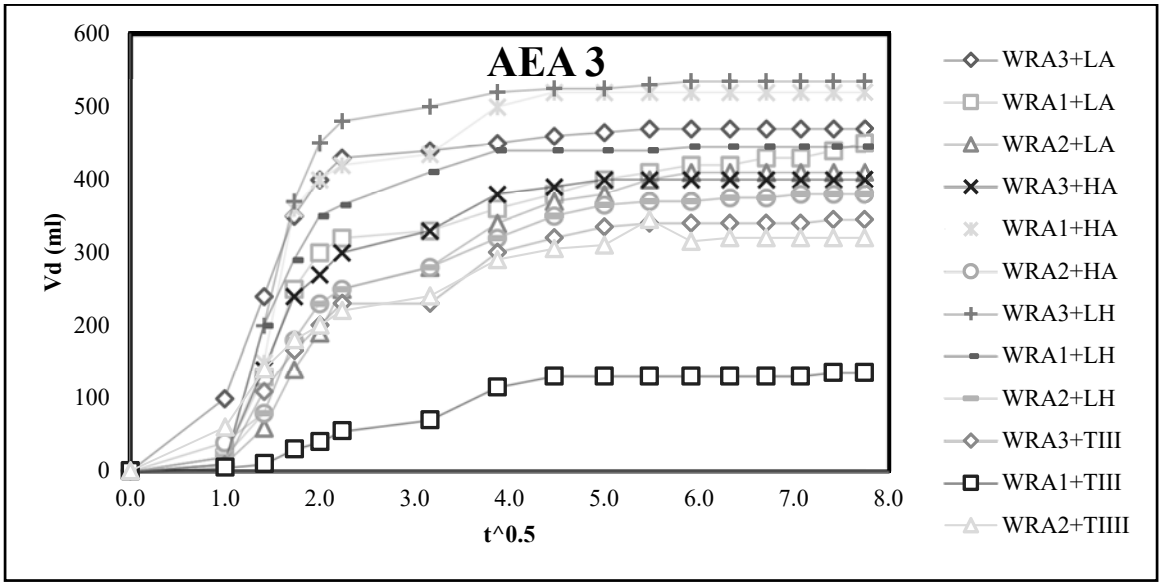

Figure 3.8. Liquid drained (Vd) vs $\sqrt{t}$ for AEA3

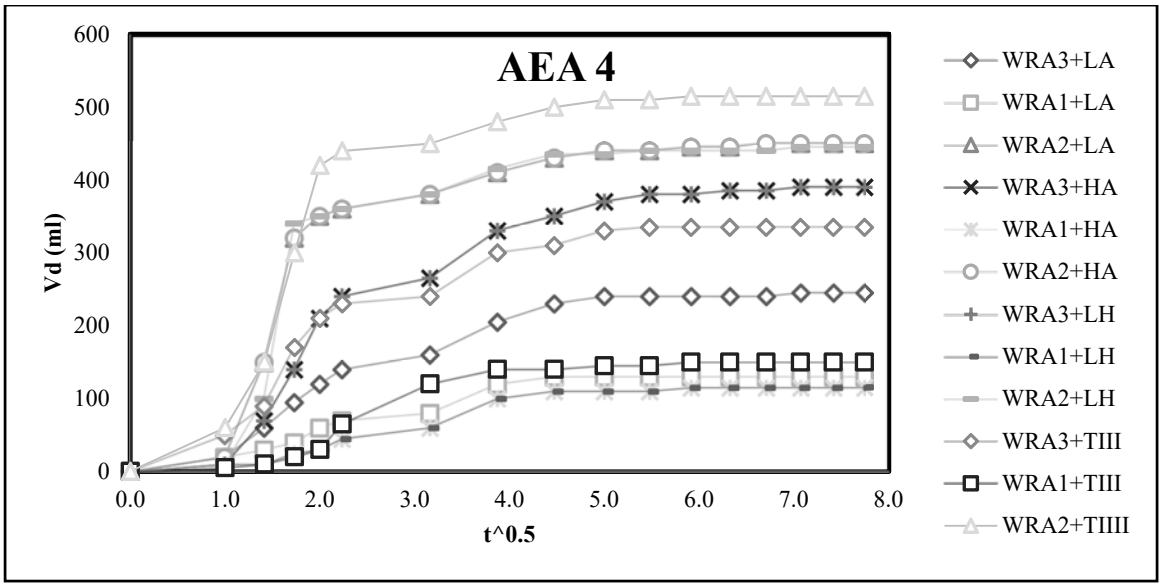

Figure 3.9. Liquid drained (Vd) vs $\sqrt{t}$ for AEA4

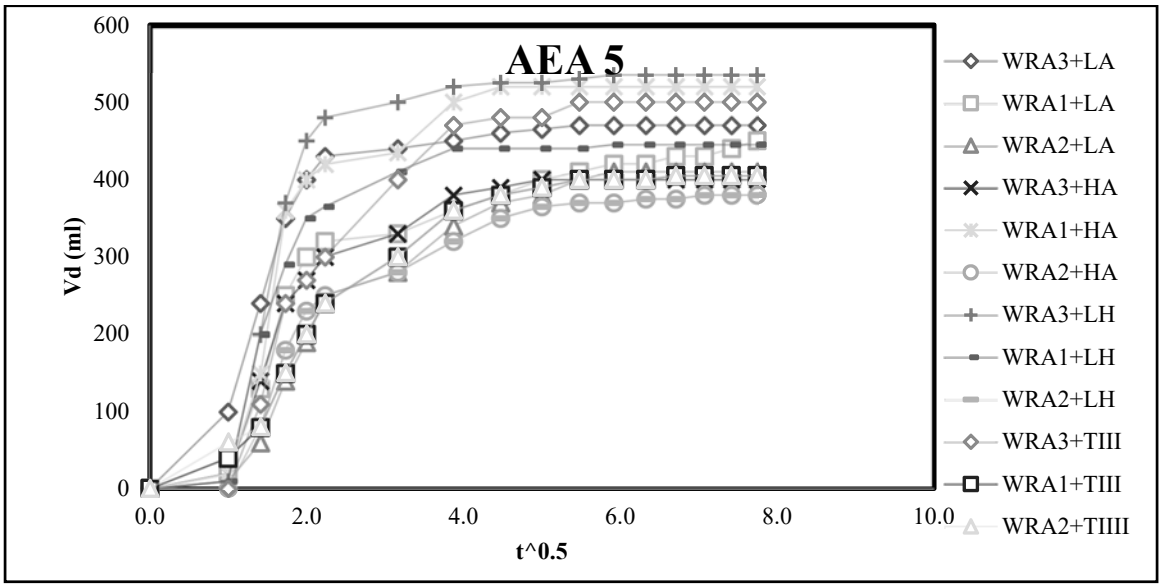

Figure 3.10. Liquid drained (Vd) vs $\sqrt{t}$ for AEA5

Two patterns can be found in Figure 6. In Figure 6 AEA 2, foam drainage rate for most of combinations tend to be linear. On the other hand, for many other combinations, including all of those for AE5 there is a change of slope at approximately $\sqrt{t}$ = 2.2 (i.e. t = 5).

Observation of the plots, in light of the preveious work that indicated that AEA 2 was generally stable and AEA 5 was generally unstable, shows that selecting a single pass / fail limit

based on only the slope of the line or the maximum volume of fluid drained may not be sufficient.

AEA 5 was considered as unstable. Therefore the lowest V_{60} from this data set was selected as a potential lower limit to define a potentially unstable system (V_{60} = 350 mL).

Likewise AEA 2 was considered as generally stable. Therefore the highest V_{60} from this data set (excluding the non-linear sample WRA 1 + TIII) was selected as a potential upper limit to define a potentially stable system (V_{60} = 250 mL).

S_5 and V_{60} was plotted in Figure 7 for all combinations with the limits discussed here. S_5 shows some correlation with V_{60}, but the scatter is wide. Therefore both parameters should be used for acceptance purposes.

For a stable combination, S_5 <100 and V_{60} < 200 ml should both be satisfied. For unstable combination, either S_5 > 150 or V_{60} > 350 ml means this combination is not stable and likely to have a unstable air void system. Marginal systems falling between these boundaries should be carefully monitored during construction.

Based on Figure 7, two combinations of admixtures (Compatible and Incompatible) were selected for testing in Step III with each type of cement. Selected admixtures are listed in Table 7.

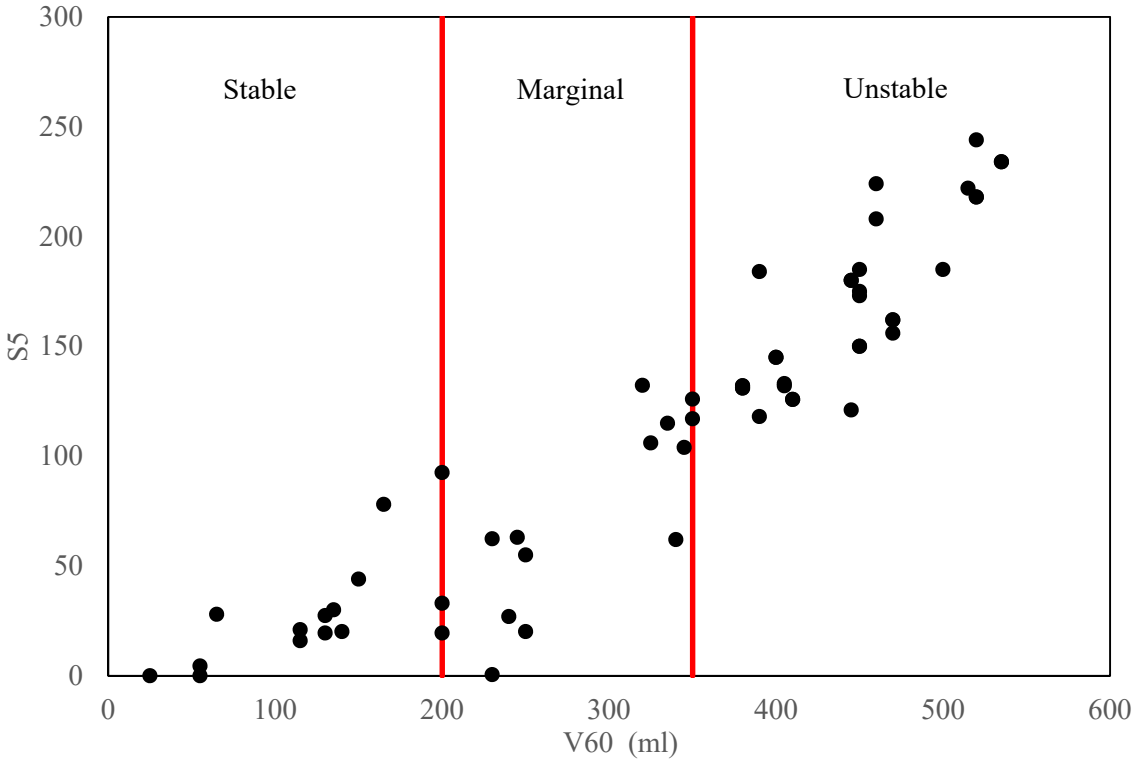

Figure 3.11. V_{60} vs. S_5 for all 60 mixes

3.4.3. Step III concrete analysis on stability and incompatibility

Air content of fresh concrete was tested by the pressure method at initial, 10 minutes of mixing+20 minutes waiting, and 60 minutes. Results are shown in Figure 8. All compatible mixes show similar level of air content loss in each stage, while incompatible mixes lost air in first 30 minutes. Less air was lost in these mixtures from 30-60 minutes, likely because there was less air in the system to be lost. Air contents of all incompatible mixes was lower than 4% after 30 minutes. Results of hardened air content analyses are presented in Figure 9, showing trends similar to those observed in the fresh tests.

Spacing factor of hardened concrete is presented in Figure 10. For compatible mixes, even after 60 minutes, most mixes still had a spacing factor lower than 0.2 mm, which indicates a desirable stability. On the other hand, although all incompatible mixtures had spacing factors

below 0.2 mm initially, all of them were well above 0.2 mm after 60 minutes. Such concrete, which was acceptable in terms of spacing factor and air concrete right after mixing, would likely have a problem during the service life since the air void system is likely poor after placing.

3.5. Conclusions

By varying parameters in the foam drainage test in terms of testing conditions and data processing methods, this study was able to recommend more specific details on how to conduct the test. At the same time, by testing combinations of a wide range of cements and admixtures, this study was able to recommend an alternative approach to interpreting the data along with pass/fail limits.

Using the suggested limits, eight concrete mixes were prepared to evaluate the relationship between foam drainage results and air void system stability. The performance of the concrete mixtures was similar to that predicted by the foam drainage test in that air void systems were observed to decay faster in mixtures prepared using unstable admixture combinations.

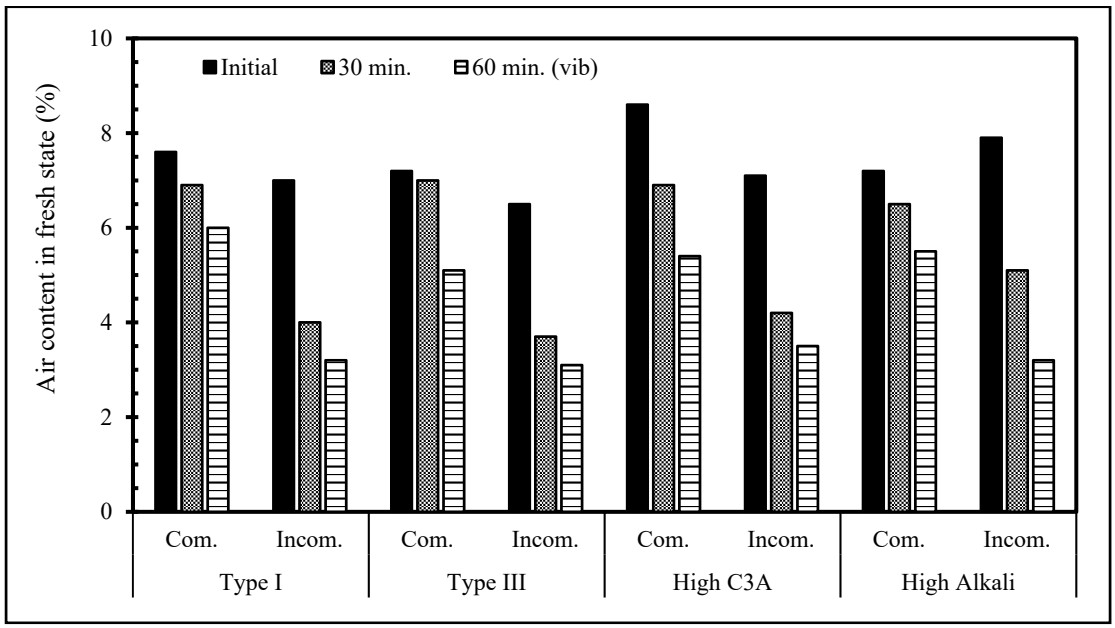

Figure 3.12. Air content and air loss up to 60 minutes (Fresh concrete)

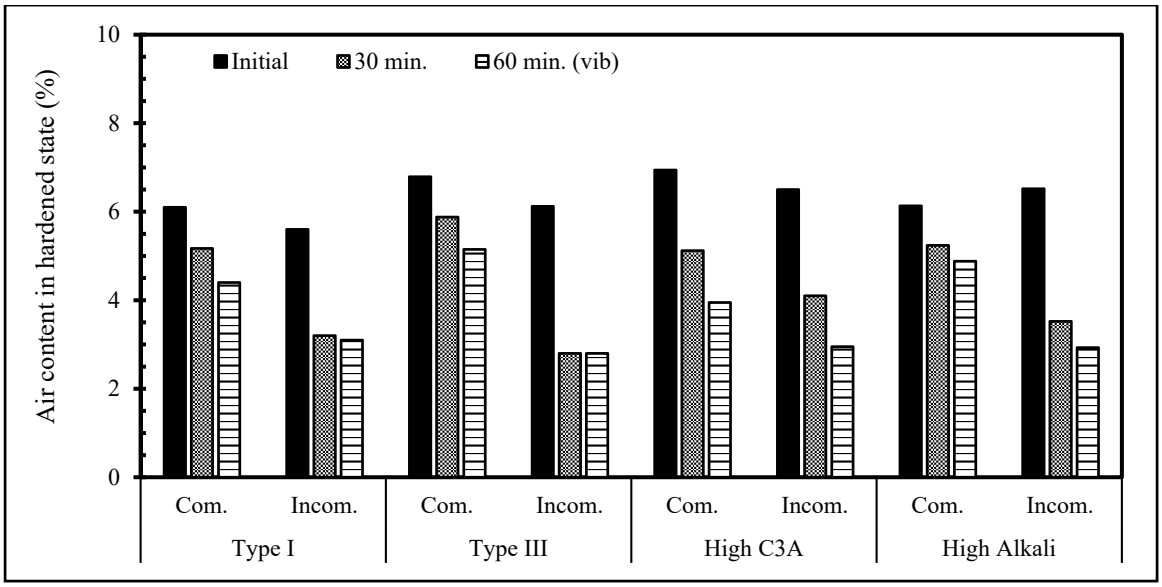

Figure 3.13. Air content and air loss up to 60 minutes (Hardened)

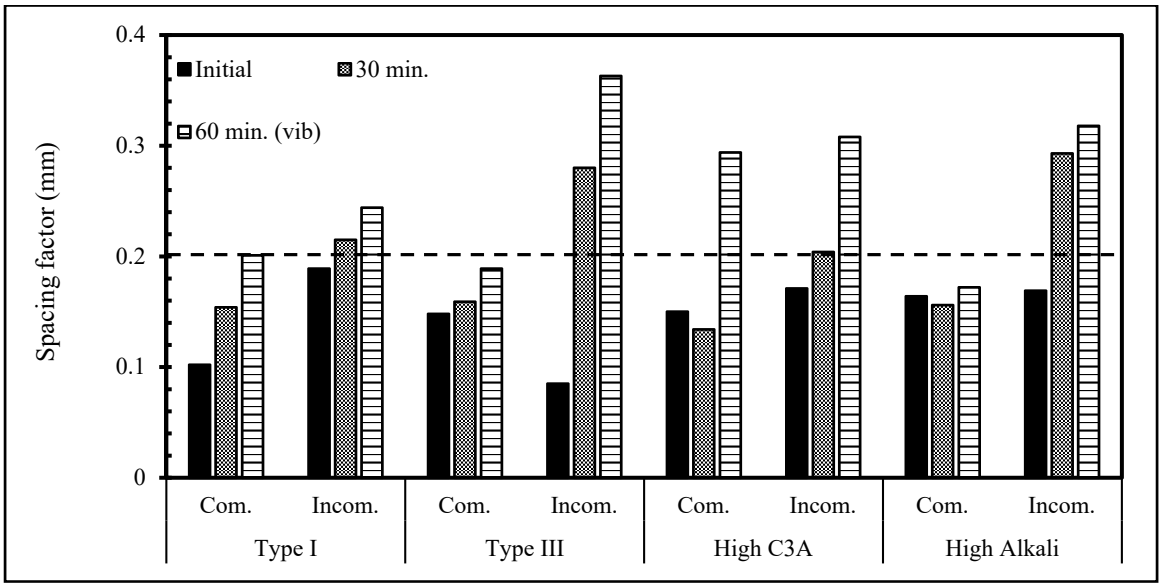

Figure 3.14. Spacing factor for hardened concrete up to 60 minutes

3.6. References

(1) ACI 201.2R, 2016, "Guide to Durable Concrete," American Concrete Institute

(2) Kosmatka, S.H., Wilson, M.L., 2016, *Design and Control of Concrete Mixtures*, 16th edition

(3) ACI 211, 1991, Standard Practice for Selecting Proportions for Normal, Heavyweight and Mass Concrete, American Concrete Institute

(4) Plante, P., et al., 1989, "The Influence of Water-Reducers on the Production and Stability of the Air Void System in Concrete," *Cement and Concrete Research*, Vol. 19, pp. 621–633

(5) Nagi, M.A., Okamoto, P.A., Kozikowski, R.L., and Hover, K. 2007. *NCHRP Report 578: Evaluating Air-Entraining Admixtures for Highway Concrete*, National Cooperative Highway Research Program, Washington, DC

(6) Taylor, P., Wang, X., and Wang, X.H, 2016, *Concrete Pavement Mixture Design and Analysis (MDA): Evaluation of Foam Drainage Test to Measure Air Void Stability in Concrete*. National Concrete Pavement Technology Center, Iowa State University, Ames, IA

(7) Taylor P.C., Johansen V.C., Graf L.A., Kozikowski, R.L., Zemajtis J.Z., and Ferraris C.F, 2006, *Identifying Incompatible Combinations of Concrete Materials, Volume II—Test Protocol*. Federal Highway Administration, Research, Development, and Technology, Turner-Fairbank Highway Research Center, McLean, VA

(8) Cross, W., Duke, E., Kellar, J., and Johnston, D. 2000. *Investigation of Low Compressive Strengths of Concrete Paving, Precast and Structural Concrete. South Dakota Department of Transportation*, Office of Research, Pierre, SD

(9) Torrans, P.H., Ivey, D.L., 1968, "Review of Literature on Air-Entrained Concrete," *Air Entrainment in Concrete*, Research Study Number 2-5-66-193, the Texas Highway Department

(10) Dodson, V.H., 1990, *Concrete Admixtures*, Van Nostrand Reinhold, New York

(11) Klieger, P. and Perenchio, W.F., 1976, "Further Laboratory Studies of Portland-Pozzolan Cements," Research and Development Bulletin RD041.01T, PCA, Skokie, IL

(12) Gebler, S. and Klieger, P., 1983, "Effect of Fly Ash on the Air-Void Stability of Concrete," *Fly Ash, Silica Fume, Slag and Other Mineral By-Products in Concrete*, SP-79, American Concrete Institute, Detroit, MI

(13) Baalbaki, M. and Aitchin, P.C. 1994. *Cement/Superplasticizer/Air-Entraining Agent Compatibility*, ACI SP-148, pp. 47–62

(14) Okkenhaug, K. and Gjørv, O.E., 1992, "Effect of Delayed Addition of Air Entraining Admixtures to Concrete," *Concrete International*, Vol. 14, No. 10, pp. 37–41

(15) Gutmann, P. F., 1988, "Bubble Characteristics as they Pertain to Compressive Strength and Freeze-thaw Durability," *ACI Materials Journal*, pp. 361-366.

(16) Bruere, G.M., 1955, Air Entraining in Cement and Silica Paste," *Journal of the American Institute*, Vol. 26, No.9, pp. 905-920

(17) ASTM C231 / C231M-14, 2014, "Standard Test Method for Air Content of Freshly Mixed Concrete by the Pressure Method," ASTM International, West Conshohocken, PA

(18) ASTM C457 / C457M – 12, 2013, "Standard Test Method for Microscopical Determination of Parameters of the Air-Void System in Hardened Concrete, American Society for Testing and Materials," West Conshohocken, Pennsylvania,

(19) Miles, G.D., Shedlovsky, L., and Ross, J., 1944, *Foam Drainage*, Division of Colloid Chemistry and the Division of Physical and Inorganic Chemistry, American Chemical Society, New York

CHAPTER 4. VARIATIONS IN AIR VOID SYSTEM FOR MORTAR AND CONCRETE TESTED WITH PRESSURE METHOD OR SEQUENTIAL AIR METHOD

Xin Wang, Seyehamed Sadati, Xuhao Wang, Peter Taylor, Kejin Wang

Abstract

The entrainment of air voids into fresh concrete has been the major requirement for concrete pavement to ensure a good freeze-thaw durability. The total air content is a commonly measured property of fresh concrete and is usually tested according to ASTM C231. Other parameters (spacing factor, specific surface) of the air void system in concrete are available but hard to measure in fresh concrete. Ley and Tabll (2014) proposed a new method called the Super Air Meter (SAM) to measure some of the these more nuanced air void system parameters mentioned above in fresh concrete using sequential pressure stages rather than one pressure used in ASTM C231. Though the correlation between results from SAM and hardened air void analysis is good, the reason why there is correlation between SAM measurement and hardened air void system is not clear.

The work presented here seeks to explain the mechanism behind the SAM by studying volume change of air voids during different pressure stages, which is part of the SAM's test protocol. Mortar mixtures were prepared and exposed to different pressure stages and durations. The hardened air void system of these samples was obtained using the linear-traverse method (ASTM C457). Volume changes from mortar samples were used to estimate the volume changes in concrete during the sequential pressure. Concrete mixtures were prepared and tested using both SAM and ASTM C457 to evaluate the accuracy of the estimation. It was found that data obtained by SAM at 100-kpa pressure stage was able to predict multiple hardened air void system parameters, providing insight into the mechanism of underlying the SAM test.

4.1. Introduction

Air content of concrete is critical for both quality control and concrete freeze-thaw (F-T) durability. Fresh air content is measured frequently during concrete delivery (usually right in front of paver) to ensure the consistency of concrete quality. At the same time, a good air content provides an indication of F-T resistance for hardened concrete. Total air content is defined as the proportion of the total volume of air voids to the bulk volume of concrete including all the constituents and the total volume of air (1). Klieger (2) reported that for concrete with 19 mm maximum size coarse aggregate, air content needs to be approximately 6% for effective freeze-thaw resistance. Iowa DOT requires an 8.0% ± 2.0% air content for slip form paving. It is generally believed that concrete with air content over 5.0% will display a good F-T resistance.

Power (1) introduced "spacing factor" as a parameter for describing the air void system in hardened concrete that, can be determined by a hardened air void system analysis using ASTM C457 (4). Spacing factor is defined as the distance water needs to travel to reach the nearest air void. ACI 201 (5) recommends a spacing factor less than 0.2 mm for concrete to have a sufficient F-T durability. The problem with spacing factor (or any other parameter of hardened air void system in concrete) is the time necessary to conduct the test. It can take between 7 to 14 days to complete a hardened air void system test, rendering it useless for quality control during construction. Over decades, researchers have found that a good air content does not necessarily mean good F-T durability (6). Even today, air content of 5.0% is still used as a rule of thumb in most pavement construction in the U.S.A, since spacing factor o(r other critical parameters like chord length distribution or specific surface) is not available at the fresh stage.

Table 1 summarized the fresh air void system test methods. The volumetric method uses unit weight of concrete and specific gravity of each ingredient to calculate air content. The

gravimetric method also needs unit weight of the concrete and displacement in water of a weighed sample of concrete. An air indicator determines the air content for fresh concrete by displacing the air with alcohol and recording the change of liquid in a tube. The air void analyzer (AVA) is an efficient fresh air void system test that can present both air content and spacing factor of fresh concrete. The downside to AVA is that due to the mechanism of the test, it is very sensitive to test environment, even shaking the table on which the test was performed or changing of room temperature may induce errors, which makes it difficult to use in the field. Acoustic bubble spectrometer is able to provide bubble size distribution in fresh concrete by measuring sound speed and attenuation at various frequencies. Pressure method is commonly used in practice. Fresh air content can be tested using pressure method without knowing unit weight or mix proportion. The recently developed Super Air Meter (SAM) was developed to measure air void system in fresh concrete. Ley and Tabll first introduced SAM in 2014 (8), then modified the test procedure in 2017 (9). Compared with the pressure meter which used 1 atmospheric pressure (100 kPa) to compress fresh concrete, SAM uses two more pressure stages (207 kPa and 310 kPa) to further compress the sample and as a result, a more accurate air content is obtained. A so-called 'SAM number' is obtained from this test. SAM number is the difference between equilibrium number (the pressure reading after open the valve between upper and bottom chamber) at 310 kPa of round two and round one. Though it correlates well with spacing factor and F-T test, the physical/chemical meaning behind SAM number is unclear, in fact, the mechanism of air voids changing and pressurization is not yet explained. The SAM number did however correlate well with spacing factor from hardened air void system analysis and durability factor from ASTM C666 F-T durability test (citation) making understanding the physical basis for the measurement all the more intriguing.

Table 4.1. Air content test method for fresh concrete

Method	Parameters				References
	Total Volume	Sizes, Chord Length, SS	Spacing, SF	Distribution, Frequency	
Pressure meter	✓				ASTM C231 (10)
Volumetric method	✓				ASTM C173 (7)
Gravimetric	✓				AASHTO T196 (11)
Chace Air Indicator	✓				AASHTO 199 (12)
Super Air Meter	✓		✓		Ley et al. 2017 (9)
Air Void Analyzer, AVA	✓	✓	✓	✓	AASHTO TP 75 (13)
Acoustic Bubble Spectrometer	✓	✓	✓	✓	Wu and Chahine 2010 (14)

The objective of this study is to investigate the volume change of air bubbles in concrete under multiple pressures and study the mechanism underlying the SAM. Mortar mixes were made and pressured at exposed to multiple pressure stages and then the air void system of these samples were tested using ASTM C457. Subsequently, concrete mixtures were prepared to evaluate if the SAM's multiple pressure stages used were able to predict hardened air void properties.

4.2. Backgrounds and theory

Klein and Walker proposed the pressure meter in 1946 (15). Since then, few researchers have studied air dissolution or air transition between air voids for concrete under pressure. Mielenz et al. (16) conducted a series of studies on the air transfer between voids in concrete. In their research, they found that air in bubbles may dissolve in the pore solution or merge with other bubbles. Whether one bubble is receiving or losing air depended on the size of bubble and the average bubble size of the system. Smaller bubbles will dissolve and lose air to bigger

bubbles relatively faster. Hence, the average bubble size will increase. Research has shown that bubbles smaller than 50 μm tend to vanish after pumping (17). Ley et al. (18) observed behavior of bubbles and diffusion of gas in the bubble under fluid pressure for different chemical based air entraining agent (AEA). They found that bubbles with diameter of 300-400 μm would shrink under pressure up to 70 kPa and will be about 5% smaller than the original diameter once the pressure is released, meaning there was a reduction in diameter of bubble. They proposed that this reduction is caused by dissolution of air into the surrounding fluid. Changes observed in bubbles of different diameters are presented in Table 2. In general, bubbles under pressure experienced both dissolution and compression, so in most of cases both factors need to be considered.

Table 4.2. Bubble size change with and without pressure (16,17,18)

Bubble size (μm)	No pressure	Under pressure (up to 70 kPa)
<50	Dissolve and vanish	Dissolve and vanish faster
50<diameter<500	grow first and shrink	shrink
500<diameter<1000	Shrink or grow , depending on pressure and average diameter	

Hover (19) examined the hypothesis that internal pressure of bubbles is equal to atmospheric pressure, which is used to calculate air content in an ASTM C213 Pressure Meter (Figure 1). Under this assumption and assuming that all bubbles in the concrete are initially the same radius, total air volume in concrete is:

$$V_{a1} = n(4\pi/3)R_1^3 \quad (1)$$

Where V_{a1} is initial air content, R_1 is initial average bubble radius, n is bubble count

The reduction in air volume after compression can be written as

$$\Delta V_1 = n(4\pi/3)(R_1^3 - R_2^3) \quad (2)$$

Where R_2 is average bubble radius after applying pressure,

Applying Boyle's law,

$$P_1V_{c1} = P_2V_{c2} = P_2(V_{c1} + \Delta V_1) \quad (3)$$

Apply Equation (2) to Equation (3) and reorganize,

$$K_1 = (R_2/R_1)^3 = \frac{Vc1P2 + Va1P2 - P1Vc2}{P2Va1} \quad (4)$$

Where P_2 is the equilibrium pressure after applying 100-kPa pressure on concrete.

With higher pressure used in SAM, same relationship can be built using Boyle's law

$$K_2 = (R_2/R_3)^3 = \frac{Vc1P3 + Va2P3 - P2Vc1}{P3Va2} \quad (5)$$

Where R_3 is average radius of bubbles in concrete after 207-kPa pressure, P_3 is the equilibrium pressure after this pressure, and V_{a2} is the volume of air voids for concrete after 100-kPa.

Respectfully,

$$K_3 = (R_3/R_4)^3 = \frac{Vc1P4 + Va3P4 - P3Vc1}{P4Va3} \quad (6)$$

Where R_4 is average radius of bubbles in concrete after 310-kPa pressure, P_4 is the equilibrium pressure after this pressure, and Va_3 is the volume of air voids for concrete after 207-kPa pressure.

With Equation 4, 5, and 6, it is possible to calculate the volume ratio between each pressure stage (K_1, K_2, K_3). In each equation, P_n is the reading of each pressure stage, so the only unknown is V_{an}, which is the volume of voids under each pressure stage.

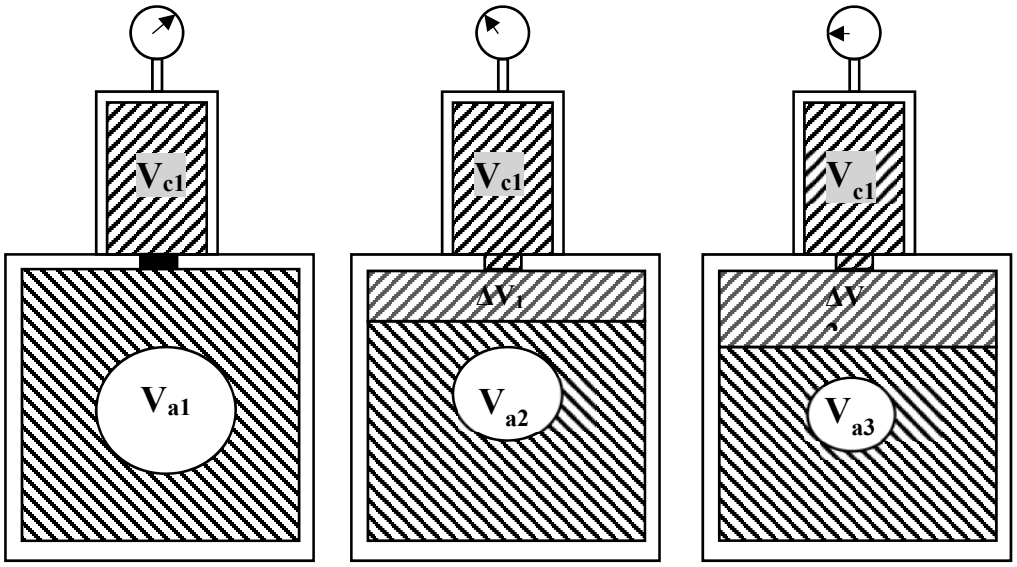

Figure 4.1. Schematic diagram of air meter at multiple pressure stages

A). Schematic diagram of a Type B air meter (or Super Air Meter) showing volume change which occur when the valve between top and bottom chamber is opened; B). Schematic diagram of an air meter (or Super Air Meter) showing volume of concrete and upper chamber after apply 207-kps pressure; C). Schematic diagram of Super Air Meter showing volume of concrete and upper chamber after apply 310-kps pressure

As stated above, voids under pressure are experiencing both compression and dissolution. With Ley et al.'s observation (18), it can be assumed that the volume reduction caused by compression is *reversible*, while air dissolution is *irreversible*, which is why bubbles in their study did not grow back to original size after the pressure is released. Another assumption is that dissolution can be accomplished in a short period, i.e., during the testing period of each pressure stage (roughly 10 seconds). Another assumption may be that given enough time until concrete is hardened (8 hours), both compression and dissolution reach equilibrium. This means subtraction

of volume change in 8 hours sample and 10 seconds sample is volume change caused by compression. Therefore:

$$\Delta V_{8h} = V_{comp} + V_{dis} \quad (7)$$

$$\Delta V_{10s} = V_{dis} \quad (8)$$

$$V_{comp} = \Delta V_{8h} - \Delta V_{10s} \quad (9)$$

Where ΔV_{8h} is volume change after 8 hours of pressure, V_{comp} is volume change due to compression of pressure, V_{dis} is volume change due to dissolution of air, and ΔV_{10s} is volume change after 10 second of pressurization

To calculate these volume changes, mortar mixes were prepared to determine volume change under each pressure stage with different pressurization timse. Mortar was used to avoid voids in coarse aggregate confounding the data. Concrete mixtures were made with the same pressure stages for comparison.

Concrete mixes were then prepared and tested using SAM, and thus equilibrium p P_2, P_3, and P_4 in Equation (4), (5), (6) is measured in each concrete mix. Using volume reduction calculated in mortar mixes, volume ratios K_1, K_2, and K_3 can be calculated.

4.3. Experimental methods

4.3.1. Materials and mix proportions

The cementitious materials used in this study include Type I/II Portland Cement and Class C fly ash. Their chemical compositions are listed in Table 3.

Table 4.3. Chemical composition of cementitious materials (wt%)

Element	SiO_2	Al_2O_3	Fe_2O_3	CaO	MgO	SO_3	LOI	Na_2O	K_2O
Type I cement	20.05	4.38	3.07	64.29	3.38	2.78	2.81	0.14	0.58
C-Fly Ash	42.46	19.46	5.51	21.54	1.42	1.20	0.19	1.42	0.68

River sand with a fineness modulus of 2.63 was used as fine aggregate. Crushed limestone with a nominal size of 4.75-9.00 mm was used as coarse aggregate.

Vinsol-resin air entraining agent (AEA) and polycarboxylate water reducing agent (WRA) were used as admixtures. For mortar mixtures, dosage of AEA was 20 ml/100 kg cement. For concrete mixtures, dosage of AEA was dependent on target air content of the mixture: high (6-8%), marginal (4.5-6%), and low (2.5-4.5%).

Mix proportions for mortar mix and concrete mix are listed in Table 4.

Table 4.4. Mix proportion for mortar and concrete mixtures

Mix Type	Amount kg/m^3							
	Coarse Aggregate	Fine Aggregate	Cement	Fly Ash	Water	w/c ratio	WRA	AEA
Mortar	-	1500	480	120	252	0.42	590 ml/100 kg cement for WRA, Usage of AEA was dependent on target air content	
Concrete	1023	838	270	65	141	0.42		

4.3.2. Test methods

For mortar mixture, cylinders with dimension of 10.2 cm diameter and 20.3 cm in height were cast and then stored in a pressured pot. Pressure and duration of the pressurization is listed in Table 5. Pressure stage is selected based on operation procedure for SAM (Ley et al. 2017). Two rounds of pressurization are part of procedure for SAM. Each sample was pressurized all previous pressure stages. For instance, M4A was at 100-kpa in Round 2, so it experienced 3 pressure stages in first round, and then be pressured at 100-kpa. Eight hours was allowed for

equilibration to ensure concrete is hardened and dissolution and compression of bubbles is accomplished at such pressure. One extra concrete mixture was prepared and pressured according to Table 6. All samples were then cured and cut into discs for hardened air void system analysis according to ASTM C457.

Table 4.5. Pressure stage and duration of pressure for mortar samples

Pressure kPa	100	207	310	100	207	310
Round	Round 1			Round 2		
Duration	10 seconds					
Sample ID	M1A	M2A	M3A	M4A	M5A	M6A
Pressure kPa	100	207	310	100	207	310
Round	Round 1			Round 2		
Duration	8 hours					
Sample ID	M1B	M2B	M3B	M4B	M5B	M6B

Table 4.6. Example of sample ID and pressure stage for Mix 1

Sample ID	C1	C2	C3	C4	C5	C6
Pressure kPa	100	207	310	100	207	310
Round	Round 1			Round 2		
Duration	10 seconds					

For concrete mixtures, slump of concrete is determined according to ASTM C1611. Air content and SAM number for fresh concrete is determined according to Ley et al. (2017). Equilibrium number at each pressure stage were recorded for all mixtures. Samples were cured 28 days and then cut into discs for hardened air void system analysis according to ASTM C457. Data for fresh and hardened air void system parameters for concrete mixtures are presented in Table 7.

Table 4.7. Fresh and hardened air void system parameters for concrete mixtures

Mix No.	1	2	3	4	5	6	7
Slump mm	25	22	25	20	22	25	25
Fresh air content %	7.6	6.6	6.65	5.9	4	3.45	3
SAM number	0.20	0.26	0.26	0.16	0.72	0.62	0.88
Hardened air content %	5.66	6.18	6.18	5.21	3.97	3.85	2.36
Spacing factor mm	0.117	0.187	0.187	0.159	0.261	0.271	0.572

4.4. Results and discussion

4.4.1. Volume change for mortar samples M1-6 and concrete samples C1-6

According to findings from Mielenz et al. (1958), air in small bubbles tend to dissolve faster, and dissolved air will transfer into bigger bubbles. The size of 'small' or 'big' is subjective, depending on average bubble size in the system. When the water in the system is saturated with air from small bubbles the system will stabilize, therefore the average diameter of bubbles at this time can be used to determine if one bubble would lose or gain air volume.

When comparing chord length distribution for the same pressure stage in two rounds. The tendency of air transfer can be seen from Figure 2 to Figure 4. Under the same pressure, the volume change due to compression is the same, the volume difference seen in Figure 2 to Figure 4 between two rounds is likely caused by dissolution of air. At 100-kPa two rounds intersected at 260 μm, and number of bubbles with size below to this decreased from round one to round two, indicating in general bubbles above 260 μm lose air due to dissolution. For 207-kPa, this diameter is 190 μm, and for 310-kPa it is 50 μm. This shows that a second round of pressurization would enhance the dissolution. At the same time, higher pressure is able to force smaller bubbles to lose air due to dissolution compared with lower pressures

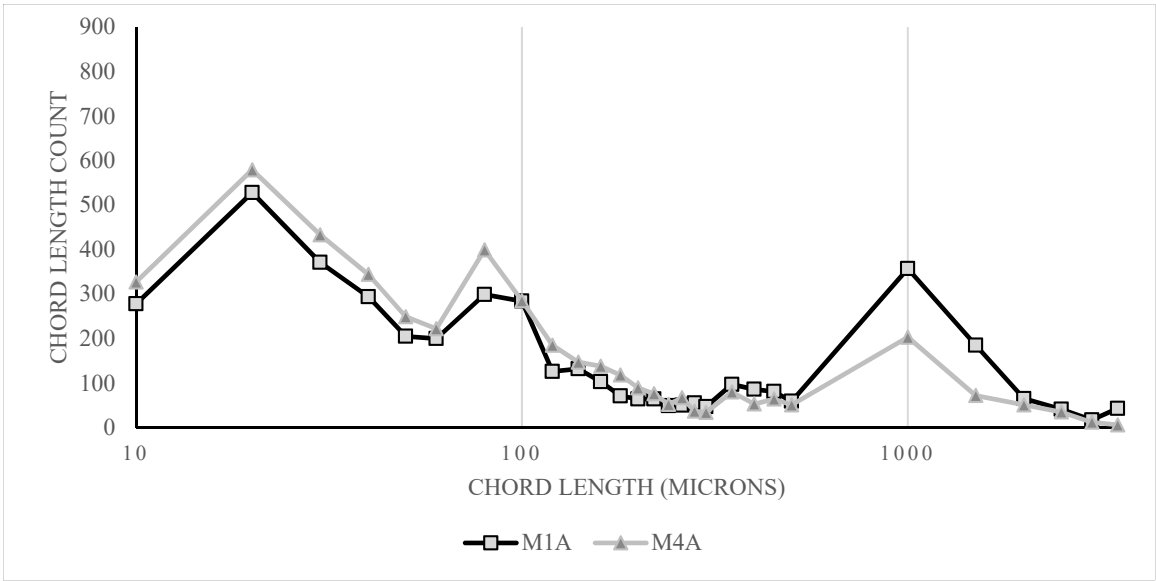

Figure 4.2. Chord length distribution for 100-kPa samples

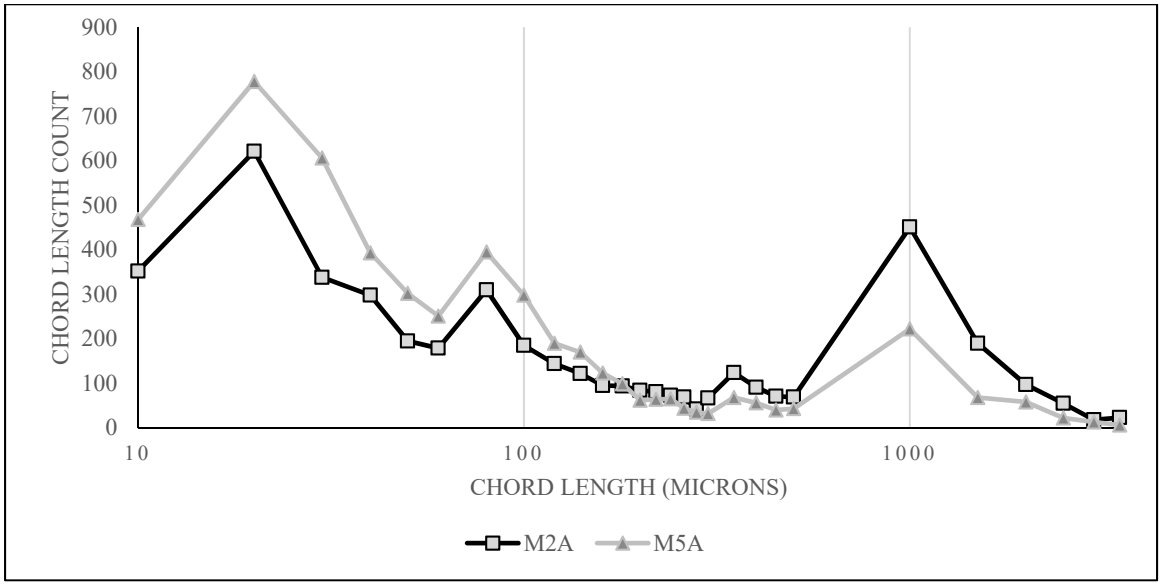

Figure 4.3. Chord length distribution for 207-kPa samples

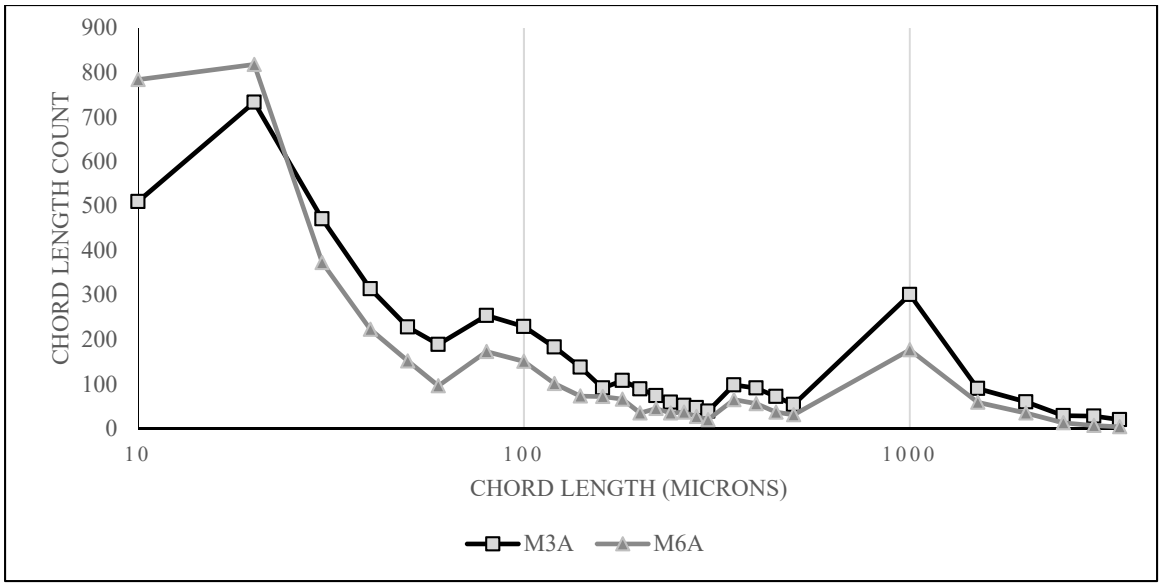

Figure 4.4. Chord length distribution for 300-kPa samples

Chord length distributions for samples pressurized for 8 hours are less conclusive, and complete figures are presented in the appendix. This is expected because in these samples, air bubbles were experiencing both dissolution and compression.

Volume change caused by compression (V_{comp}) can be calculated by subtracting volume of voids in 8 hour samples from the volume of voids in 10 second samples. Volume reduction caused by dissolution (V_{dis}) is calculated by subtracting volume of voids in 10 seconds sample from volume of voids in the original sample. Volume change for both compression and dissolution is presented in Table 8.

It can be seen from Table 8 that with higher pressure, influence of compression on voids grew, while dissolution caused by pressure decreased. Higher pressure will compress bubbles more than lower pressure, and dissolution volume is decreasing with pressure. Comparing each pressure in different rounds, compression volume is similar for each pressure stage after two rounds, and dissolution volume after round two is higher than after round one. Figure 2 to Figure

4 shows the reason for more dissolution. After each pressure stage for round two, diameter of bubbles that loss air due to dissolution is decreasing with increasing pressure, which as a result, more bubbles are losing air due to dissolution, causing more volume reduction .

Table 4.8. Volume change calculations for both compression and dissolution

Initial Volume (mm^3)	Pressure (kPa)	V_{comp} (mm^3)	% reduction	V_{dis} (mm^3)	% reduction
0.26	100	0.03	12	0.09	35
	207	0.04	16	0.08	31
	310	0.07	27	0.07	27
	100	0.01	4	0.14	54
	207	0.03	4	0.13	50
	310	0.06	8	0.1	39

Figure 5 shows the chord length distribution for concrete samples with difference pressure stages. Besides bubble shrinkage and air dissolution, pores in coarse aggregate will also contribute to air transmission in concrete. Similar trend as mortar samples was found for round one, where bubble count for 500-1000 μm decreases and bubbles in 10-30 μm increases. For round two this trend is less clear, which could be caused by air getting into aggregates due to higher pressure, but in general the trend in concrete samples for pressure stages is similar to mortar samples. Volume change for concrete at each stage was calculated and presented in Table 9.

Table 4.9. Volume change in concrete samples

Stage	Initial	100-kPa	207-kPa	300-kPa	100-kPa	207-kPa	300-kPa
Volume mm^3	0.027	0.003	0.004	0.005	0.006	0.001	0.007
Volume change %		10	16	18	21	23	25

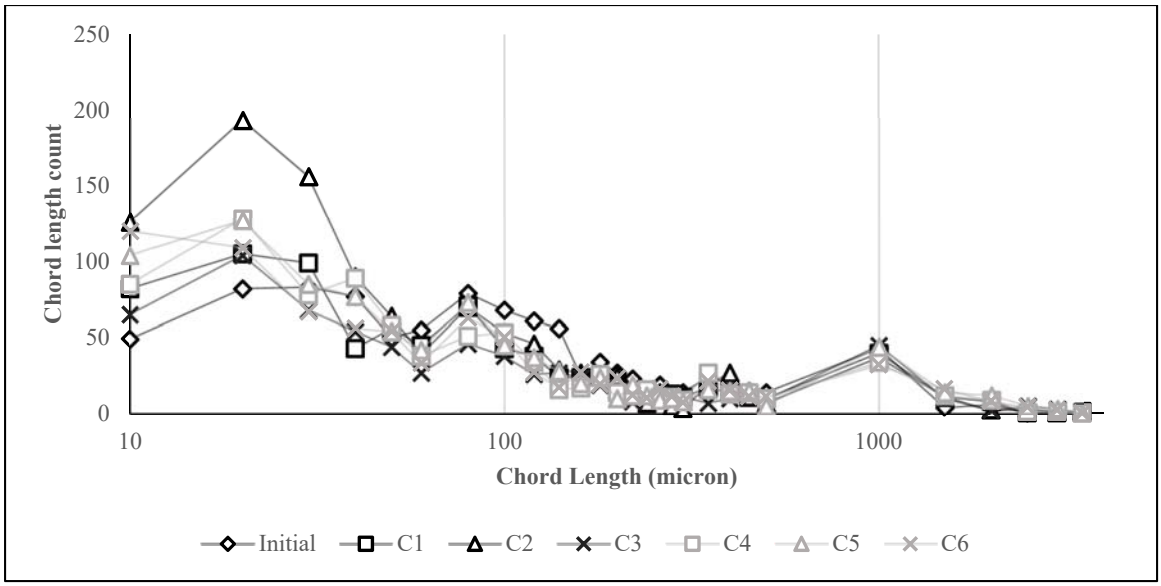

Figure 4.5. Chord length distribution for pressured concrete samples

4.4.2. Concrete mixtures tested by Super Air Meter

Using V_{comp} and V_{dis} calculated for each pressure stage in Table 8, volume ratio for each stage defined in Equation 4, Equation 5, and Equation 6 can be calculated. Volume change at each level and volume difference at each pressure level between each round were calculated and are presented in Table 10. Bubble counts for each range are calculated according to ASTM C457 hardened air voids analysis results. Volume ratio at each pressure stage is calculated using Equation 4, Equation 5, and Equation 6. Volume ratio rate is the slope of volume ratio rate and pressure stages.

Volume ratio at each pressure stage vs. chord length counts is presented in Figure 6. In general, 100-kPa stage can predict the total bubbles counts for bubbles from 10 μm to 1000 μm, while 207-kPa pressure stage can predict bubbles between 190 to 1000 μm and volume change ratio 310-kPa pressure stage failed to predict any chord length. Air content for fresh and hardened concrete is often quite comparable, though hardened concrete used image analysis while fresh concrete used Boyle's law. Volume change ratio at 100-kPa explained why two

methods can provide results that are similar. It is because volume change ratio caused by 100-kPa, which represents the air dissolve during 100-kPa pressure stage, correlated with bubbles from10-1000 μm, which is essential for hardened air content calculation.

The dissolution rate at each round (K_1 and K_2) is the slope of volume rate vs. pressure stage is calculated and presented in Table 10, and difference between K_1 and K_2 is presented in Table 10 as well. Figure 7 shows the relationship between $D(K_1-K_2)$ and spacing factor and chord length for each mix. Concrete with higher $D(K_1-K_2)$ usually has a lower spacing factor, and likely to have more bubbles in 10-1000 μm range

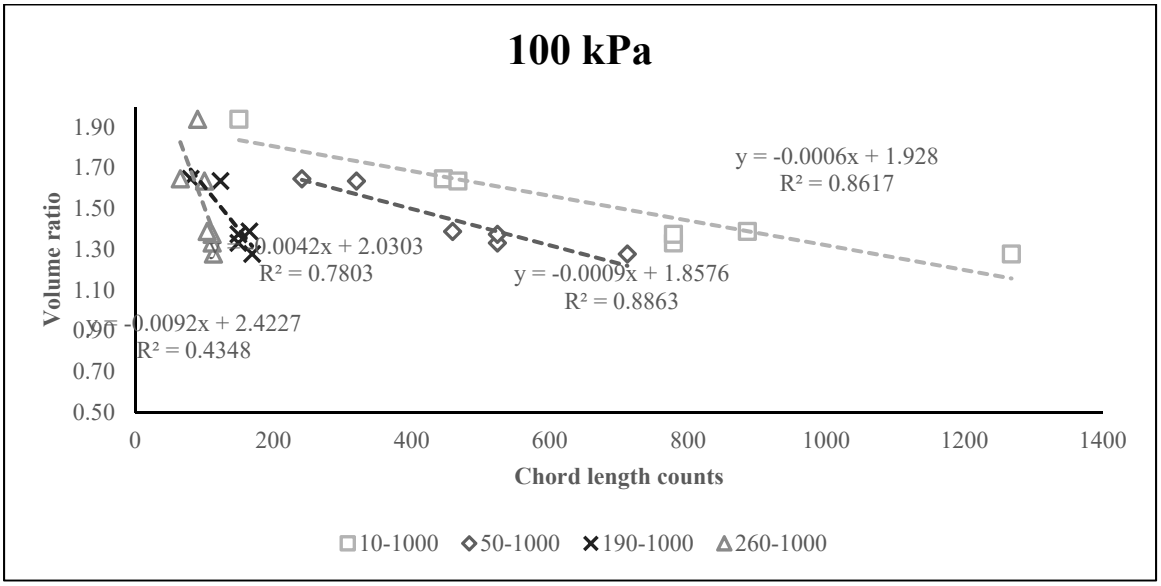

Figure 4.6. Prediction of volume ratio to chord length counts

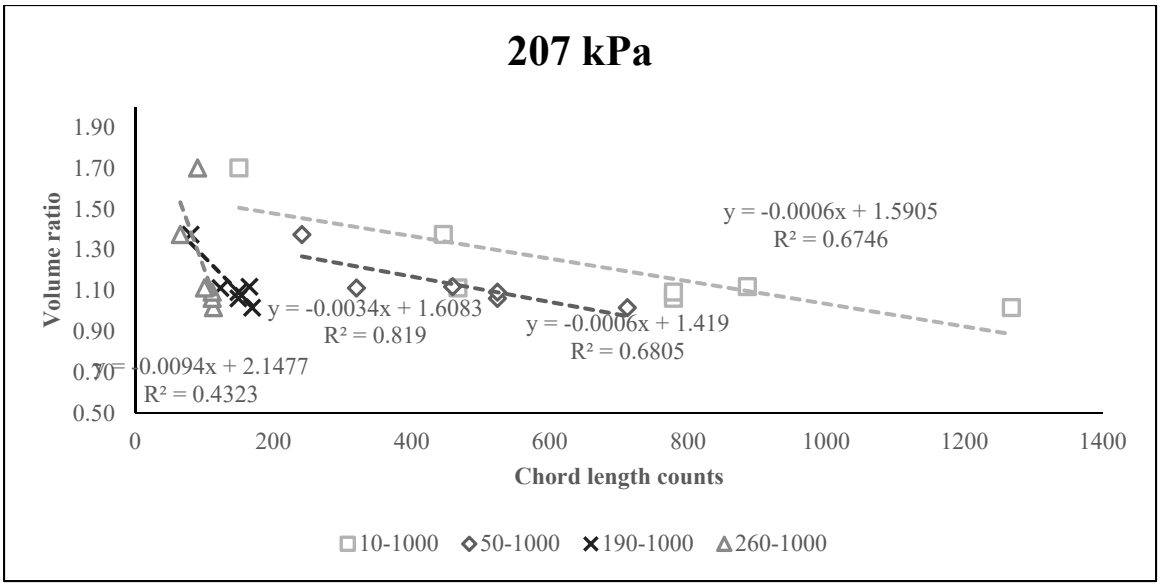

Figure 4.7. Prediction of volume ratio to chord length counts

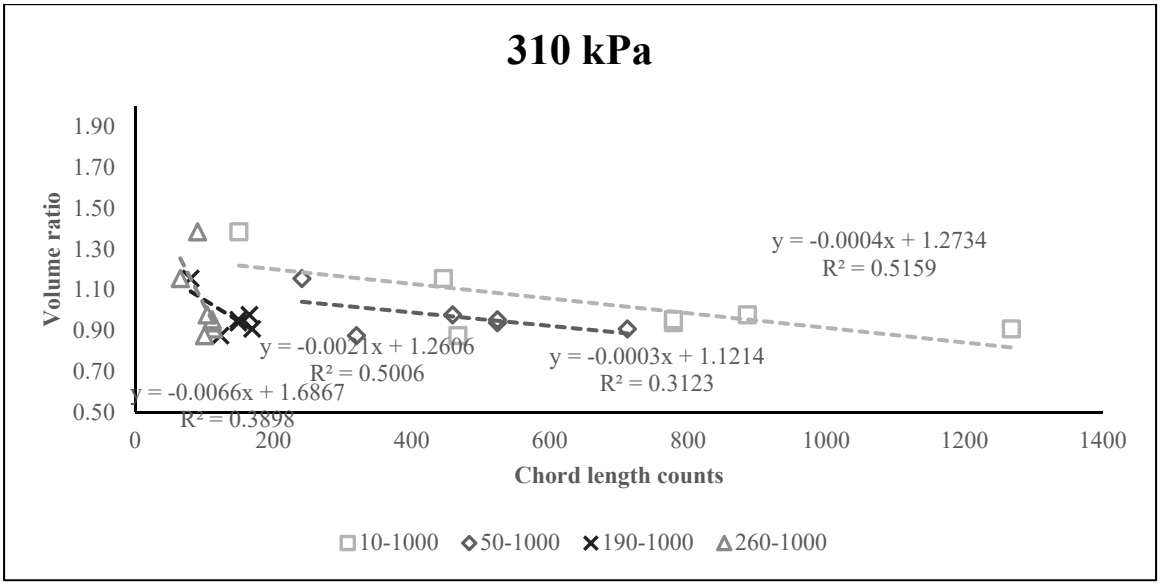

Figure 4.8. Prediction of volume ratio to chord length counts

.

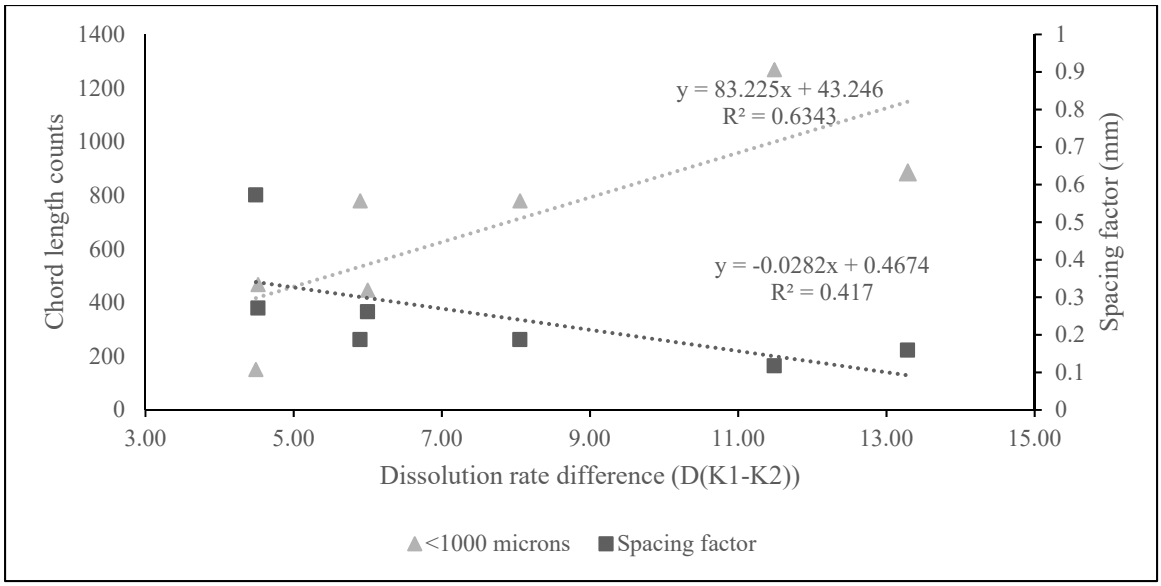

Figure 4.9. Prediction of dissolution rate difference

Difference between volume change ratio at each pressure stage is calculated (D_1, D_2, D_3) and presented in Table 10. This difference shows how much more (or less, if it is negative) volume change occurred between rounds, and predicts air dissolution volume. Figure 8 to Figure 10 shows the correlation these differences and chord length counts, spacing factor, and SAM number. Figure 8 show the similar results as Figure 6, 100-kPa pressure stage is able to predict chord length counts between 10-1000 μm while higher pressure fail to do so. Figure 9 shows the correlation between spacing factor from hardened air void system analysis and volume difference. Volume difference at each pressure stage correlates well with spacing factor. Considering that spacing factor is calculated using traverse length and total bubble counts and D_1 correlates well with bubble counts, there is no surprise that D_1 will correlates well with spacing factor. Concrete with lower volume ratio difference at each pressure stage at fresh stage is likely to have a low spacing factor when concrete is hardened. Figure 10 shows the correlation between SAM number and D. Though physical meaning of SAM number is not defined, it is purposed to represent the difference of air dissolve between 310-kPa at first round and second

round. D shows the volume difference caused by dissolution at each round, and SAM number correlates well with each stage, which could potentially be an indicator for D at each stage.

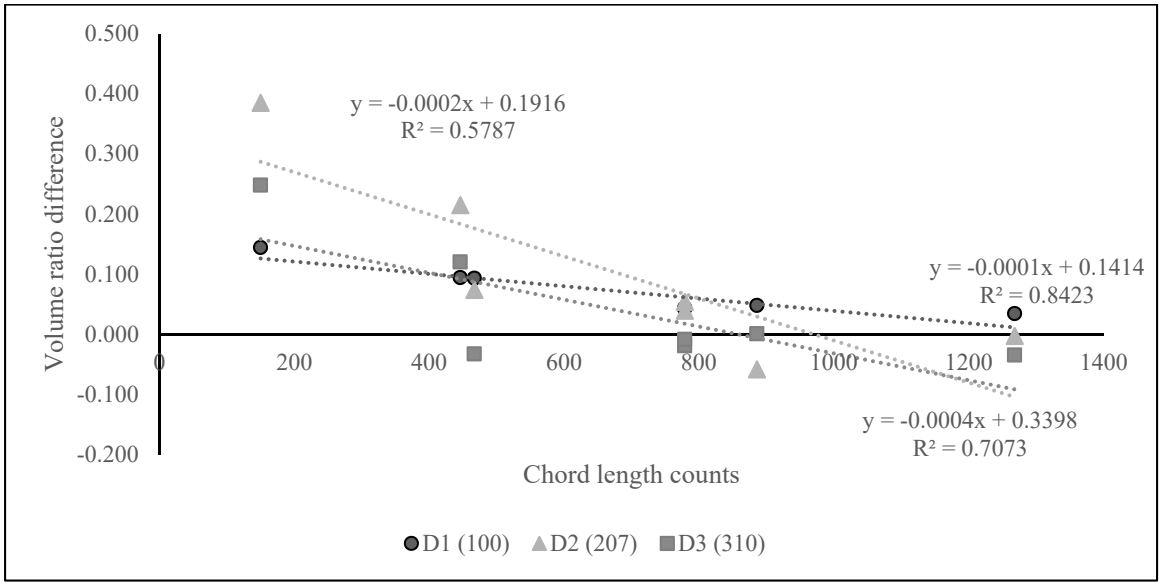

Figure 4.10. Prediction of chord length counts

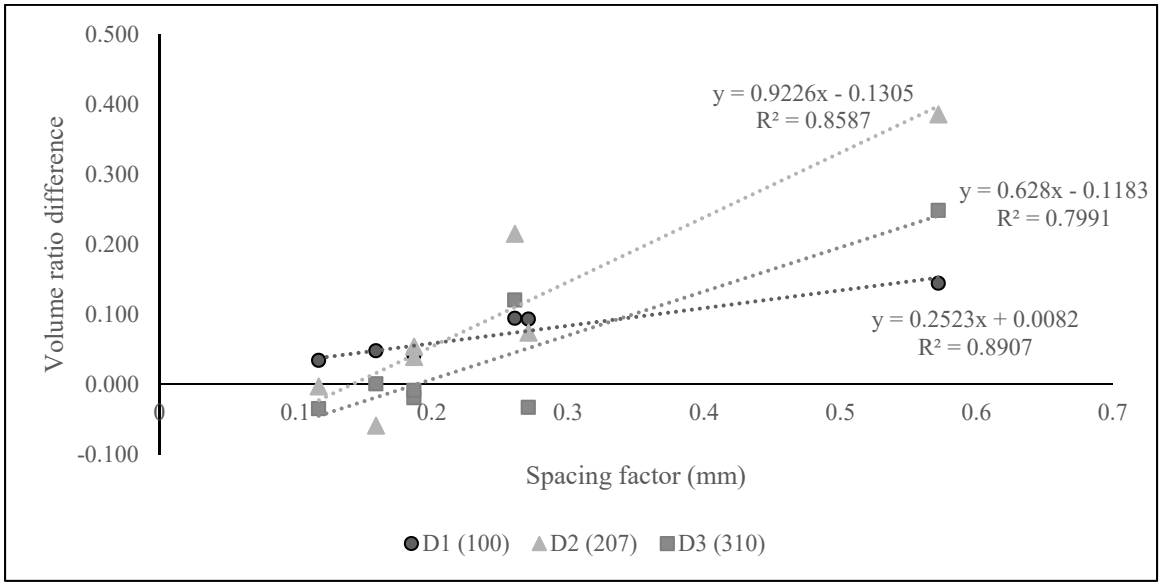

Figure 4.11. Prediction of spacing factor

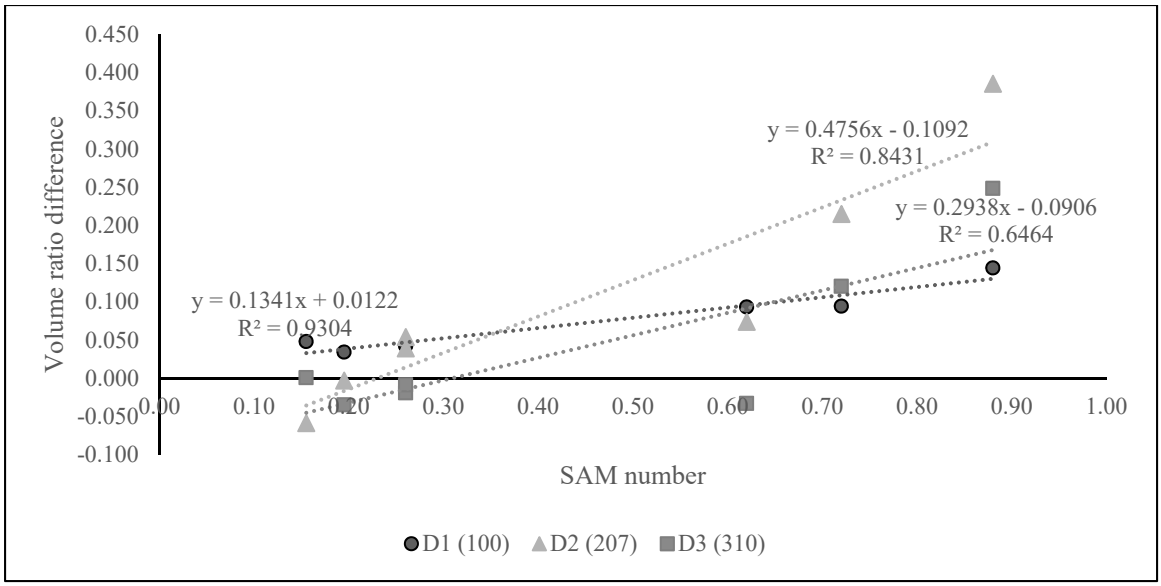

Figure 4.12. SAM number vs. volume ratio difference

4.5. Conclusions

This work presents the volume change for concrete and mortar under pressure up to 310-kPa, and provides a method to explain data from the newly developed fresh air void system test Super Air Meter. Tendency of air transition when concrete and mortar is under pressure is studied by comparing chord length distribution from each pressure stage for mortar and concrete.

Moreover, volume change ratio under each pressure stage is calculated. Using volume change ratio calculated from pressured mortar and concrete, data collected from seven fresh concrete mixtures with various air systems were used to calculate actual volume change for concrete tested by SAM, and results of this volume change was used to compare with hardened air void system parameters. Following conclusions have been made:

- At 100-kPa, bubbles with chord length larger than 260 μm are receiving air due to dissolution. For 200-kPa, this chord length becomes to 190 μm, and for 300-kPa it is 50 μm.

- During pressurization, bubbles experience both compression and dissolution. Volume loss caused by compression increased with higher pressure while volume loss due to dissolution decreased with higher pressure.

- Using equilibrium pressures collected from SAM test, it is possible to calculate volume change ratio at each pressure stage at each round. The difference between each round at same pressure stage correlates well with spacing factor from hardened air void system analysis.

4.6. References

1) ASTM C125-18a, *Standard Terminology Relating to Concrete and Concrete Aggregates,* ASTM International, West Conshohocken, PA, 2014

2) Klieger, P., "Further Studies on the Effect of Entrained Air on Strength and Durability of Concrete with Various Sizes of Aggregate," Proceedings, Highway Research Board, 1956, pp. 16-17; Bulletin No. 77, Research and Development Laboratory, Portland Cement Association, Skokie, IL

3) Power, T.C., "Void Spacing as a Basis for Producing Air-Entrained Concrete," ACI 50th Annual Convention*, Journal of The American Concrete Institute*, V.25, No.9, 1954

4) ASTM C457 / C457M – 12, *Standard Test Method for Microscopical Determination of Parameters of the Air-Void System in Hardened Concrete*, American Society for Testing and Materials, West Conshohocken, Pennsylvania, 2013

5) ACI 201. 2R-01, *Guide to Durable Concrete*, American Concrete Institute, 2001

6) Power, T.C., Willis, T., "The Air Requirement of Frost Resistant Concrete," in: Highway Research Board Proceedings, 1950

7) ASTM C173 / C173M-14, *Standard Test Method for Air Content of Freshly Mixed Concrete by the Volumetric Method*, ASTM International, West Conshohocken, PA, 2014

8) Ley, T.M., Tabb, B., "A Test Method to Measure the Freeze Thaw Durability of Fresh Concrete Using Overpressure," T&DI Congress, ASCE, 2014

9) Ley, T.M., Welchel, D., Peery, J., and LeFlore, J., "Determining the Air-void Distribution in Fresh Concrete with the Sequential Air Method," Construction and Building Materials, Vol. 150, 2017, pp. 723-737

10) ASTM C231 / C231M-14, *Standard Test Method for Air Content of Freshly Mixed Concrete by the Pressure Method*, ASTM International, West Conshohocken, PA, 2014

11) AASHTO T196M/T196-11, *Standard Method of Test for Air Content of Freshly Mixed Concrete by the Volumetric Method*, American Association of State Highway and Transportation Official, 2011

12) AASHTO T 199, *Standard Method of Test for Air Content of Freshly Mixed Concrete by the Chace Indicator*, American Association of State Highway and Transportation Officials, 2000

13) AASHTO T75, *Air-Void Characteristics of Freshly Mixed Concrete by Buoyancy change*," American Association of State Highway and Transportation Official, 2008

14) Wu. X., and Chahine, G.L., "Development of an acoustic instrument for bubble size distribution measurement," Journal of Hydrodynamics, Ser. B, Volume 22, Issue 5, Supplement 1, October 2010, pp. 330-336

15) Klein, W., Walker, S., "A Method for Direct Measurement of Entrained Air in Concrete," in: Journal Proceeding, 1946

16) Mielenz, R.C., Wolkdorf, V.E., Backstrom, J.E., and Burrows, R.W., "Origin, Evolution, and Effects of the Air Void System in Concrete: Part 4: The Air Void System in Job Concrete," in Proceedings of the American Concrete Institute, Vol. 30, No. 4, 1958, pp. 507-518.

17) Pigeon M, Marchand J, Pleau R (1996) Frost resistant concrete. Constr Build Mater 10(5):339–348

18) Ley M.T., Frazier R.M., and Tabb B.M., "System And Method For Rapid Measurement of The Air Void Distribution Of Fresh Concrete," United States Patent Application Publication Us 2014/0096593 A1, April 10, 2014

19) Hoover, K.C., “Analytical Investigation of the Influence of Air Bubble Size on the determination of the Air Content of Freshly Mixed Concrete,” *Cement, Concrete, Aggregates*, Vol.10(1), 1988

20) ACI 211, Standard Practice for Selecting Proportions for Normal, Heavyweight and Mass Concrete, 1991. American Concrete Institute

CHAPTER 5. INCREASING OF AIR CONTENT IN CONCRETE MOLDS CONSOLIDATED BY INTERNAL VIBRATOR

Xin Wang, Xuhao Wang, Seyehamed Sadati, Peter Taylor, Kejin Wang

Abstract

Internal vibration is the most commonly used consolidation method during concrete construction. It is commonly known that internal vibration on can remove the entrapped air voids from a concrete's air void system or entrained air voids if excessive vibration is applied. It is less well known, however, that air voids can be added into the system during vibration, causing increasing of air content. The consequence of this air entraining process during vibration is an uneven distribution of air voids, resulting in a concrete with heterogeneous strength and freeze-thaw durability.

To study the mechanism of this increasing of air content and how air voids are distributing after vibration, concrete mixtures were prepared and vibrated in multiple frequencies and durations. Air voids distribution within each sample was then obtained by linear-traverse method from ASTM C457, dividing each sample into 18 sections for a 15 cm × 30 cm cylinder. The mechanism of air increment was found to be that rotary movement caused by vibrator created a vortex inside of liquefied fresh concrete that sucks air voids into concrete. Meanwhile, air entraining agent (AEA) in the system would help stabilize these newly entrained air voids up to the point that AEA is used up. Frequency of vibration and duration of vibration both affect the amount of added air. In general, a high frequency of vibration will cause more air addition, while the amount of air added due to increasing the duration of vibration is dependent on the amount of AEA left in the system.

5.1. Introduction

The use of vibration on concrete was to ensure the placement of dry concrete into complex forms and through congested reinforcement. At the same time, vibration will release larger (or entrapped) air voids in concrete, producing a dense and more durable concrete (Banfill et al. 2011, ACI 309 1.R, Jagger 1910). Copious research on vibration and concrete has been produced over the past 100 years (ACI 309.1). The primary mechanism of action for vibration is to eliminate internal friction between particles. To achieve this purpose, energy transmitted to concrete by vibration is essential. Energy input by vibration is described with frequency, amplitude, time, and acceleration. Most of these parameters affect the rheology of fresh concrete, which is essential for concrete finishing and placing. Concrete vibration techniques include surface, form, table, and internal vibration, with the latter being the most commonly used vibration method. When concrete is under internal vibration, there is a visible liquefied zone around vibrator, while regions with greater distance are not affected. The radius of this liquefied zone is defined as radius of action (Banfill et al. 2011, Ghadban 2016). In general, this radius increases with higher frequency, while there is an optimum frequency for a given amplitude and vibration duration (Banfill et al. 2011, Forssblad 1965).

Vibration can enhance the air void system by removing entrapped air voids, defined as voids with diameter of 1 mm or above and irregular in shape, which are produced due to insufficient mixing or consolidation (ASTM C125). Entrapped air voids provide no increase in freeze-thaw (F-T) durability and may decrease concrete strength. The effect of vibration, however, is not limited to removal of entrapped air voids in the system (Power 1954). Backstrom (1958) found a reduction in air content and specific surface with a longer vibration duration while the effect on spacing factor was not significant. Blandin and Larsen (1959) found the lose

of air content deepened on slump of each mixture, and it was easier for high slump concrete to lose more air during vibration. Simon et al. (1992) studied air void system in vertical direction within a slab and found that impact of vibration on air system was limited to the radius of action, and the removal of voids during vibration involved the creation of smaller voids at the expense of larger voids. Plowman (1953) found that air could be sucked into concrete during vibration causing strength loss.

Even though the movement of air voids, or stability of air void system is affected by parameters of vibration, the compatibility of admixtures and cement in the system will affect stability of air void system as well . Cross et al. (2000) and Taylor et al. (2006) recognized that incompatibilities of admixtures and cementitious systems would cause unstable or unacceptable air void system. Among other ingredients, air entraining agents (AEA) are the primary factor to determine stability of air void system. The first one is to stabilize air voids by creating a film or layer of water at the interface of voids to prevent coalescence, hence making it harder to foam larger voids which can escape from the system easier (Dolch 1995). The other mechanism by which AEAs operate is that molecules adsorbed to the surface of air voids have their polar heads oriented in the water phase, causing separation between each other due to electrostatic repulsion (Dodson 1990, Nagi et al. 2007). Even though it is generally believed that air entrainment happens during mixing, AEAs stabilize air voids when there is air entraining into the system happening.

Stability of air void system can be determined by the foam drainage test (Taylor et al. 2006). Initially proposed by Gutmann (1988), this test method explains the potential stability of entrained air voids in paste. The foam drainage test involves preparing a mixture of paste ingredients, and agitating in a blender to create 1000 mL of foam. This foam is poured into a

graduated cylinder, and the rate at which fluid collects at the bottom of the cylinder is monitored over 60 minutes. It can also be used to determine the capacity of an AEA to produce voids in certain dosages.

Concrete internal vibrators act mostly in a rotary manner, where oscillations are generated by imbalanced rotating, and the imbalanced rotation is usually achieved by setting distance between center of weights of the vibrator and center of rotation (Anderson 1967, Ghadban 2016,). The rotation creates harmonic waves which eventually excite compression wave and shear wave in the fresh concrete. Banfill et al. (20011) found that the flow inside of radius of action is controlled by the shear waveform, while rotary motion of materials outside of this is governed by the compressive waveform. The rotation of vibrator and liquefied zone in radius of action make it possible to form a vortex in concrete(Hayduk and Neale 1978). Most vortex formation research are done with rotation on the surface (Gowda et al. 2013, Torre et al. 2006), suggesting that depth of vortex is dependent on the frequency of rotation. Formation of a vortex caused by vibration in concrete can justify the air entrainment reported by Plowman (1953).

The objective of this study is to study the changes in the air void system of hardened concrete during internal vibration with different vibration speed and durations, as well as the mechanism responsible for such change. The foam drainage test was conducted to evaluate the potential capability of AEA used in this study to stabilize voids. Concrete mixtures using the same AEA were then cast and vibrated at different vibration speed and durations. The air void system was tested in both fresh and hardened states to determine the modification in air void system caused by vibration.

5.2. Materials and mix proportion

Type I/II Portland Cement was used as chemical composition of cement is listed in Table 1. Crushed limestone with maximum size of 25 mm and specific gravity of 2.66 was used as coarse aggregate. River sand with a fineness modulus of 2.63 and specific gravity of 2.64 was used as fine aggregate.

Table 5.1. Chemical composition for Type I/II Cement

Description	wt%
SiO_2	20.05
Al_2O_3	4.38
Fe_2O_3	3.07
CaO	64.29
MgO	3.38
SO_3	2.78
LOI	2.81
Na_2O	0.14
K_2O	0.58
CO_2	1.85
Limestone	-
C_3S	66.5
C_2S	7.32
C_3A	6.42

Mix proportion for this study contained 1023 kg/m^3 coarse aggregate, 838 kg/m^3 fine aggregate, cement 335 kg/m^3 and water to cement ratio is 0.42. Target air content was 7 ± 1% and target slump was 2.5 to 5.1 cm. Chemical composition for admixtures used in this study is listed in Table 2.

5.2.1. Foam drainage test

Proposed by Gutmann (1988) and reviewed by Cross et al. (2000) and Taylor et al. (2006), foam drainage test is to used to measure the potential stability of entrained air voids in a paste. The foam drainage test comprises preparation of a mixture of paste ingredients agitating in

a blender to create 1000 mL of foam. The foam is then poured into a graduated cylinder, and the rate at which fluid collects at the bottom of the cylinder is then monitored over 60 minutes.

Using foam drainage test in this study was to determine the capability of AEA to produce foam in certain conditions. To achieve this objective, modifications were made. To simulate the similar rotational movement as vibrator, spinning speed of the test included 4K, 8K, 10K, and 12K VPM, and test durations included 10, 20, 40, and 60 seconds. Since the focus of the study was on the amount of the bubbles formed, only foam volume after spinning was recorded instead of recording changes within 1 hour.

Table 5.2. AEA and WRD combinations and compositions

Admixture	AEA	WRA
Chemical base	Fatty Acid Salts	Polycarboxylate
Density(kg/m^3)	1.006	1.07
Dosage (ml/100 kg cement)	50	325

5.3. Test Methods

5.3.1. Fresh property tests for concrete mixture

Slump for each mixes was determined according to ASTM C1611. Fresh air content was determined according to ASTM C231 Pressure method. Consolidation methods used for fresh air content test included rodding and internal vibration in various rotational speeds. Details of consolidation method are listed in Table 3. For samples using internal vibration and pressure method, the penetration depth of vibrator was 22.5 cm, which was the depth of air meter (Figure 1).

Table 5.3. Test matrix for fresh air content test

Sample ID	Vibration method/vibration rate (VPM)					Vibration duration (seconds)			
	Rod	4K	8K	10K	12K	10	20	40	60
R	✓								
4K-10		✓				✓			
8K-10			✓			✓			
10K-10				✓		✓			
12K-10					✓	✓			
12K-20					✓		✓		
12K-40					✓			✓	
12K-60					✓				✓

5.3.2. Hardened air void system for concrete mixture

After the fresh air content test, concrete was cast into 15 cm x 30 cm cylinders and consolidated using the same method and vibration rate as fresh air content test (Table 3). The penetration depth of vibrator was 12.7 cm (Figure 1), and the purpose of this depth was to investigate the influence of vibration on both top and bottom of samples. After curing, samples were cut into two pieces (top and bottom, Figure 2) for hardened air void system test according to ASTM C457.

As described in Table 4, two sets of samples were vibrated while covered with a cap on (8K-10-C, 12K-10-C) to prevent air getting into concrete during vibration. Two sets of samples were vibrated with the same vibration frequency and duration with no cap (8K-10-N, 12K-10-N). Then five sets of samples were vibrated using various frequencies with 10s vibration duration (R-10, 4K-10, 8K-10, 10K-10, and 12K-10). Three more durations with 12K vibration rate was tested (12K-20, 12K-40, and 12K-60).

Table 5.4. Test matrix for hardened sample

Sample ID	Vibration method/vibration rate (VPM)					Vibration duration(seconds)				CAPPING	
	Rod	4K	8K	10K	12K	10	20	40	60	CAP	No CAP
8K-10-C			✓			✓				✓	
8K-10-N			✓			✓					✓
12K-10-C					✓	✓				✓	
12K-10-N					✓	✓					✓
R	✓										
4K-10		✓				✓					
8K-10			✓			✓					
10K-10				✓		✓					
12K-10					✓	✓					
12K-20					✓		✓				
12K-40					✓			✓			
12K-60					✓				✓		

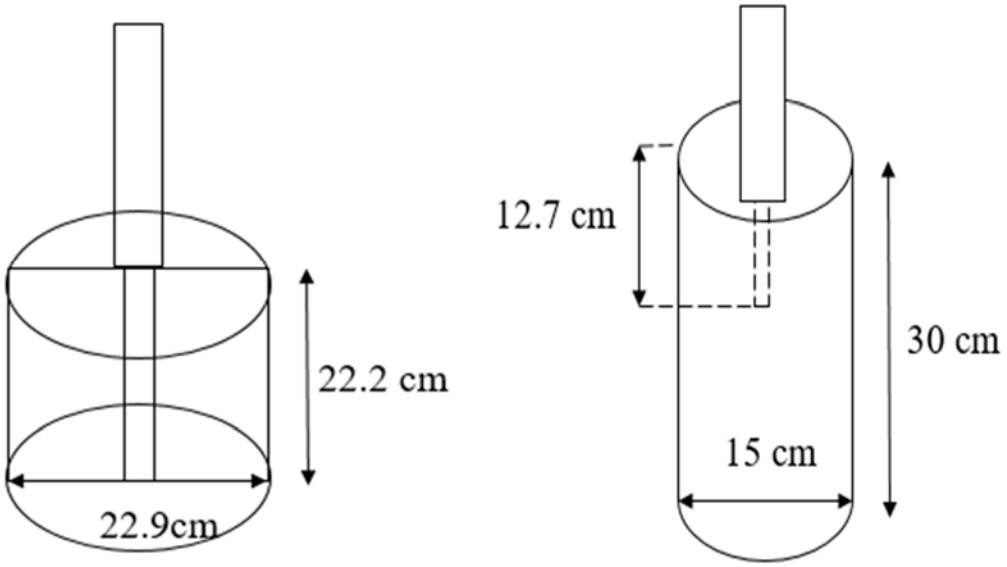

Figure 1.1. Dimensions and depth of insertion for specimens,

Left: measuring bowl for fresh air content, Right: 15 cm x 30 cm cylinder

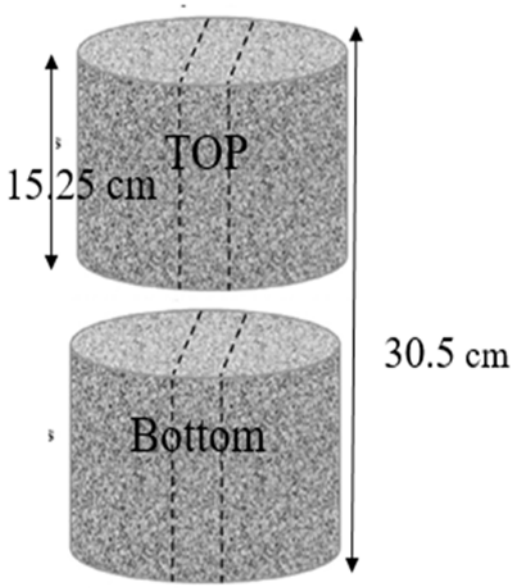

Figure 1.2. Specimen cut in to two pieces for further investigations

In order to analyze the hardened air void, the specimens were cut in half. Slices measuring 15× 15 cm were obtained from the center of the half cylinders (Figure 2). Each slice was analyzed as combination of nine subsections, with each of them measuring 5 × 5 cm. As stated earlier, the vibrator was penetrated to a depth of 12.5 cm from the surface of the investigated 30 cm height cylinders.

Average air content was determined for each sample, which is the average hardened air content for all 18 sections (9 from top, 9 from bottom). Standard deviation within each specimen was also calculated.

A contour map for air content was plotted for each sample. Based on the hardened air content determined by ASTM C457 from each section.

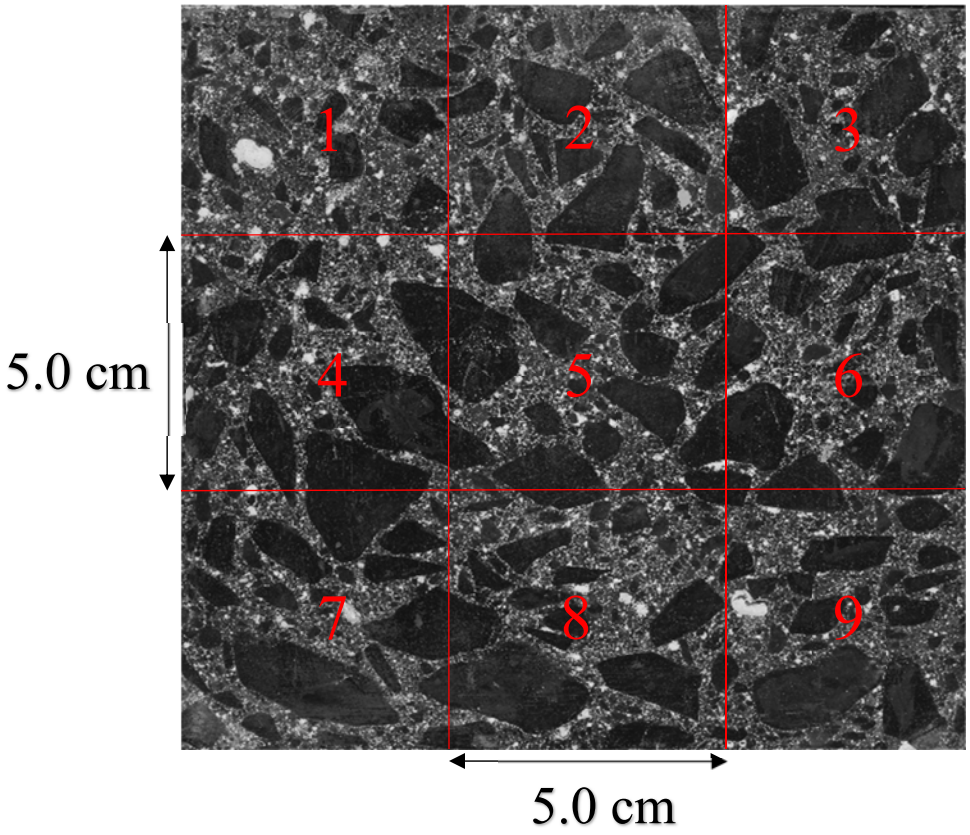

Figure 5.3. Nine sections for half of each specimen for air void system evaluation

5.4. Results and discussion

5.4.1. Foam drainage test

Figure 4 presents the foam drainage data obtained for paste system after 10 seconds of mixing with the same dosage of AEA but different mixing frequency. In general, results indicate an increase in the volume of the foam with mixing speed. However, as the volume of the foam reached a maximum amount at 10K VPM, the volume of foam was similar for 10K and 12K VPM mixing.

Similar trends were observed when the paste system was mixed for up to 60s. At a frequency of 12K VPM, the amount of developed foam reached the maximum value of 400 ml, regardless of the longer mixing time. When the mixing frequency was lower (e.g. 4K VPM) a

mixing time of 20s was necessary to reach the maximum foam content of 400 ml. This means before 20s, there is small amount of AEA in the system.

Results of this test show that for certain amount of AEA, the potential foam (or voids) produced is related to spinning speed and spinning duration, i.e., the energy input of the system. If the energy exerted to the system is not enough, either in terms of time or frequency, some of AEA will not contribute in generating/stabilizing air bubbles.

Assuming the same situation occurs in concrete mixing, the amount of AEA used in mixing stage stabilized 300 ml of voids due to the mixing conditions, but it can produce 400 ml with faster mixing speed or longer mixing time. In this case, part of AEA is not reacted or used during mixing, stirring in the system, mixing with water. Normally it will not be an issue, but if concrete sucks air voids during vibration due to the rotary movement generated by internal vibrator, then this "left-over" AEA is able to stabilize these newly entrained air voids and help them to remain in the system, until the remaining AEA is fully consumed.

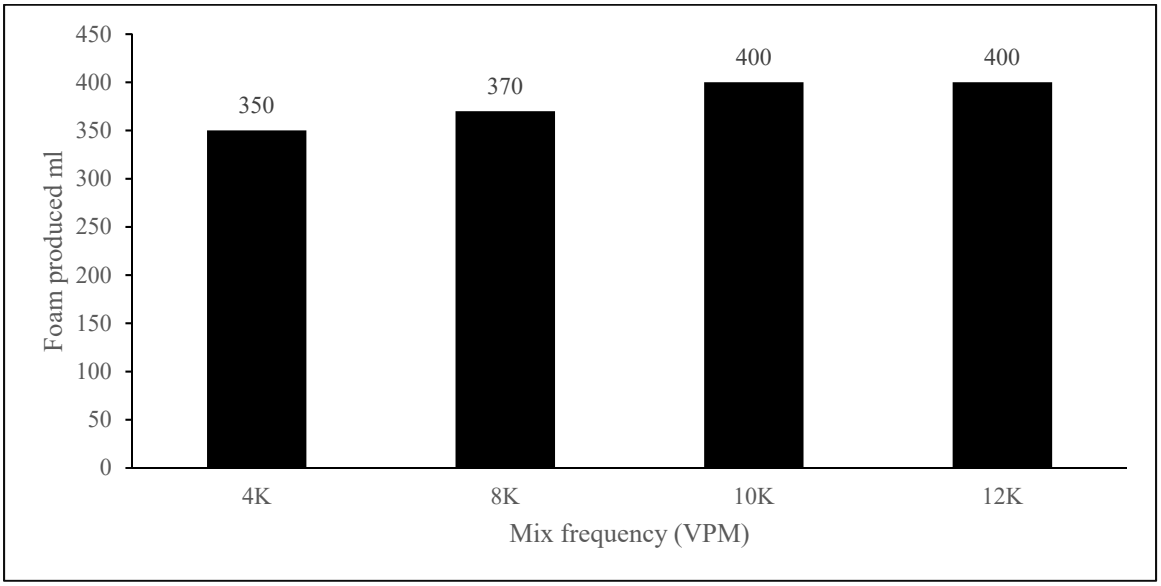

Figure 1.4. Foam produced with different speed for 10 seconds

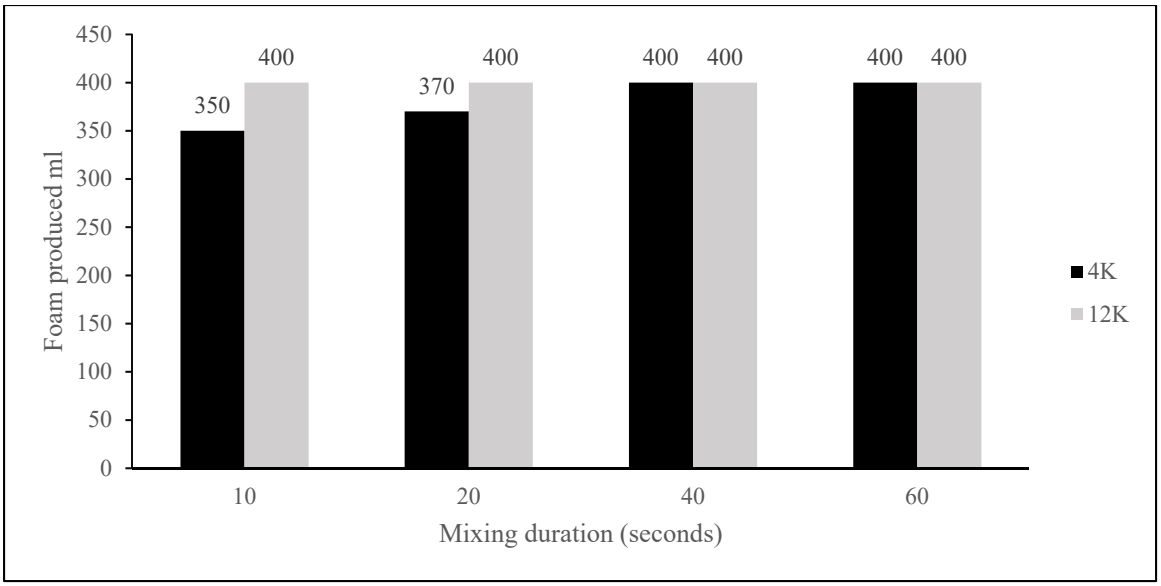

Figure 5.5. Foam produced with different durations

5.4.2. Air content of samples with cap and no cap

To confirm Plowman's finding (1953) that rotary motion of vibration may increase air content and to investigate the source of air increment during vibration, two sets of samples were covered with a plastic cap to prevent extra air getting into concrete during vibration (Figure 6), and another two sets of samples were consolidated using the same method with no cap. Average air content of hardened concrete for each set is presented in Figure 7. Fresh air content was 6%. It is generally observed that the air volume tested freshly using ASTM C 231 Pressure Method or ASTM C 173 Volumetric method would be higher than it tested by linear traverse method following ASTM C 457 (Khayat et al., 1991). This difference is usually within 0.5-1.5%, especially when air content of concrete is more than 4%. Both capped samples gave a normal hardened air content of 6.3% and 5.6%, indicating that there was no air entrainment during vibration. The no capped samples gave a higher air content with an average air content of 10.6%, which indicates an increase of up to 4.7%. This indicates that when exposed to the environment,

concrete under vibration can add air and as a result, average air content will increase, and this increment tend to be larger when using higher vibration rate.

Figure 1.6. Sample vibrating with cap to prevent air voids getting into system

It was also observed that the vibration tends to cause the cylinder molds to rotate. This is another explanation of extra air getting into concrete. Internal vibrator is making rotary movement inside the concrete, which will produce both compression and shear waves (Ghadban 2016). The rotation of the vibrator creates a forced vortex. One should also note that there is a liquid zone and rapid decay of energy near the internal vibrator because of the liquefaction and flow of the concrete (Banfill et al. 2011). Combining the two mechanisms, one can conclude that a liquefied zone is created during vibration, and the rotational movement created by vibrator

makes it possible to form vortex and suck air into the system from top. Previous observations have indicated suction of air into concrete during vibration (e.g. Plowman 1953). ACI 309 .1R (2008) also mentions that with increasing vibration intensity and decreasing pressure due to sinusoidal compression waves, large clusters of air voids can be observed.

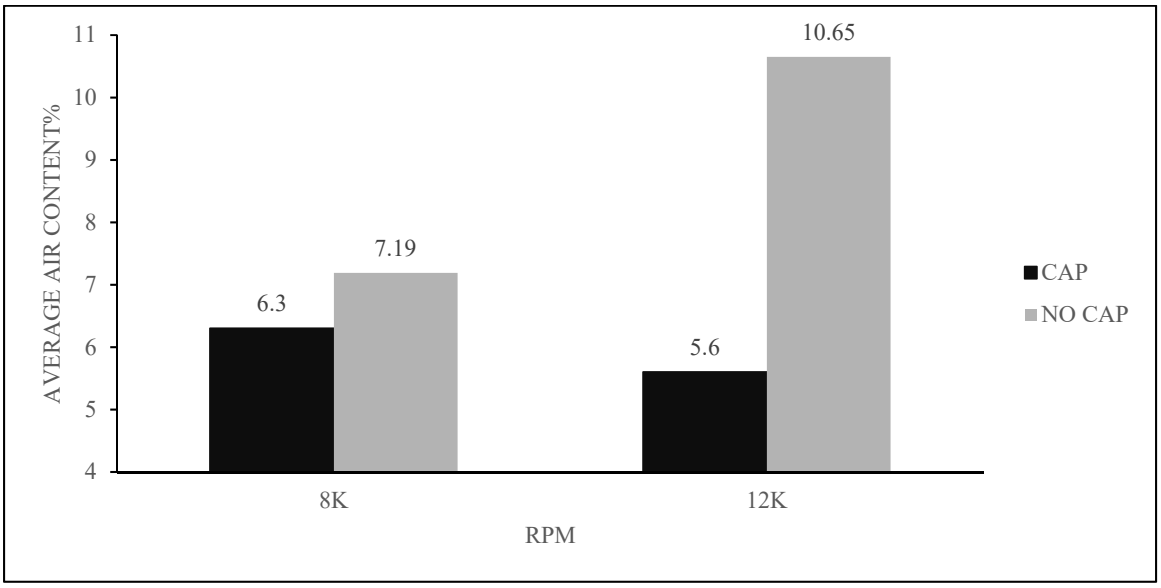

Figure 5.7. Hardened average air content with and without CAP

5.4.3. Samples vibrated using different vibration rates

5.4.3.1. Air content

Figure 8 presents the fresh air data obtained from samples vibrated at various frequencies. In general, no significant difference in fresh air content was observed for the investigated scenarios. All mixtures exhibited a fresh air content of 8.9 ± 0.2%, regardless of consolidation scenario of rodding or vibration at 4K to 12K for 10 seconds. Average air contents for hardened concrete are presented in Figure 9. Unlike the fresh stage, average air contents from hardened samples. There is a trend of increasing air content with increasing vibration rate. The average air content obtained for the rodded sample and the one vibrated at 4K VPM were slightly lower than at the fresh stage, and this is in line with the typical drop of 0.5-1.5 % as mentioned earlier.

However, an increase in hardened air content was observed at the high vibration frequency over 8K VPM. This air content increase indicates that there is air entrainment during these vibrations. With increased vibration rate, this increment tends to be larger, since the variation within each specimen is quite large. The average air content, especially for samples from 10K-10, 12K-10, cannot be used as the only indicator of air void system due to the high variation within each sample.

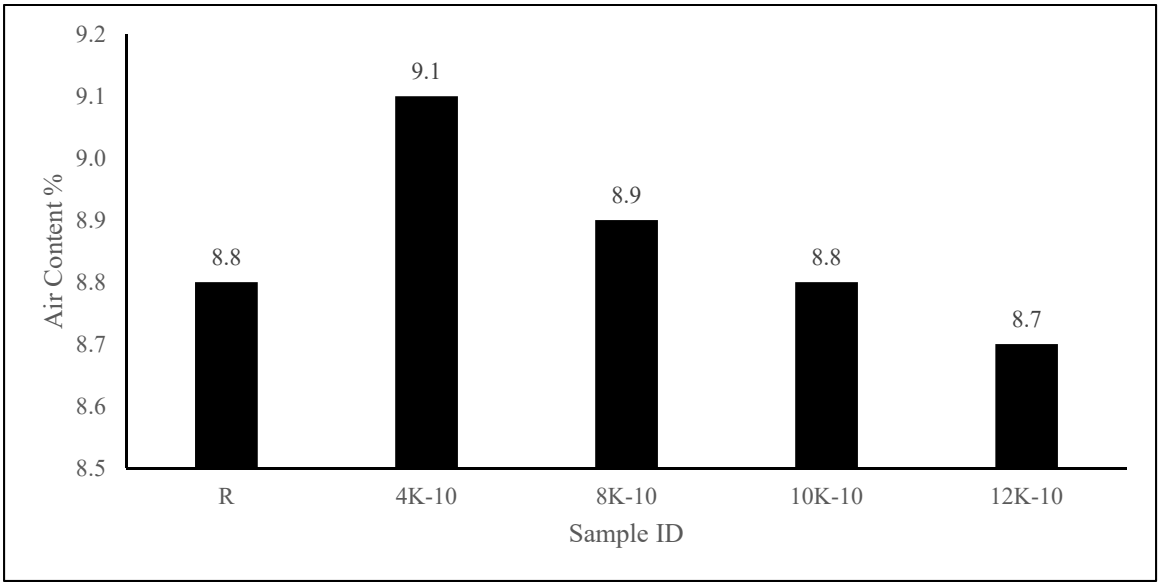

Figure 1.8. Fresh air content (%) with increasing vibration rate

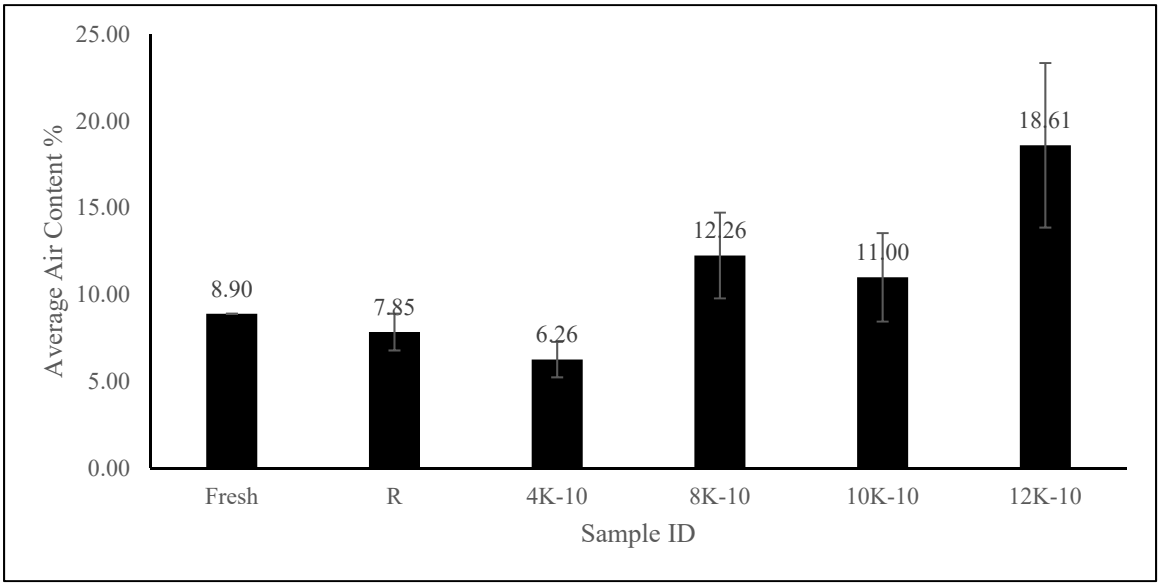

Figure 1.9. Average air content for Mix 1 increasing vibration rate (Standard deviation from left to right: (No for Fresh), 0.64, 0.96,1.72, 1.99, and 4.33)

Variation of air content within each sample is also increased with vibration rate. In addition, for samples from 12K-10 the standard deviation reached 4.33. This variation indicats that air increment observed in Figure 9 is not uniformly distributed, instead, as stated in ACI 309, it could be a cluster of air voids. Figure 4 shows a contour map for air content in each section. Vertical axis is the distance from top of specimen. There is no apparent air void cluster observed in the case of samples that were consolidated by rod and 4K vibration. However, clustering was observed for vibration frequency higher than 8K VPM, Moreover, the spots of this cluster are at 5 cm below the depth of vibrator penetration

Combining the observations from Figure 10 and the vortex theory mentioned above, the source and path of this abnormal air increment can be explained. At high vibration rate, concrete is liquefied, which makes it possible to form a vortex since the internal vibrator is making rotary movements. This vortex can suck air voids into concrete from the surrounding environment. As proved in the foam drainage test and for covered samples, if there is an access for air to entrain into concrete system during vibration, along with the non-reacted AEA, it is possible for AEA to stabilize more air voids during vibration. The trend that there is an increment of average air content can correlate with foam test results in Figure 5. Higher vibration frequencies will entrain more air voids up to the point of AEA is fully consumed.

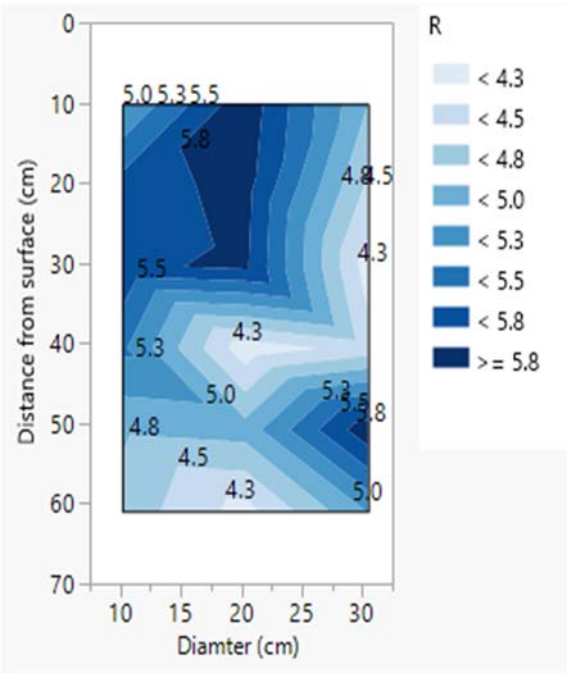

Rod

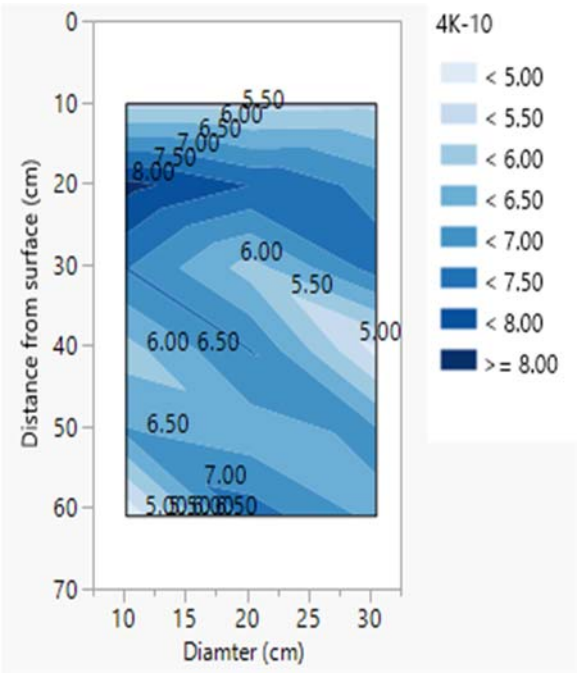

4K-10

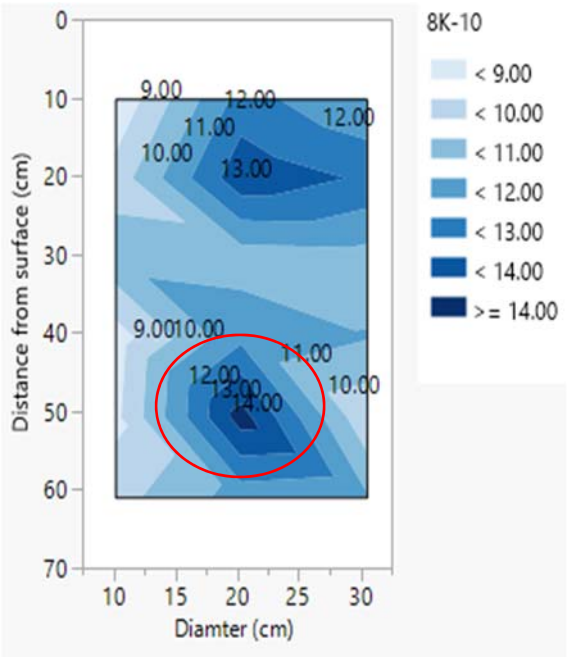

8K-10

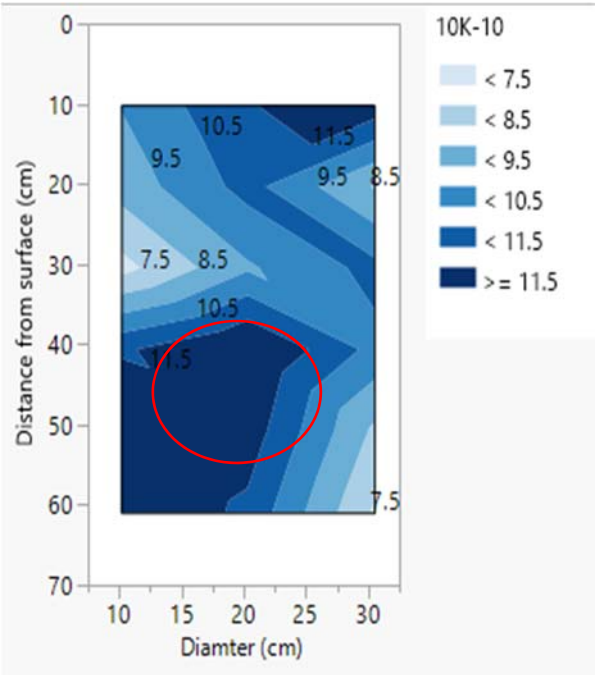

10K-10

Figure 1.10. Contour map of hardened average air content

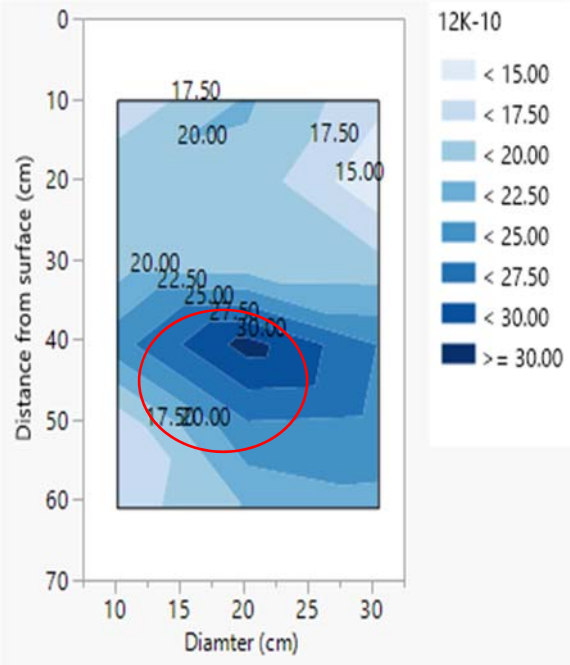

12K-10

Figure 1.10. (continued)

Fresh air content tested by air meter using various vibration rates did not change as much as the hardened state. As a matter of fact, one can conclude from these fresh air contents, that vibration, even with high frequency, has minor or no influence on fresh air content. Besides the maturity of tested concrete is widely different in pressure meter and cylinder mold. The other two major differences are the dimension of the containers and the depth of vibration. According to ASTM C231/C213 M, measuring bowl should have a capacity at least 5663 cm^3 and a minimum diameter equal to 0.75-1.25 times the height, leading to minimum of 21.3 cm as the diameter of measuring bowl. Diameter of measuring bowl used in this research is 23 cm, and the depth of penetration for vibrator was 23 cm for pressure meter.

ACI 309.1R suggests a correlation between radius of action and amplitude with 10s vibration (Figure 11). Based on Figure 11, with 1 mm amplitude, the radius of action for 8K, 10K, and 12K RPM are 19.1, 30.5 cm, and 38.1 cm, At lower frequency, even with higher amplitude (0.18 cm) at 6K VPM, the radius of action is about 17.8 cm. In other words, when vibration rate is higher than 6K VPM, depending on the depth of vibrator, it is possible that entire sample is liquefied. For air meter, only higher frequency vibrations (10K and 12K VPM) have this wide radius of action to cover entire specimen. This may explain the sudden increase of air content around of 8K. If liquefied concrete is stirred by vibrator to create vortex, then for frequency above 6K VPM, more concrete will be liquefied (perhaps entire volume of the concrete in a standard test cylinder), transferring air voids into the concrete. This increase did not happen in air meter for fresh concrete since the penetration depth is too deep to create a vortex, and loss of air did not happen given the vibration time was not long enough for air voids to escape from the system.

5.4.3.2. Chord length

Distribution of chord length at 5 cm beneath vibrator corresponding to section 5 of the tested slices is presented in Figure 12. This section was selected as the location of cluster of high air content found in Figure 10. The main difference observed for the rodded and 4K samples was the chords ranging from 10 to 100 microns. With no air entraining during this vibration, the higher number of small voids in this range indicates redistribution of air voids, which is expected for vibrated samples because it is supposed to provide a denser and more durable concrete. Results were not the same in the case of samples 8K-10, 10K-10, and 12K-10. From 8K, increase air content was no longer restrained to the 10-100 microns range. Instead, increase was observed in every range. If this increase in air content happens at certain range (say 10-100 microns) of

chord length, one could argue that this is a redistribution of air voids instead of air entrainment. In this case, increase in all ranges more likely suggests that air has been entrained from the environment.

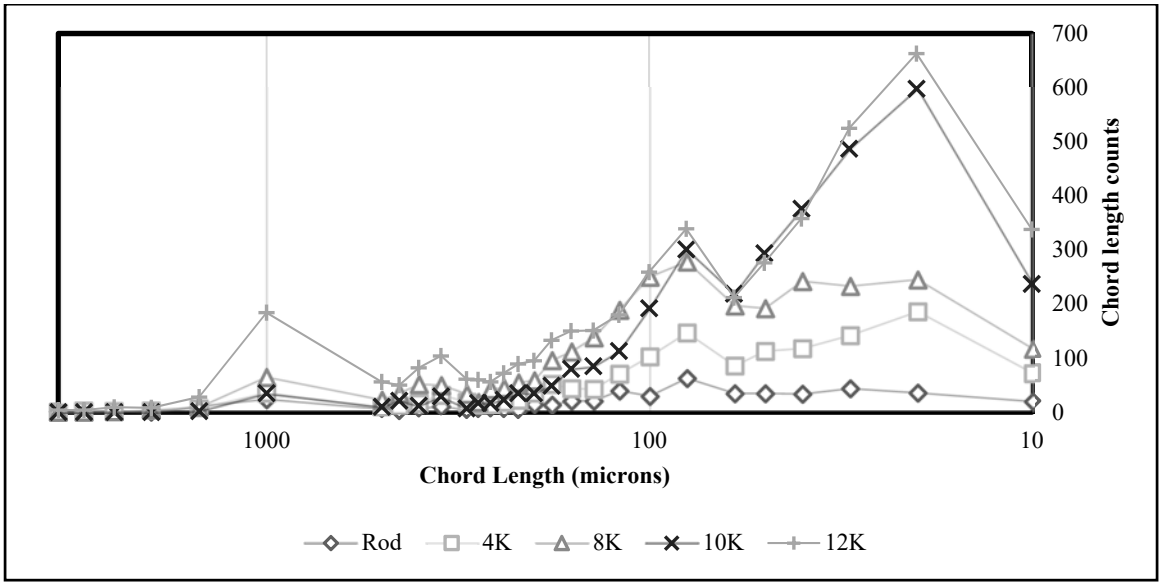

Figure 5.11. Chord length distribution for Mix 1 at 5 cm below vibrator

5.4.4. Vibration with longer durations

5.4.4.1. Air content

Fresh air content for samples vibrated using different durations are presented in Figure 13. No less of air content was observed when samples were vibrated for 10 seconds. However, samples vibrated for longer durations lose air content with increased vibration duration. As discussed above, vibrator penetration was too deep to create a vortex in air meter used for fresh air content test. However loss of air content could be observed with longer vibration durations, since voids need time to raise to the top and escape from the system.

Hardened average air content for samples vibrated using different durations are presented in Figure 14. Increased average air content was observed in all samples, and increased standard deviation within samples was also observed. In general, longer vibration duration generated

higher average air content increment. To study the difference of between increasing vibration rate and increasing vibration duration on air content, contour map for 12K-10, 12K-20, 12K-40, and 12K-60 are presented in Figure 15. It can be seen that clusters of air voids no longer occurs at the bottom of samples, instead, with increasing frequencies, these clusters occurred at the top of the samples. Raising of air voids, which is defined as merging of small voids to big voids and escaping from the system, always happens during vibration. Even during the vortex formation there are still voids that raise simultaneously, with the maximum air increase limited by AEA concentration in concrete. As discussed above, the function of AEA is to stabilize individual voids preventing them from merging to large voids and escaping from the system. With longer duration of vibration, the 'left over' AEA gets used up, so no more stabilizing the air bubbles. Hence, the vortex entrained air voids merge with each other and escape from the system, or at least to leave the system.

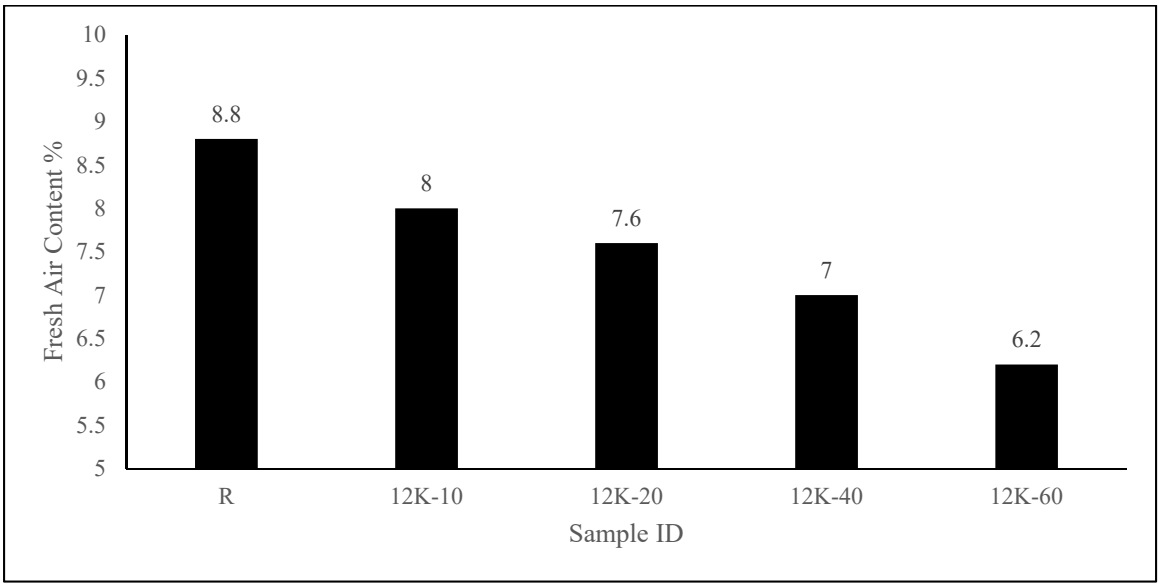

Figure 1.12. Fresh air contents with different durations

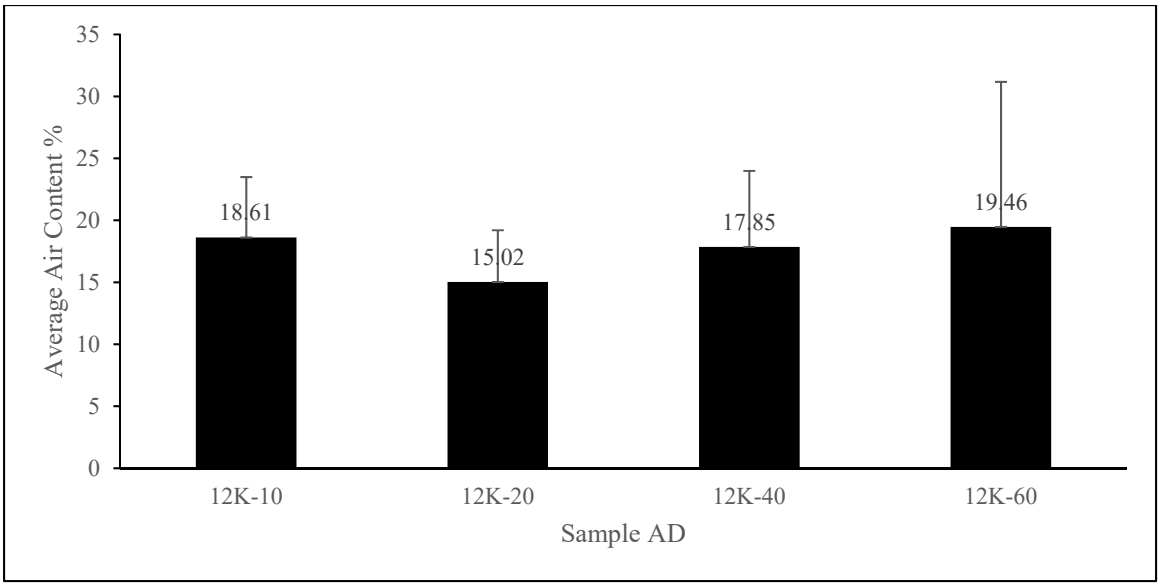

Figure 5.13. Hardened air contents with different durations

(Standard deviation 4.88, 4.18, 6.14, 11.17)

5.4.4.2. Chord Length

Chord lengths in the top parts of the specimen subjected to elongated vibration are presented in Figure 16. Longer vibration resulted in an increase in large voids (>1000 microns) and loss many voids in 10-100 microns chord length rage. As confirmed in the foam test, this vortex-air entraining would stop once AEA was used up. After this, vibration is still creating a vortex that sucks air voids into concrete, but the potential to store these voids and keep them apart from each other as small voids is no longer possible because the AEA has been consumed. The newly formed air voids have no choice but to merge with each other to become large voids ≥1000 microns and rise up to the top of the sample, eventually leaving the system, according to the observation of a considerable amount of voids over 1000 microns on top of 12K-60 sample.

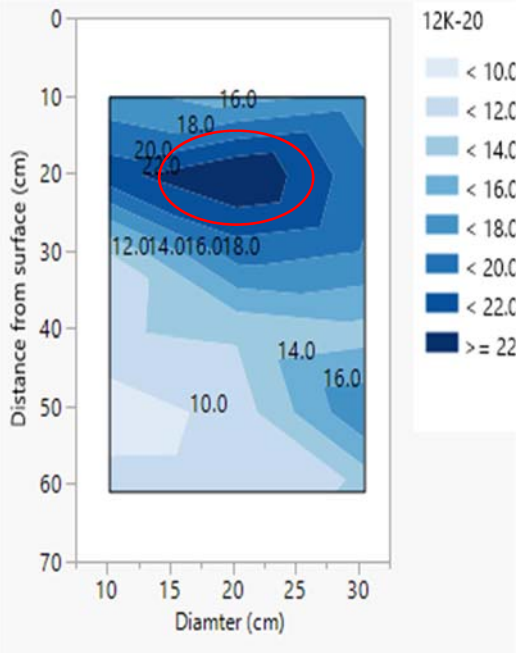

12K-20

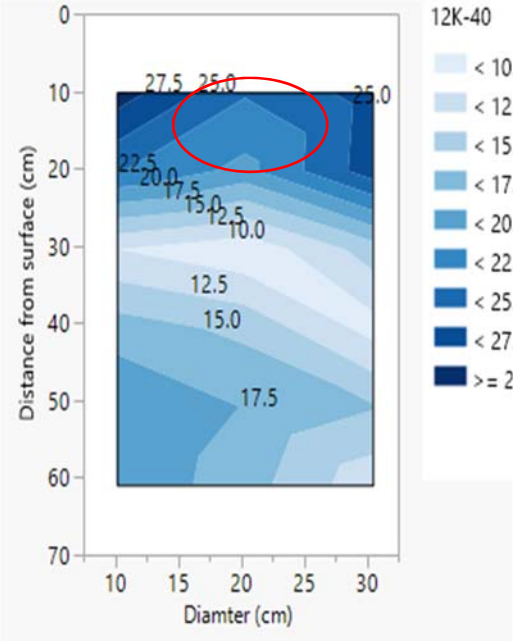

12K-40

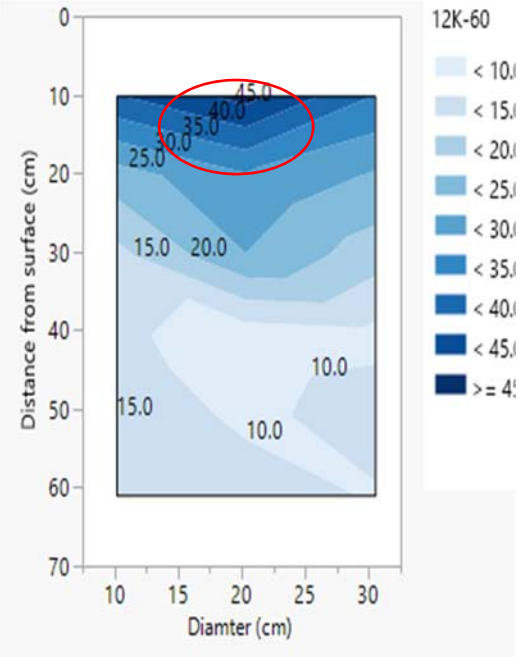

12K-60

Figure 5.14. Contour map for average air content using vibration with longer durations

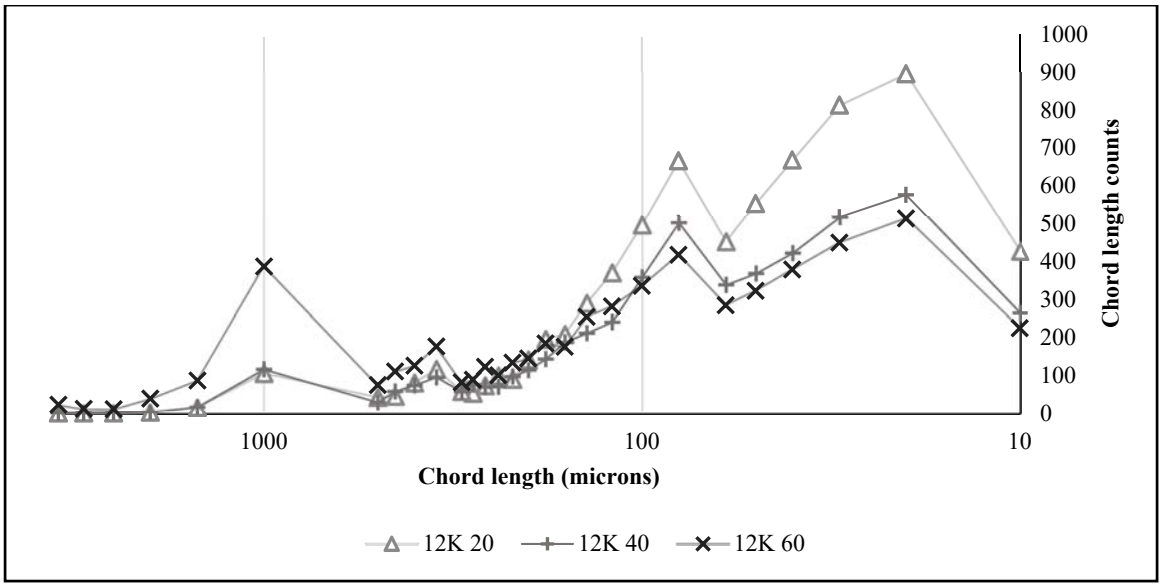

Figure 5.15. Chord length distribution for samples vibrated with different durations

5.5. Conclusions

The foam drainage results indicated that unless enough mixing energy is provided, the AEA will not reach the maximum potential for stabilizing air bubbles. Increasing mixing energy beyond this point yields negligible air entrainment because the AEA has been consumed.

Comparing the data obtained for samples vibrated with or without cover, it was found that increasing of air content during vibration is possible, and the source of air voids was from the surrounding environment. The mechanism of air increment was then proposed that rotary movement caused by vibrator created a vortex inside of liquefied fresh concrete that sucks air voids into concrete.

To confirm this mechanism and to study the influence of frequency and duration on air increment during vibration, the air void system for samples vibrated with different speed and duration were tested in both fresh and hardened status. The influence was proved dependent on size of samples, depth of vibrator injection, vibration speed, and vibration durations. At the fresh stage, there was no increase in air content increment when samples were vibrated for 10 seconds,

regardless of vibration speed. Loss of air content was observed with longer vibration time up to 60 seconds. For hardened air void systems, increasing of average air content was observed with increasing vibration speed and vibration duration, and the variation within each sample also increase with increasing vibration frequency and duration. With short vibration duration of 10s, cluster of air voids was observed at 5 cm beneath penetration point of vibrator, while no such cluster was observed at 20, 40, and 60 seconds vibration. This was believed to be caused by the fact that AEA was used up and concrete could no longer stabilize air voids, and observing that the air voids had risen to the top of the sample

5.6. Reference

Anderson, R.A., Fundamentals of Vibrations, New York: The Macmillan Company, 1967.

ASTM C125, "Standard Terminology Relating to Concrete and Concrete Aggregates," ASTM international, West Conshohocken, PA, 2018

Backstrom, J.E., Origin, Evolution and Effects of Air Void System in Concrete, Part 3- Influence of Water-Cement Ratio and Compaction, American Concrete Journal Vol.55,ACI Index, 1958

Banfill, P.F.G; Teixeira, M.A.O.M; Craik, R.J.M.; "Rheology and vibration of fresh concrete: Predicting the radius of action of poker vibrators from wave propagation", Cement and Concrete Research, 2011.

Blandin, F.H, Larsen, O. Effect of Internal Vibration of Concrete Mixtures upon the Entrained Air, Illinois Highway Engineer, Vol 11, 1959

Cross, W., Duke, E., Kellar, J., and Johnston, D. 2000. *Investigation of Low Compressive Strengths of Concrete Paving, Precast and Structural Concrete*. South Dakota Department of Transportation, Office of Research, Pierre, SD

Dodson, V.H., *Concrete Admixtures*, Van Nostrand Reinhold, New York, 1990.

Dolch, W.L., "Air-Entraining Admixtures," Concrete Admixtures Handbook, Properties, Science, and Technology, Second Edition, 1995

Forssblad, L., Investigation of Internal Vibration of Concrete, Civil Engineering and Building Construction Series, No.29, Stockholm, 1965

Ghadban, A.A.; PhD Dissertation, Kansas State University, 2016.

Gowda, B.H.L., Akhuli, S., Anudeep, B.R., Kishore, K., Influence of Base Inclination on Vortex Formation during Draining from Cylindrical Tanks, Indian Journal of Engineering & Materials Sciences, Vol. 20, 2013.

Hayduk, W., Neale, G., T, Vortex Formation in Stirred Draining Vessels, The Canadian Journal of Chemical Engineering, Vol. 56, 1978

Jagger, P.B., "Vibrating Table to Ensure Homogeneity in Cast Concrete Pieces," Cement Age, Vole 11, 1910.

Legg, F.E., Efficiency of Vibrators in Consolidating Paving Concrete, Final Report, DRDA Project 320351, 1974

Nagi, M.A., Okamoto, P.A., Kozikowski, R.L., and Hover, K., "Evaluating Air-Entraining Admixtures for Highway Concrete," NCHRP Report 578, Transportation Research Board, 2007.

Plowman, J.M. The Influence of Variables in the Vibration of Concrete, Concrete Building Construction Products, 28, 1953

Power, T.C., "Void Spacing as a Basis for Producing Air-entrained concrete," *Research Bulletin,* 49, Portland Cement Association, Journal of the American Concrete Institute, 1954, pp. 741-760

Simon, M.J., Jenkins, R.B., and Hover, K.C., The Influence of Immersion Vibration on the Void System of Air Entrained Concrete, Durability of Concrete, G.M.Idorn International Symposium, ACI Speical Publication, SP-131, American Concrete Institute, 1992

Taylor P.C., Johansen V.C., Graf L.A., Kozikowski, R.L., Zemajtis J.Z., and Ferraris C.F. 2006. *Identifying Incompatible Combinations of Concrete Materials, Volume II—Test Protocol*. Federal Highway Administration, Research, Development, and Technology, Turner-Fairbank Highway Research Center, McLean, VA.

Taylor, P; Wang, X; and Wang X; “Concrete Pavement Mixture Design and Analysis (MDA): Evaluation of Foam Drainage Test to Measure Air Void Stability in Concrete" (2015). InTrans Project Reports. 119.

Torre, J.P., Fletcher, D.F., Lasuye, T., Xuereb, C., An Experimental and Computational Study of the Vortex Shape in a Partially Baffled Agitated Vessel, Chemical Engineering Science, 62, 2007.

Zheng, X.H., Yong, G., Yuan, J., Influence of Air Content and Vibration Time on Frost Resistance of Air Entrained Concrete, Advaced Material Research, Vol.857, 2013

CHAPTER 6. INFLUENCE OF INTERNAL VIBRATOR ON AIR VOID SYSTEM AND AGGREGATE DISTRIBUTION

Xin Wang, Xuhao Wang, Seyehamed Sadati, Peter Taylor, Kejin Wang

Abstract

Internal vibration is a commonly used consolidation method for concrete. Influence of internal vibration on air void system is believed to remove entrapped air voids and some entrained air voids if excessive vibration is applied. However, air voids can be sucked into the system during vibration and cause increasing of air content, and if this phenomenon is affected by chemical base of air entraining agent (AEA) is not clear. At the same time, this excessive vibration could cause segregate of coarse aggregate in concrete.

This study is aim at evaluating the influence of chemistry of AEA on increasing air content caused by internal vibration. To develop a method to evaluate potential of segregation in pavement concrete, concrete mixtures were prepared and cast into 15 cm × 30 cm cylinders. Using foam drainage test and linear traverse method from ASTM C457, it was found that increasing air content for samples experienced excessive vibration would occur when using different types of AEA, but the distribution of air voids within sample will be different. Using digital image processing method, spacing between particles and mortar to aggregate ratio can be obtained, and these two parameters can be used to evaluate the potential of segregation in the system. Moreover, fabric tensor is used to measure the tendency of moving for coarse aggregates during vibration.

6.1. Introduction

Proper vibration can enhance the air void system of concrete by removing entrapped air voids, at the same time, it allows contractors to place concrete with relatively low water cement (w/c) ratio. Entrapped air voids are defined as those 1 mm or larger in width and irregular shape, which are produced due to insufficient mixing or consolidation (ASTM C125). Entrapped air voids provide little benefit to concrete hardened properties like freeze-thaw (F-T) durability and may decrease concrete strength (Power 1954). Proper consolidation, which usually involves vibration, can eliminate internal friction between particles, producing a denser and more durable concrete (Banfill et al. 2011, ACI 309 2008).

Excessive vibration will cause loss of entrained air voids and segregation of coarse aggregate (Iowa DOT 1999, Kosmatka and Wilson 2016). Concrete vibration methods include internal vibration, surface vibration, form vibration, and table vibration. Among different types of vibrations, internal vibration is most commonly used
vibration method. Internal vibration is described by its frequency, amplitude, time, or acceleration. These parameters affect the energy input of the vibrator. As a result, It will affect the quality of vibra tion (ACI 309 2008).

Researchers found that vibration could affect the air void system more than just removing entrapped air voids. Backstrom (1958) found increasing vibration durations would reduce total air content and specific surface. Simon et al. (1992) studied air void system changes in the vertical direction within a slab and found that impact of vibration on air system was limited within the radius of action, and they claimed that removal of bubbles during vibration involved the creation of smaller bubbles at the expense of larger bubbles. Plowman (1953) found that concrete cast into molds may be rotational during vibration and air could be sucked into the

system. Using foam drainage test, Wang et al. (2018) found that compatibility of admixture and cement would affect air void system stability in concrete, and stability can be determined by testing both fresh and hardened air void system parameters after mixing.

Segregation is usually associated with excessive vibration and poor quality concrete. Segregation describes the tendency of coarse aggregate to separate form mortar. There are two types of segregation in concrete, dynamic segregation and static segregation. Excessive vibration usually causes dynamic segregation (ACI 238, Hamed and Smally 1972).Segregation of concrete may provoke cracking. because of differential drying shrinkage between areas of differing paste contents (Legg 1975, Kosamtka and Wilson 2016. It is generally believed that coarse aggregate with higher specific gravity will settle causing other ingredients of concrete go up during segregation (Petrou et al. 2000). This settlement of coarse aggregate will occur when the attraction force between the cement particles is overcome by the energy input from vibrator (Banfill et al. 1999). It is related to the density difference between coarse aggregate and the mortar, size of aggregate, drag coefficient, and viscosity of fresh concrete (Navarrete and Lopez 2017). Hamed and Smally (1972) found that increasing acceleration of vibrator would increase segregation, at a constant frequency, while increasing frequency reduced segregation by little bit. They also proposed a third type of segregation, which is not restricted to concrete. During vibration, a mixture of coarse and fine particles tend to separate from each other, and coarse particles tend to rise up while fine ones go down. This type of segregation is called percolation, or Brazil nut effect (Kudrolli 2004, Tang and Puri 2004). There are no reports of percolation segregation in concrete In 2015, Wang et al. applied a digital image processing (DIP) method to evaluate cross sectional images of SCC. By determining the inter-particle spacing of coarse aggregate and average mortar thickness, they were able to use these two parameters to evaluate

the aggregate distribution system in hardened SCC samples. Han et al. (2016) used two-dimensional image analysis method to evaluate both aggregate distribution and aggregate orientation in concrete. There is a potential to apply these methods to evaluate the aggregate distribution in normal slump concrete.

In Part I of this study (Wang et al. 2018), the concrete air void system is measured before and after it was internally vibrated by at multiple speeds with the vibrator inserted vertically into the sample. It was found that when concrete was vibrated at high frequency (over 7000 VPM) there was an increase in air content inside 15 cm × 30 cm hardened concrete cylinders. By measuring the air content variation inside each sample, it was found that this increment of air content was higher than at 5 cm beneath the tip of the vibrator. It was found that the vortex formed by rotary movement of internal vibrator inside the liquefied concrete sucked air into the concrete from the surface. It was hypothesized that unused air entraining agent (AEA) inside the concrete stabilized these bubbles.

In this paper, the influence of partial merged internal vibration on concrete air void system with different types of AEA was studied. Using a foam drainage test (Taylor et al. 2006), the compatibility of two combinations of AEA and WRA were determined, and these two combinations were then used for concrete mixtures. Aggregate distribution characteristics included inter-particle spacing and mortar thickness index were determined using DIP method to study the potential of segregation for concrete consolidated with internal vibrator. Fabric tensor was used to determine the orientation of coarse aggregate in concrete, indicating the tendency of aggregate movement.

6.2. Experimental program

Two concrete mixtures with two combinations of admixtures were prepared to evaluate the influence of internal vibration on air void system and aggregate distribution.

6.2.1. Materials and mix proportion

Two combination of admixtures were tested using foam drainage test to determine the compatibility between admixture and cement. These two combinations were then used in concrete mixtures. Chemical composition of admixtures is listed in Table 1, and chemical composition for Type I cement used in this study is listed in Table 2.

Table 6.1. Chemical base of admixtures

Combination	AEA chemical base	WRA chemical base
1	Visol-Rosin	polycarboxylate
2	Fatty Acid Salts	polycarboxylate

Table 6.2. Chemical composition for Type I cement

Description	%
SiO_2	20.05
Al_2O_3	4.38
Fe_2O_3	3.07
CaO	64.29
MgO	3.38
SO_3	2.78
LOI	2.81
Na_2O	0.14
K_2O	0.58
CO_2	1.85
Limestone	-
C_3S	66.5
C_2S	7.32

Mix proportion for both mixtures is listed in Table 3.

Table 6.3. Mix proportion for Mix 1 and Mix 2

Materials	Specific gravity	Amount (kg/m^3)
Coarse Aggregate	2.66	1023
Fine Aggregate	2.63	838
Cement (Type I)	3.15	335
Water	-	141
w/c ratio	-	0.42
Target Air %	5-6	
Admixture dosage	Combination 1 for Mix1 (50 ml/100kg cement for AEA, 325 ml/100kg cement for WRA) Combination 2 for Mix 2 (20 ml/100kg cement for AEA, 325 ml/100 kg cement for WRA)	

6.2.2. Testing and analysis methods

6.2.2.1. Foam drainage test

Two combination of admixture were tested using foam drainage test to evaluate compatibility of each combination. Proposed by Gutmann (1988) and reviewed by Cross et al. (2000) and Taylor et al. (2006), foam drainage test was developed to measure the potential stability of entrained air bubbles in paste. The foam drainage test comprises preparing a mixture of paste ingredients, and agitating in a blender to create 1000 mL of foam. This foam is poured into a graduated cylinder, and the rate at which fluid collects at the bottom of the cylinder is then monitored over 60 minutes. . The volume of fluid (V_d) is plotted against the inverse of time (1/t). The data are modeled to estimate the volume (V_0) of fluid collected (Equation 1). This equation was proposed by Erbring and Peter (1941) as an exponential kinetic function for final drainage stage for gravitational foam drainage (opposed to high pressure drop foam drainage). Decreasing V_0 indicates systems that may be considered more stable and less likely to collapse in the field.

$$V_d = V_0 - 1/(k \times t) \qquad \text{Equation 1}$$

Where

V_d = Volume of water at time t

V_0 = estimated initial liquid volume in the foam at t=0 (before drainage started)

t = time

k = slope of the V_d vs 1/t plot

Chapter 1 Air void system test

Concrete mixtures made with each combination were cast and vibrated using internal vibrator at different frequencies. Matrix of vibration rate and sample ID is listed in Table 4. Fresh air content was tested in accordance with ASTM C231 using pressure method.

Table 6.4. Matrix for frequency of internal vibration and sample ID

Mixture	Sample ID	Rod	Frequency vibration per minute (VPM)			
			4,000	8,000	10,000	12,000
1	1-R	✓				
	1-4		✓			
	1-8			✓		
	1-10				✓	
	1-12					✓
2	2-R	✓				
	2-4		✓			
	2-8			✓		
	2-10				✓	
	2-12					✓

After mixing, concrete was cast into cylinders with 15 cm diameter and 30 cm height, and then cylinders were consolidated according to Table 4. The internal vibrator used in this

study was a controlled speed vibrator with 1 mm amplitude and 2.4 mm head diameter. The depth of insertion of vibrator was 12.7 cm (Figure 1). The purpose of selecting this depth was to investigate the influence of vibration on both top and bottom of samples. It also meant that part of the head of the vibrator was exposed to the air above the surface of the concrete. Samples were cast and moisture cured in accordance with ASTM C192 for 28 days. After curing, samples were cut into two pieces (top and bottom, Figure 2) for hardened air void system analysis according to ASTM C457 and aggregate distribution analysis.

For hardened air void system analysis, each specimen had a top and bottom piece with an area of 235 cm2 , and each piece was divided into 9 sections for comparison, each with an effect area of 25 cm2 (Figure 3). Each section was tested according to ASTM C457 using Rapid Air. The traverse length used in this study for Rapid Air was 2413 mm and paste content was taken to be 31% based on the mixture proportions. Average air content and standard deviation of air content were determined from all 18 sections from each sample. Air content for each section was also used to plot the contour maps with JMP®

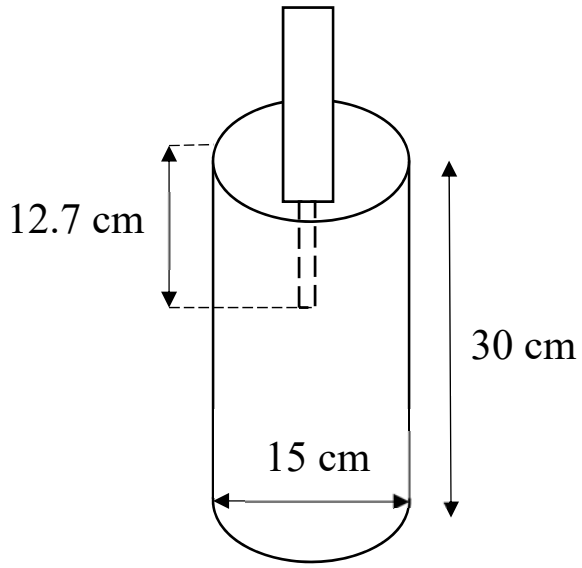

Figure 6.1. Dimension and position of vibrator for cylinders

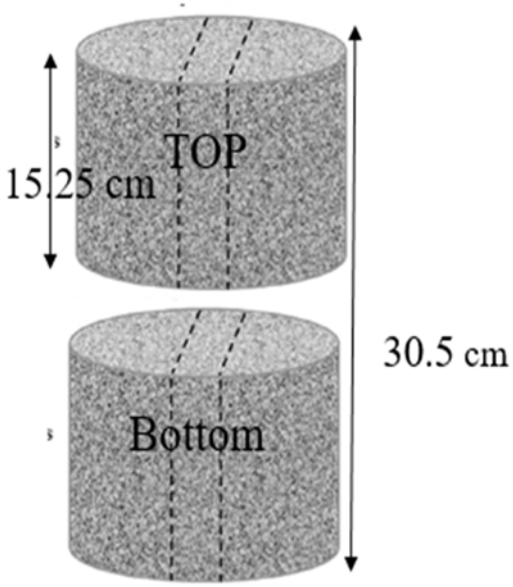

Figure 6.2. Specimen cut in to top and bottom

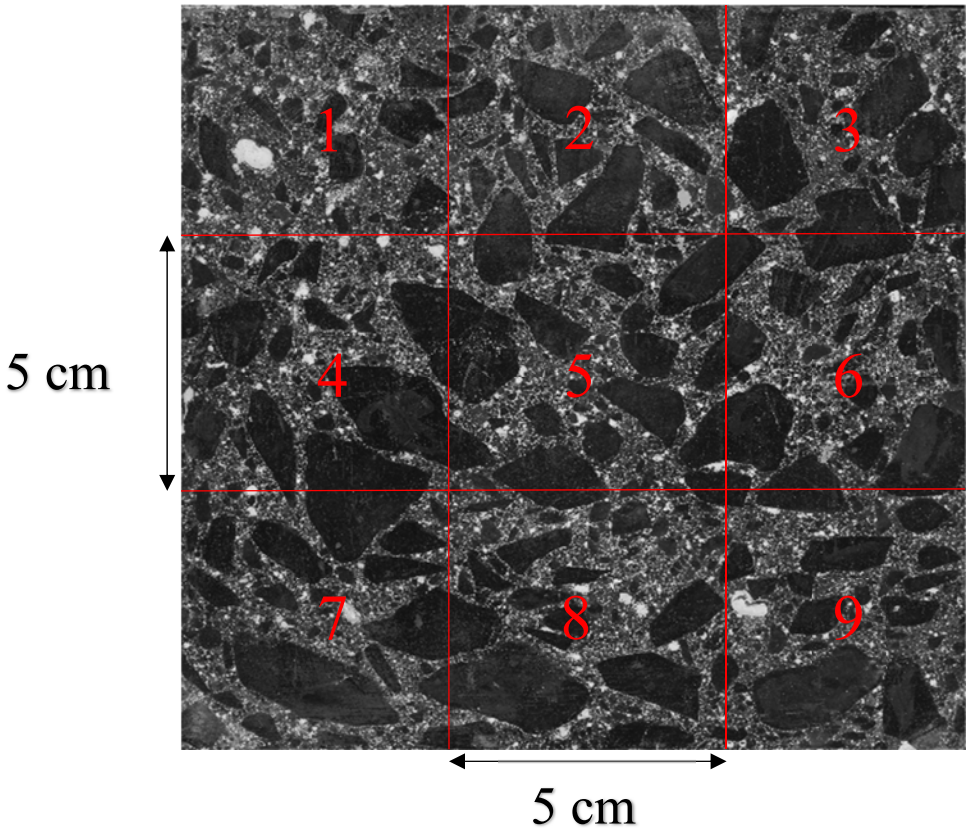

Figure 6.3. Nine sections for half of each specimen for air void system evaluation

6.2.2.2. Aggregate distribution test using digital image processing

The digital image processing method used in this study was introduced by Wang et al. (2015). Specimens were cut into discs and polished in accordance with ASTM C 457 (Fig 2). After polishing, coarse aggregates (4.75 mm to 25.40 mm in particle size) were colored manually using a black permanent marker, to enhance the contrast. After preparation samples were photographed using a single-lens reflex camera (Figure 4).

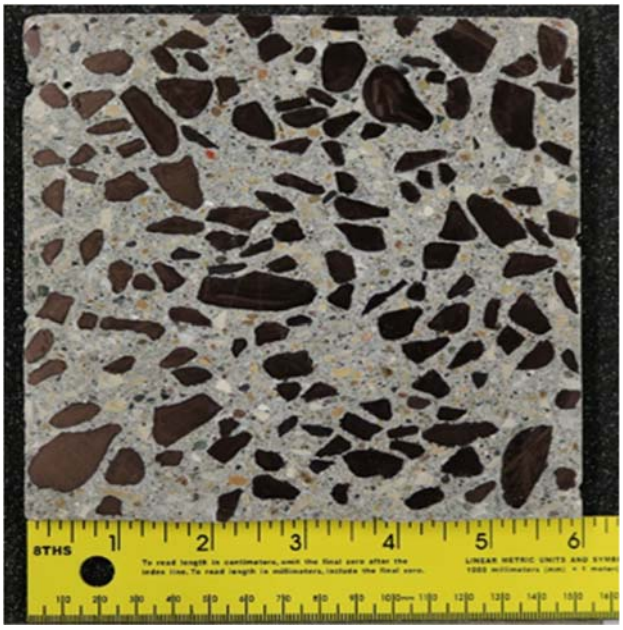

Figure 6.4. Concrete sample with marked aggregate for image analysis

Three algorithms were developed in MATLAB® to derive a binary image (Figure 5 C) for following post-processing steps. These steps include: Converting the image into a gray scale image, then apply Otsu's method (Otsu 1979) to assist with separating aggregate particles from background. An algorithm by Ozen and Guler (2014) is applied to screen out the particles whose lengths of the diameter of a fictitious circle having the same area as the particles, are smaller than 4.76 mm (#4 mesh sieve).

The centroids of each aggregate particle were found through algorithm developed in MATLAB® for each image (Figure 5 D). Delaunay Triangulation Algorithm, a surface triangulation scheme, was applied to analyze the spatial distributions of the particles. This algorithm triangulates a point set ensuring no point in the point set falls in the interior of the circumcircle of any triangle in the triangulation, meaning there will be no four points in the point set are co-circular. At the same time, the minimum angle of each triangle was maximized during triangulation process to avoid skinny triangles, so the built triangles tend to be in similar size.

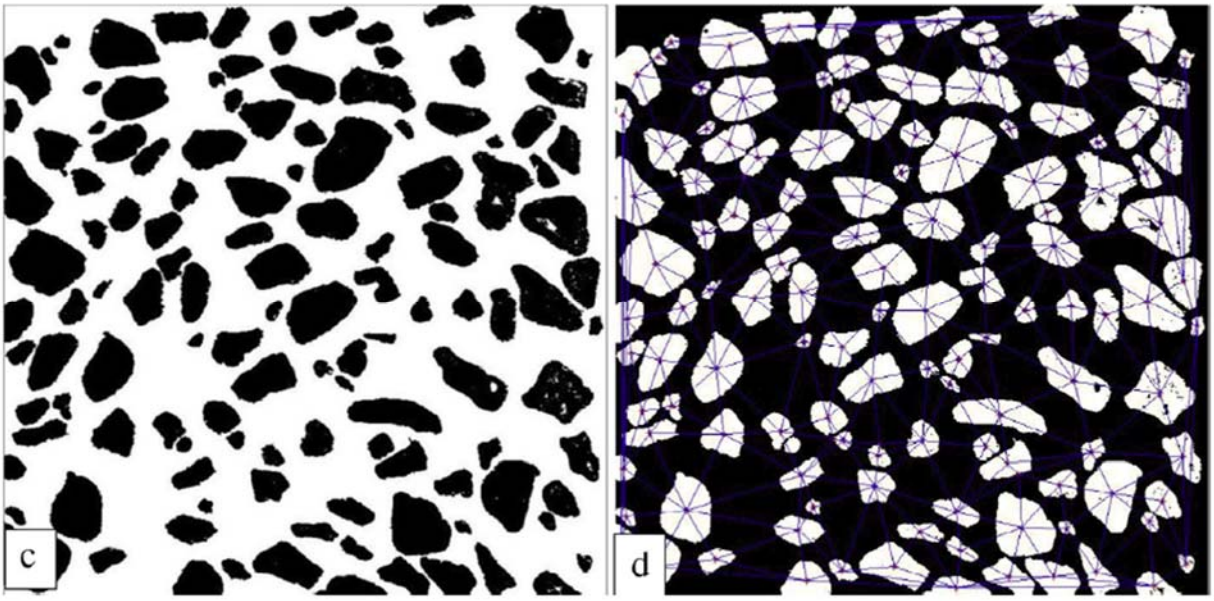

Figure 6.5. Image processing procedure

Left: Binary image used for post-processing steps

Right: Binary image with marked centroids of particles and Delaunay triangles

- Inter-particle spacing between coarse aggregates (IPS)

Inter-particle spacing, which is the length of each edge between the centroid of the particles, is calculated using Delaunay Triangulation Algorithm (Figure 6). Using all triangle lengths from each sample, a histogram of frequency is given in Figure 7, and the histogram data

from Figure 7 can be used to plot Figure 8, the curve of counts for inter-particle spacing. This curve can indicate which range of spacing is majority in aggregate distances

- Average mortar to aggregate ratio (MAR)

Using Delaunay Triangulation Algorithm, the mortar to aggregate volume ratio within each triangle formed by three aggregates (Figure 6) was determined. Mortar to aggregate ratio is determined by area of A divided by cumulative area of B1, B2, and B3. Similar histogram as Figure 7 can be built for mortar to aggregate ratio as well, and the results can be used to plot the curve of counts for mortar to aggregate ratio.

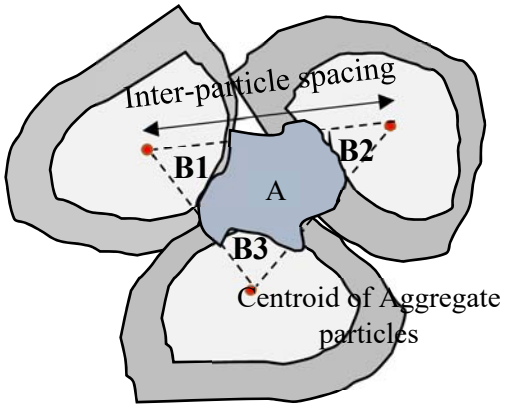

Figure 6.6. Determination of inter-particle spacing and mortar to aggregate volume ratio

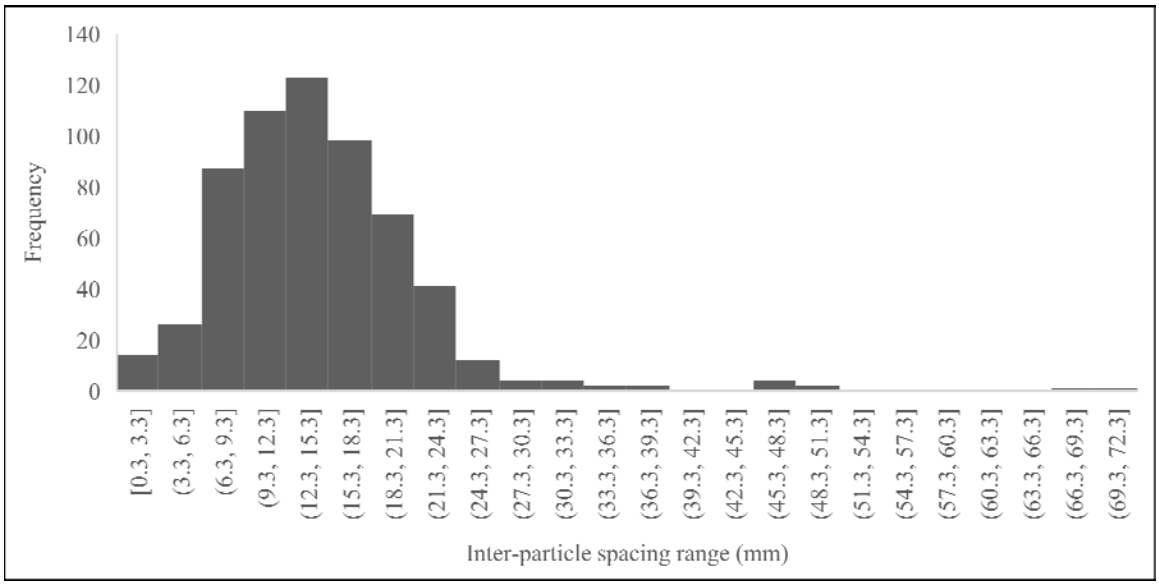

Figure 6.7. Histogram of inter-particle spacing between particles

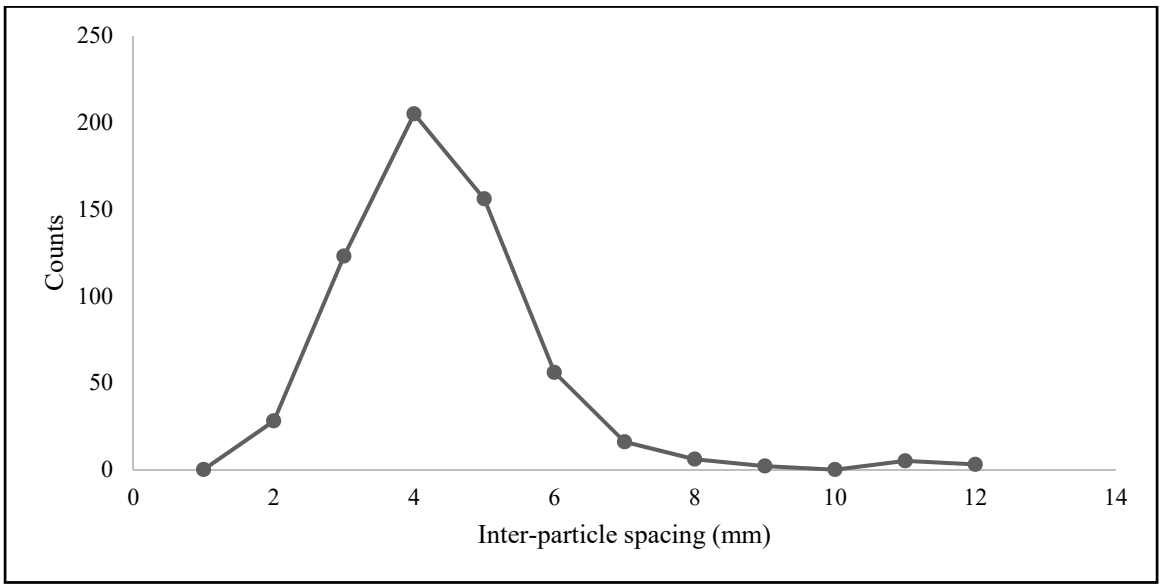

Figure 6.8. Inter-particle spacing count curve

- Aggregate Orientation

Oda and Nakayama (1989) introduced a three-dimensional index indicating the anisotropy of granular soil particles formed by preferred orientation of each particle, fabric tensor. Two unit vectors $\mathbf{n_i}$ **and** $\mathbf{n_j}$ were used to label the direction of a particle. Direction of **n** is

parallel to the longest axis if the particle is ellipsoid in shape and is perpendicular (Figure 7 A) to the major phase if a platy particle is concerned (Figure 7 B). A tensor $\mathbf{F_{ij}}$ is then introduced as

$$\mathbf{F}_{ij} = \int_n n_i n_j E(\mathbf{n}) d\Omega \quad (i,j = 1,2,3) \qquad \text{Equation 1}$$

in which n_i (i=1,2,3), n_j (j=1,2,3) = component of a unit vector **n** projected on the orthogonal reference axes x_i (i=1,2,3). Ω is a solid angle corresponding to the entire surface of a unit sphere ($\Omega = 4\pi$). The spatial distribution of **n** is described as a density E(**n**). This density should ensure that E(**n**)dΩ corresponds to the rate of unit vectors oriented within a small solid angle dΩ, and E(**n**) must satisfy

$$\int_{\Omega} E(\mathbf{n}) d\Omega = 1$$

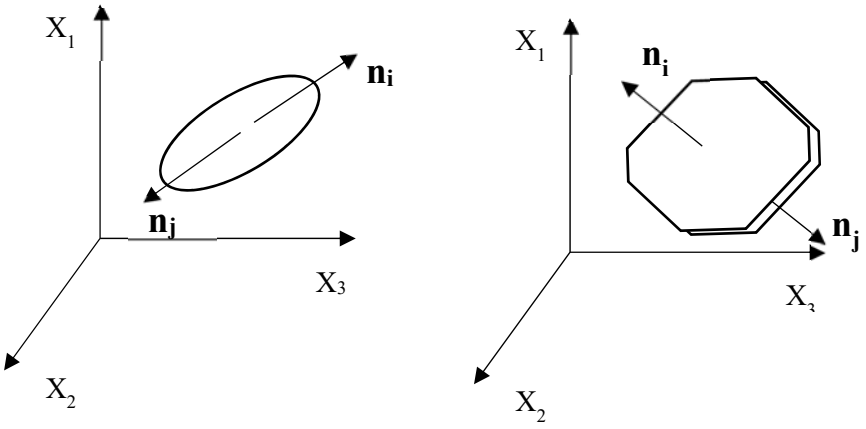

Figure 6.9. Unit victors $n^{(+)}$ and $n^{(-)}$ showing directions of typical particle

Left: Granular particle; Right: Clayey particle

Assuming particle is cut into vertical and horizontal sections (Figure 8). Let **m** be a unit vector in the direction of the longest axis of a particle on one of the sections, then Equation 1 becomes

$$\mathbf{F}_{ij} = \int_n mimj\, E(\mathbf{m}) d\Omega \ (i,j = 1,2)$$

With Ω=2π since all **m** are on a plane now.

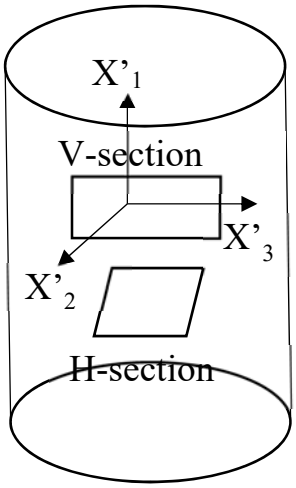

Figure 6.10. Particle cut with vertical and horizontal sections

Taking out vertical section from Figure 10, which contains only horizontal axis x'3 and horizontal axis x'1, a plane is presented in Figure 11. Let θ be an inclination angle of a unit vector m to axis x'3. Since m1 and m3 are sin θ and cos θ, the components of F ij from equation 4 becomes

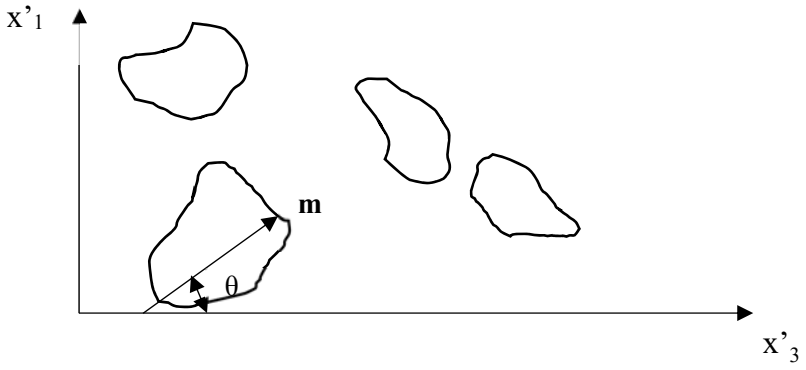

Figure 6.11. Determination of orientation and intensity of aggregate using fabric tensor

F11 $= \frac{1}{M} \sum_{k=1}^{M} \sin 2\theta$

F13 $= \frac{1}{M} \sum_{k=1}^{M} \sin\theta \cos\theta$

F33 $= \frac{1}{M} \sum_{k=1}^{M} \cos 2\theta$

In which M is the total number of measurements

The second-rank tensor **Fij** can then be converted to two principle values $\mathbf{F_1}$ and $\mathbf{F_3}$ as the following

$$\binom{\boldsymbol{F1}}{\boldsymbol{F3}} = \frac{1}{2}\ (\mathrm{F11} + \mathrm{F33}) \pm \sqrt{\left[\frac{1}{4}(\mathbf{F11} - \mathbf{F33}) + \mathbf{F13\hat{}2}\ \right]} = \frac{1}{2}\ (1 \pm \Delta)$$

where Δ is an index indicating the intensity of the preferred orientation of particles among the surface.

This study applied **Fij** on for coarse aggregate distribution analysis, to determine the orientation of each particle to X'_3 and intensity of these particle orientations among the vertical surface. The outcomes of analysis are orientated angle θ and intensity Δ. θ is the angle of aggregate to horizontal in degree, and intensity Δ is the how many aggregates are oriented in this direction. Combination of these two parameters can estimate the movement of coarse aggregates during vibration.

6.3. Results and discussions

6.3.1. Air void system

6.3.1.1. Stability of air void system

Compatibility of admixture combination 1 and combination 2 was tested by foam drainage test and presented in Figure 12. The y-intercept is recorded as V_0, which is an indication of the compatibility of a combination of admixtures. The objective is to determine the potential air stability during concrete transportation, handling, and finishing, in this case, vibration. Combination 1 yielded a V_0 of 25.0 ml, while combination 2 had a V_0 of 214.3 ml. It can be

predicted from V_0 that concrete mixtures containing combination 1 (Mix 1) would have a more stable air void system during vibration compared with those containing combination 2 (Mix 2).

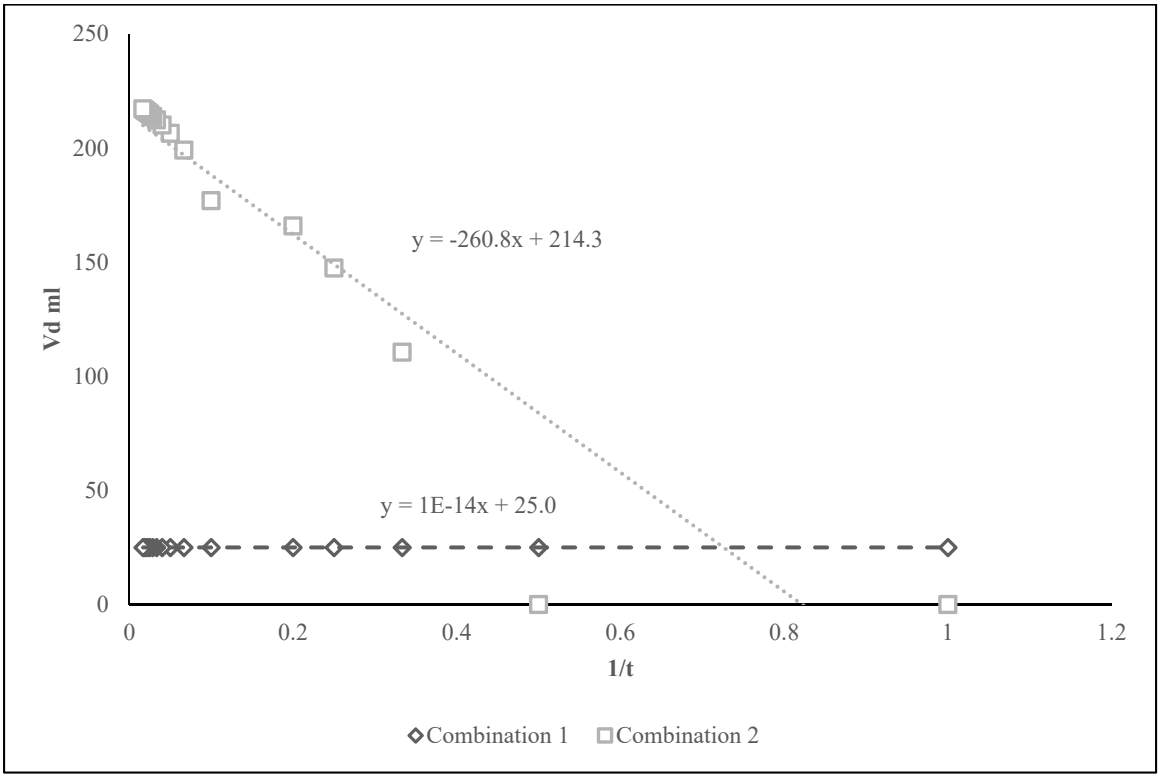

Figure 6.12. Foam drainage results

6.3.1.2. Average air content

Fresh air content for Mix 1 was 8.3%, and for Mix 2 was 8.9%. Average air content of hardened concrete for both Mix 1 and Mix 2 are presented in Figure 13. Increasing average air content higher than fresh state is observed in both Mixes with increasing frequency. It was expected that only the admixture combination with good compatibility (Mix 1) would be able to stabilize air bubbles during vibration while Mix 2 were expected to lose air. In fact, air increase was observed in both mixes. This suggests that the potential for entraining air through a vortex created by vibration is not affected by chemical base of admixtures.

The unexpected increase in average air content started from 8000 VPM in both mixes. This can be explained by radius of action. Radius of action is defined as the visible liquefied zone around a vibrator (Banfill et al. 2011). According to ACI 309.1R, With 1 cm amplitude, the radius of action for 8000, 10000, and 12000 VPM are 19.1, 30.5 cm, and 38.1 cm. This suggests that when frequency is over 5500 VPM, it is possible that entire concrete cylinder with 15 cm diameter is liquefied, which may create a stronger vacuum that suck more air in to the system.

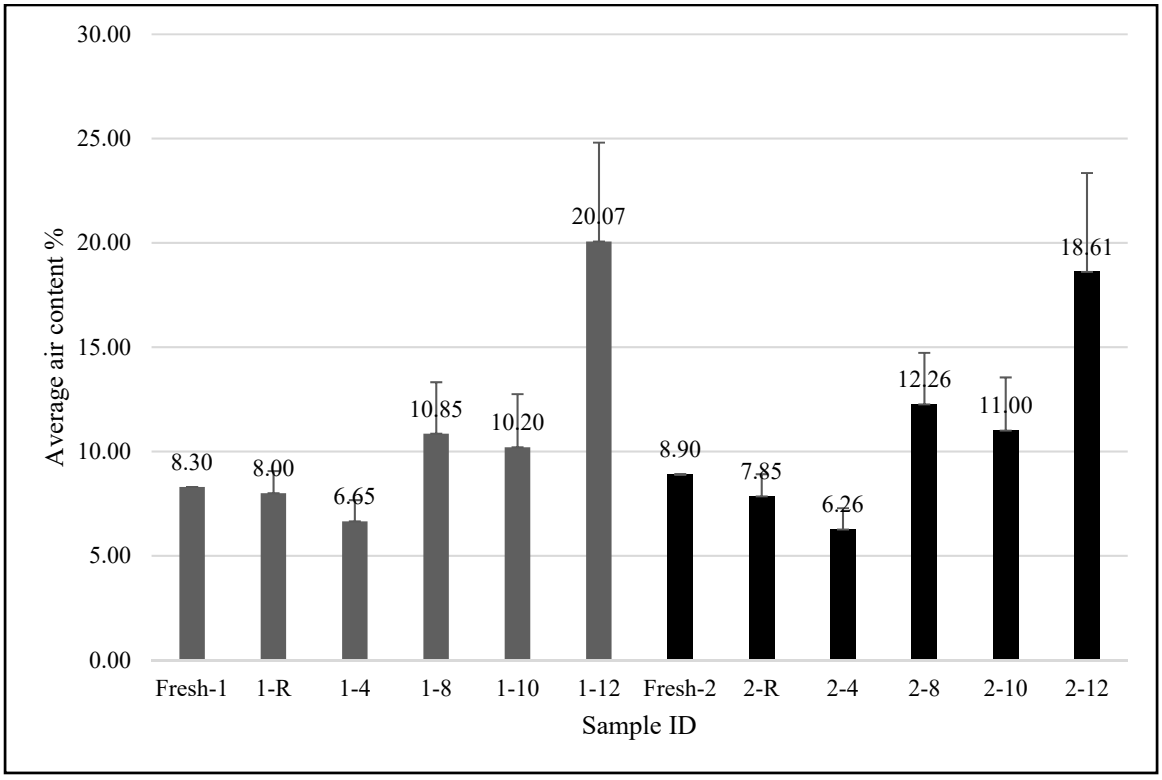

Figure 6.13. Average air content for Mix 1 and Mix 2

In samples with high average air content (above 10%), samples from Mix 2 had higher standard deviation than samples from Mix 1 vibrated with the same frequency. In order to investigate the air content distribution after vibration with various frequencies, contour maps on air content were developed based on the 18 sections of each sample (Figure 14, Figure 15).

Hardened air content for 1-R and 1-4 is close to fresh air content, which is expected. Air content for hardened samples are usually lower than fresh air content (0.5-1.5%) (Khayat et al. 1991). Standard deviations for 1-R and 1-4 are 0.64 and 1.00, showing a well distributed air void system since there is no significant difference within 30 cm below the surface of each sample. For higher frequencies, increase in air content can be found in every sample, and the amount of increase can not be explained as redistribution of air voids. Depending on the frequency, the increase of air content at one section to fresh air content was as large as 22%. At the same time, air content for section 8 of each bottom sample (5.0 cm below vibrator) is higher than most sections, proving that this could be the spot where air get into the. Air content for 2-R and 2-4 was less ideal. The standard deviations for them are 1.06 and 1.02. In 2-R, the difference of air content between top and bottom of the specimen is 3.0%, which shows instability of the system. For frequencies over 4000 VPM, a cluster of air bubbles is not observed in Mix 2 at 5.0 cm below the vibrator, instead, it was observed at the surface of specimen.

Results from foam drainage test in Figure 12 indicated that admixture combination used in Mix 2 is less stable than Mix 1. Comparison between Figure 14 and Figure 15 confirmed the instability of air void system in Mix 2. It appears that bubbles in Mix 2 merged with each other and rose up to top of the specimen, as shown in Figure 15.

6.3.2. Aggregate distribution and tendency of aggregates movement

Wang et al. (2015) and Han et al. (2016) used DIP and Two-dimensional image analysis to evaluate coarse aggregate distribution in static concrete. Inter-particle spacing (IPS), mortar to aggregate ratio (MTR), were main parameters to determine the aggregate distribution and evaluate the segregation potential. Fabric tensor was used to estimate the tendency of aggregate movement during vibration.

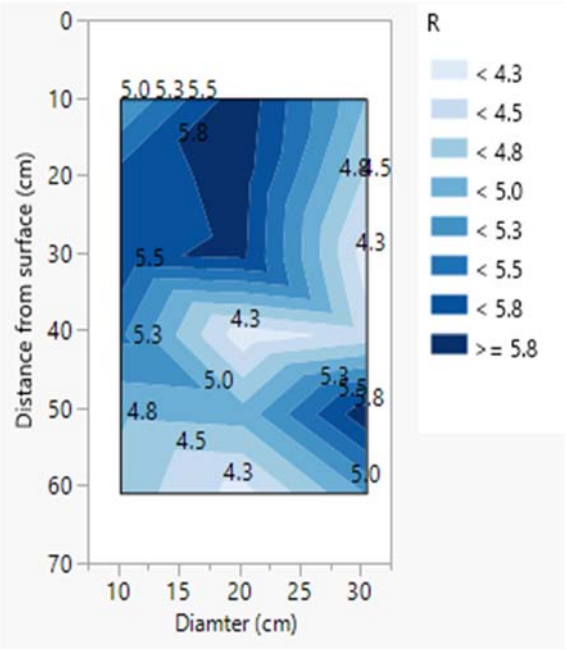

1-R

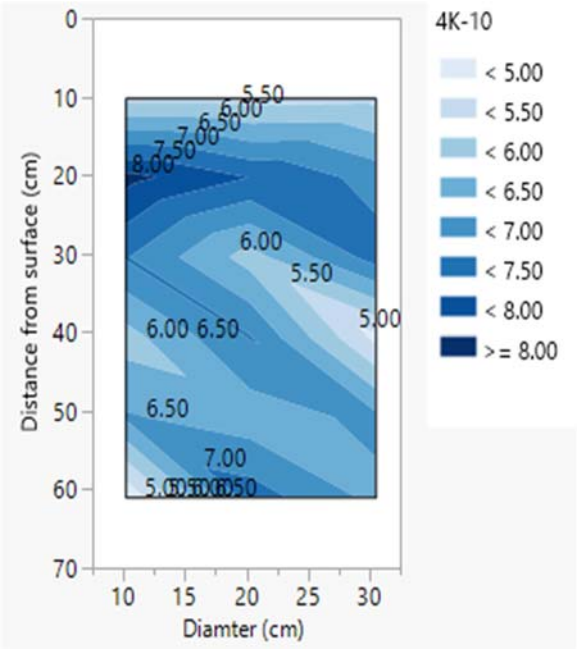

1-4

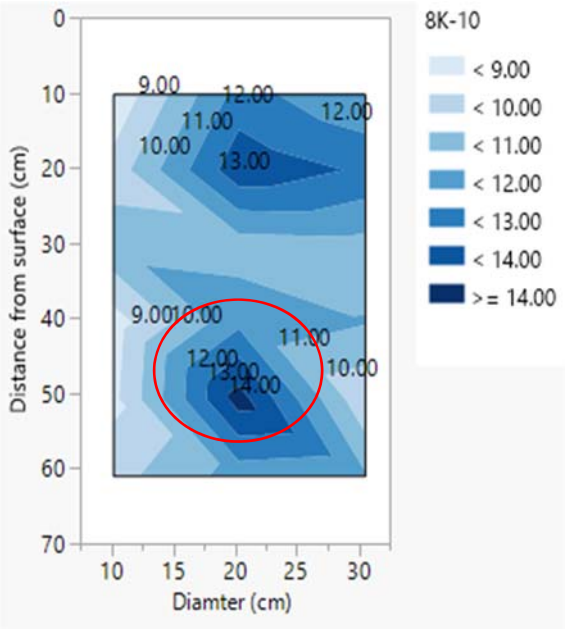

1-8

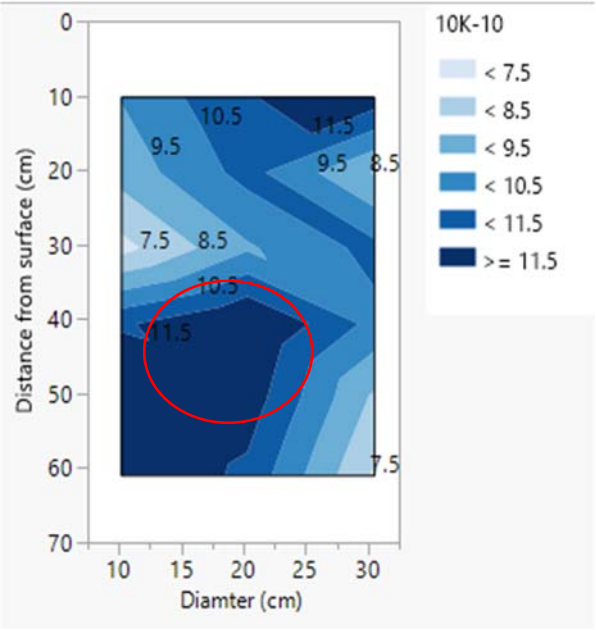

1-10

Figure 6.14. Contour map of air content for Mix 1

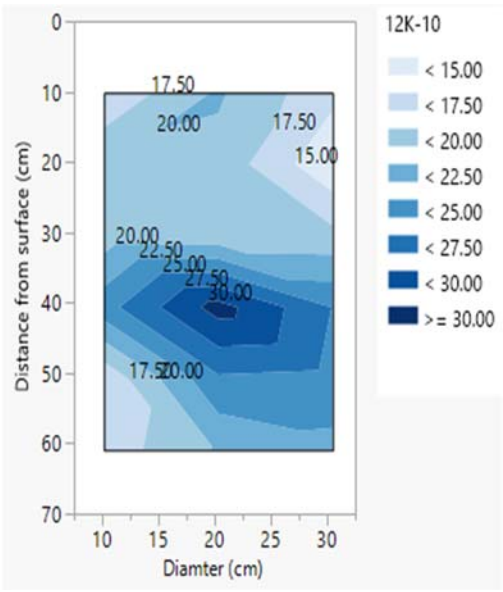

1-12

Figure 6.14. (continued)

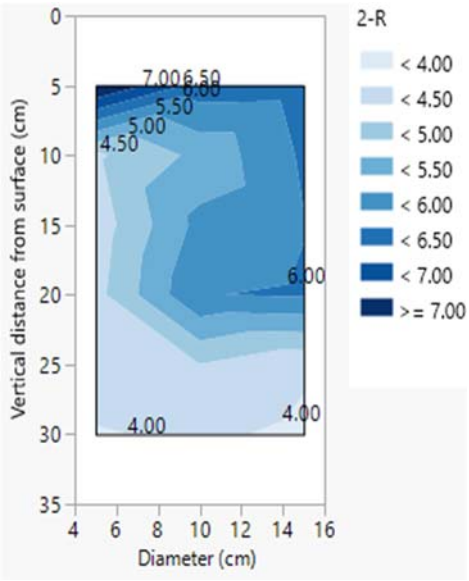

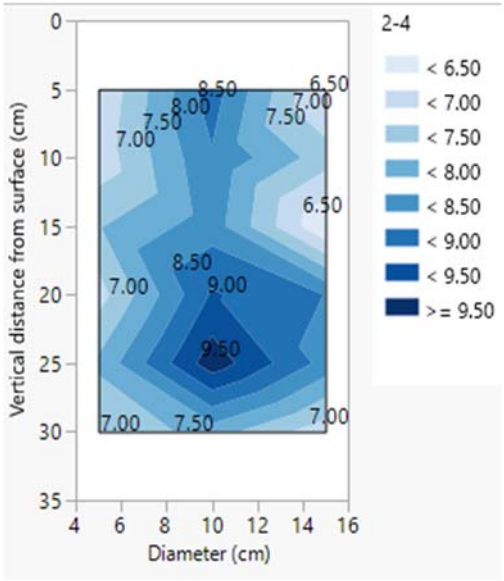

2-R **2-4**

Figure 6.15. Contour map of air content for Mix 2

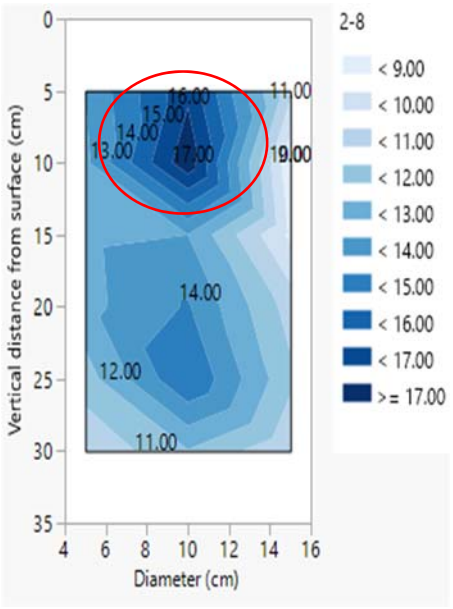

2-8

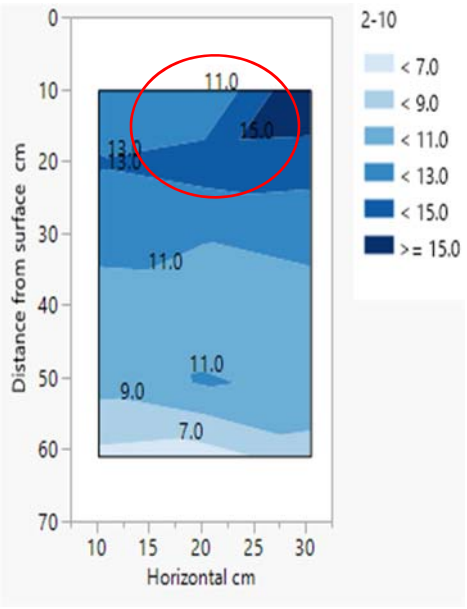

2-10

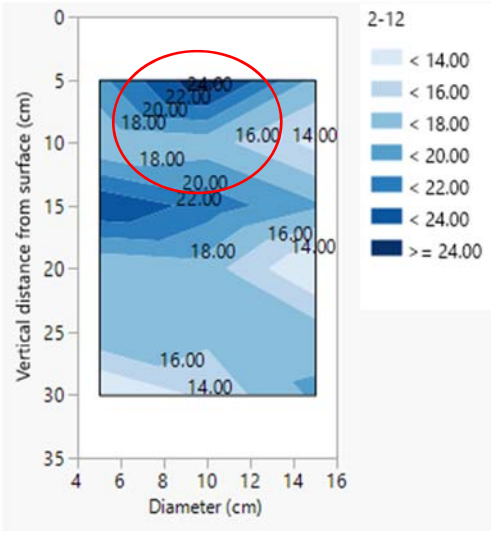

2-12

Figure 6.15. (continued)

6.3.2.1. Inter-particle spacing

Average IPS and standard deviation between aggregates with diameter larger than 4.75 mm for each vibration frequency for Mix 1 and Mix 2 is listed in Table 5. The difference in

inter-particle spacing between top and bottom is negligible for samples consolidated by R or vibration with 4000 VPM for both Mix 1 and Mix 2. This indicates that moderate internal vibration will not affect the aggregate distribution for low slump concrete, which is lower than 7000 VPM per recommended as the lowest operating rate for internal vibrator in ASTM C192C192M. For samples vibrated by frequency over 7000 VPM, difference of standard deviation between top and bottom became larger. With this and the fact that vibrator only injected into the mold at12.7 cm, it can be concluded that high frequency vibration will affect aggregate distribution, and vibration speed and injection depth of vibrator are both affecting aggregate distribution.

Lower average IPS means coarse aggregates are closer to each other, which could be a sign of segregation. During high frequency vibration, coarse aggregates that were close to vibrator (top of the sample) would sink, while coarse aggregates on bottom were less affected. As a result, coarse aggregates on top of the sample were more compacted to each other due to the vibration, while in bottom the average distance was similar to samples consolidated with rodding.

A scatter of counts for average inter-particle spacing can be plotted for each sample (Figure 16, Figure 17, and Figure 18). In Figure 16, counts for distance between particles are quite similar for top and bottom within each sample. 1-4 had more counts in 5 mm to 20 mm while 1-R has more count above 20 mm, and average distance for 1-4 was smaller than 1-R for both top and bottom. This indicates that vibration with 4000 VPM brought aggregates closer to each other comparing with rodding.

Table 6.5. Average inter-particle spacing between coarse aggregates and standard deviation for Mix 1 and Mix 2

Mix 1										
Sample ID	1-R-B	1-R-T	1-4-B	1-4-T	1-8-B	1-8-T	1-10-B	1-10-T	1-12-B	1-12-T
Avg inter-particle spacing (mm)	14.53	14.67	13.99	13.54	14.11	14.54	14.52	14.74	14.25	13.40
Std deviation (mm)	7.62	8.62	8.49	7.76	8.93	7.45	6.31	9.17	6.81	7.13
Mix 2										
Sample ID	2-R-B	2-R-T	2-4-B	2-4-T	2-8-B	2-8-T	2-10-B	2-10-T	2-12-B	2-12-T
Avg inter-particle spacing (mm)	13.39	13.82	13.74	14.17	13.42	14.11	13.56	13.54	14.69	12.69
Std deviation (mm)	8.76	7.66	7.65	7.49	8.21	8.52	7.2	11.68	8.97	8.33

In Figure 17, for both 1-10-T and 1-12-T, more counts can be seen in 5 mm to 20 mm on top of sample comparing with 1-10-B and 1-12-T, which is proving that aggregates are closer on top part than bottom. Figure 18 gives similar trend. This could happen either due to the aggregates are clustering together on top, or due to more aggregate particles were found in the top part, which was called percolation of particles (Kudrolli 2004).

Both standard deviation and count for average distance between coarse aggregates can determine the aggregate distribution of samples, and they are able to distinguish the minor difference between the top and bottom of one sample vibrated with high vibration speed. There is a potential for using average distance between particles to determine the level of segregation in low slump concrete consolidated by any types of vibrator.

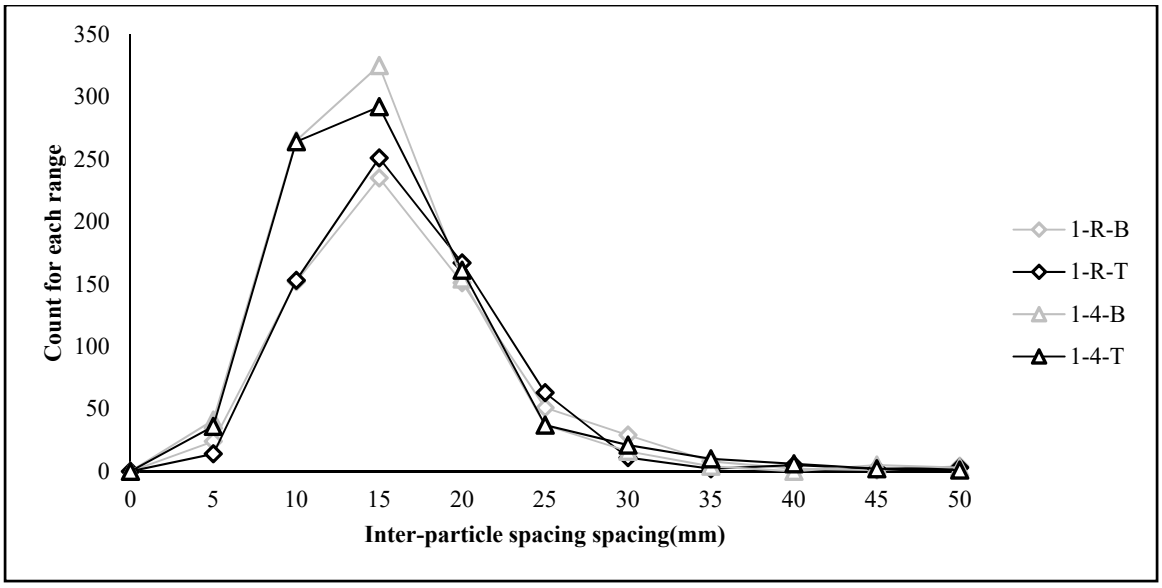

Figure 6.16. IPS counts Mix 1 (Vibration and Rodding)

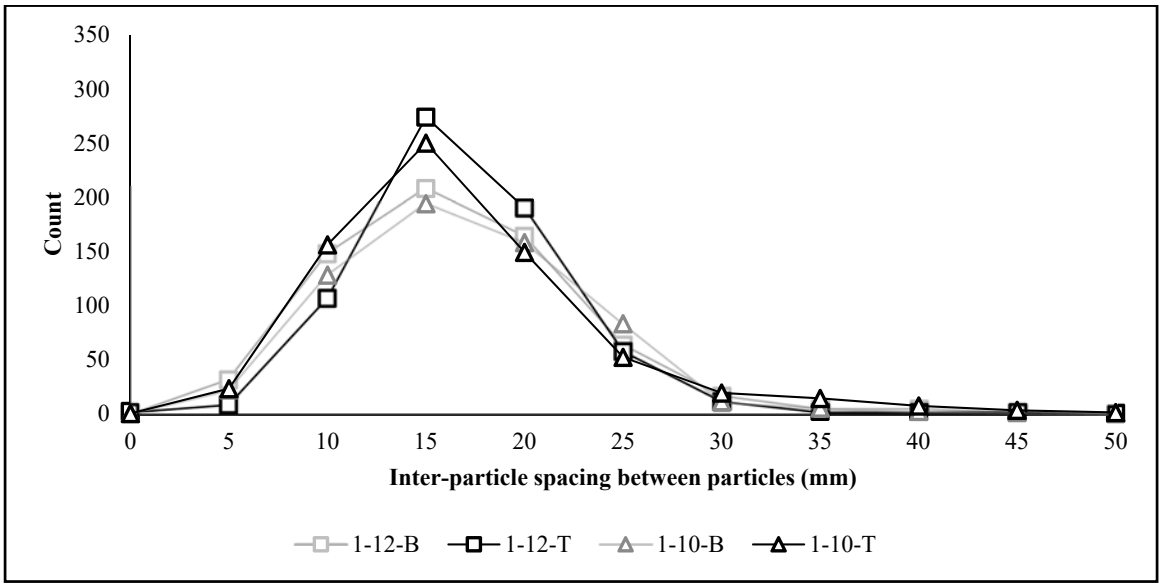

Figure 6.17. IPS counts for Mix 1 (Frequency over 7000 VPM)

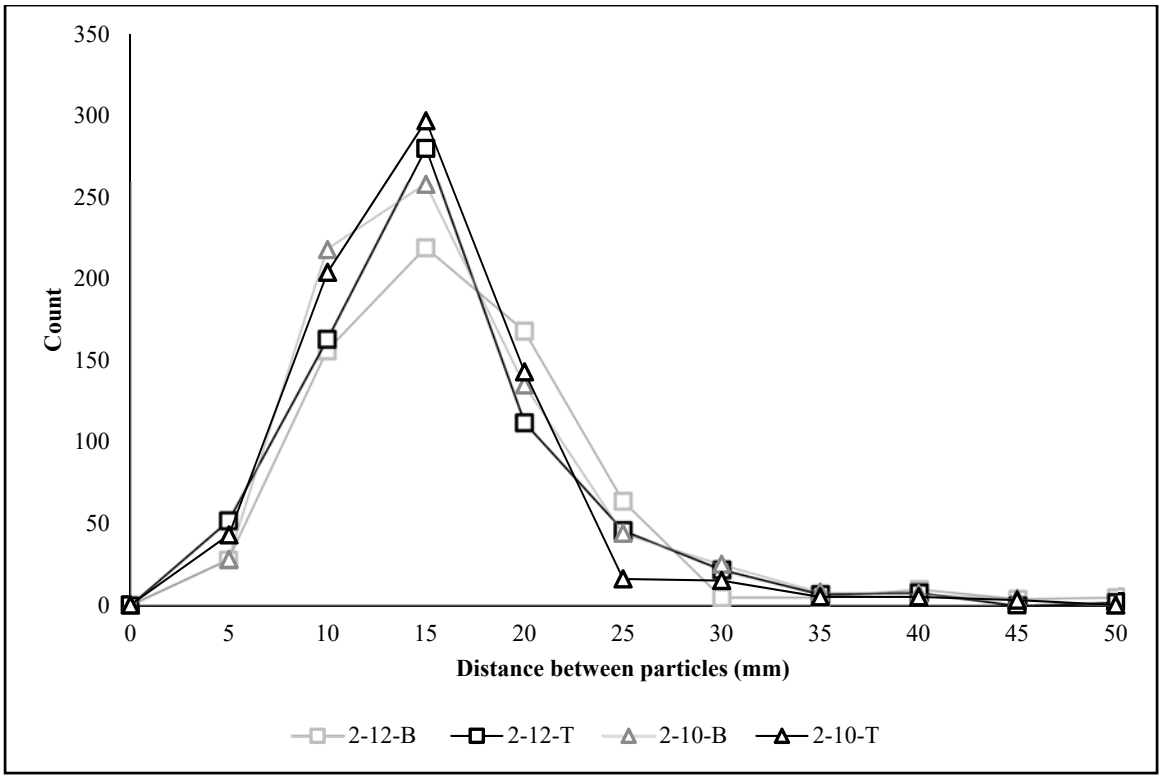

Figure 6.18. IPS counts for Mix 2 (Frequency over 7000 VPM)

6.3.2.2. Mortar to aggregate ratio

Mortar to aggregate ratio and standard deviation is presented in Table 6. Standard deviation for top and bottom of samples consolidated by rod and 4000 VPM vibration is close, while this difference between top and bottom became larger with increasing frequency. This high variation in top of samples indicates an unevenly distributed aggregate system. Similar histogram and counts for each range as average distance between particles are presented in Figure 19 and Figure 20. Sample 1-10-T has more counts in the range of 0-1 for mortar aggregate ratio than 1-10-B while 1-10-B has more counts at larger numbers, indicating less mortar and more aggregates on top of the sample than bottom. The same trend can be found for 12000 VPM, and similar situation is observed in Mix 2 for 2-10 and 2-12. This result is consistent with average

distance between particles, proving that coarse aggregates were compacted on top of the sample during vibration which caused segregation.

Table 6.6. Mortar to aggregate volume ratio for Mix 1 and Mix 2

Mix 1										
Sample ID	1-R-B	1-R-T	1-4-B	1-4-T	1-8-B	1-8-T	1-10-B	1-10-T	1-12-B	1-12-T
Mortar to aggregate ratio	2.07	1.84	2.12	2.04	1.49	2.05	2.02	2.57	1.69	1.86
Std	1.11	1.96	2.25	1.61	3.01	2.20	2.19	7.04	1.63	3.26
Mix 2										
Sample ID	2-R-B	2-R-T	2-4-B	2-4-T	2-8-B	2-8-T	2-10-B	2-10-T	2-12-B	2-12-T
Mortar to aggregate ratio	1.66	2.62	2.21	2.78	2.49	1.87	2.03	2.60	1.32	2.21
Std	1.66	1.07	3.23	5.29	4.30	3.23	1.58	3.52	1.36	3.61

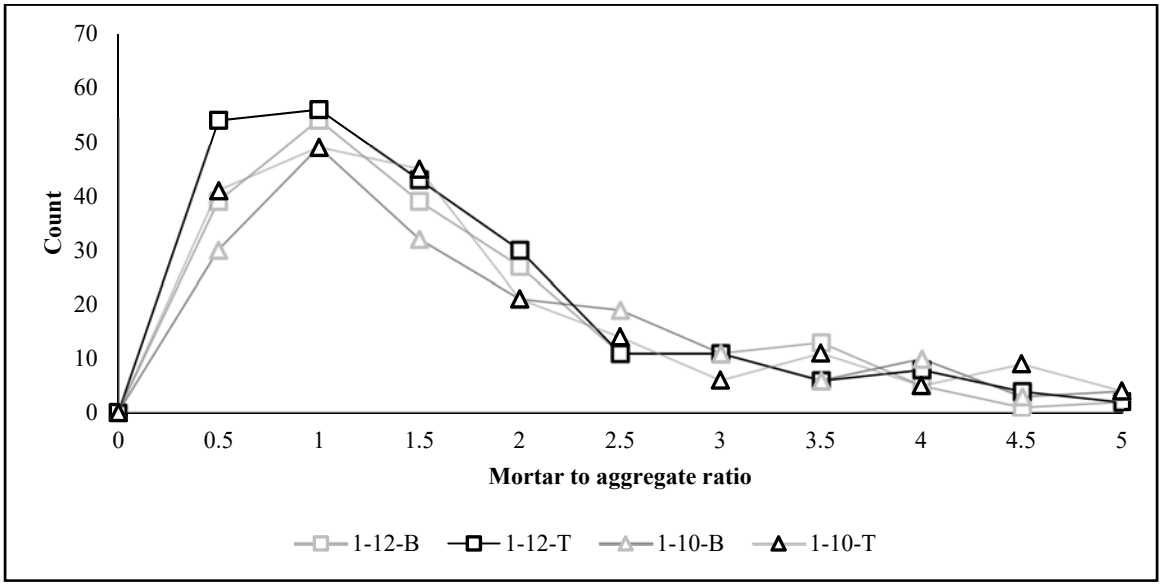

Figure 6.19. Mortar to aggregate ratio for Mix 1 at high vibration speed

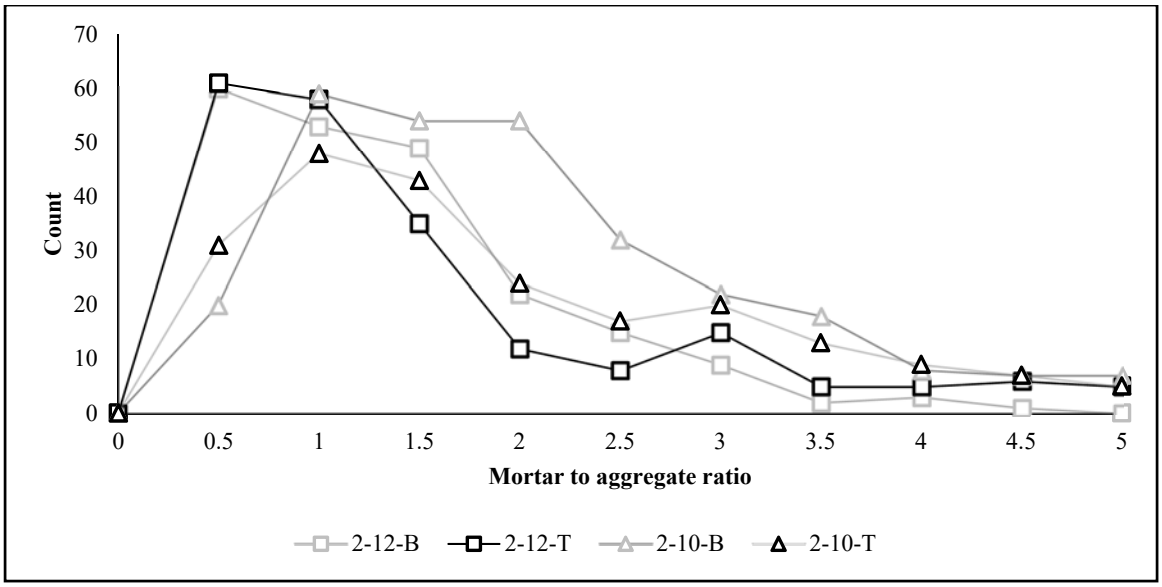

Figure 6.20. Mortar to aggregate ratio for Mix 1 at high vibration speed

Results from inter-particle spacing and mortar to aggregate ratio are both indicating that there was segregation in samples vibrated at over 7000 VPM. Due to the short period of vibration, this segregation is rather regional, and that could be the reason why there was no clear sign of severe segregation which will cause aggregates from top of the cylinder sink all the way down to bottom half of the cylinder.

The other mechanism that could explain this phenomenon is called percolation of particles. The phenomenon of large particles rising up to the top of smaller particles in a vibrated granular system is called Brazil nut effect, or sieving segregation (Tang and Puri 2010, Kurolli 2004). It happened when finer particles can sieve through voids between larger particles, and when large particle is denser than surrounding packed “bed”, large particle will first compact the bed, which will limit the movement of large particle itself from going down, since it is a compacted bed, so the tendency of coarse aggregate movement is upward (Ahmad and Samlley 1973, Williams 1963). In vibrated concrete, considering concrete is made of coarse aggregate particles and mortar, mortar will sieve down through coarse aggregate network and then get

compacted by large coarse aggregate particles and resulting coarse aggregates rising up as a respond to vibration. Either mechanism would cause the closer distance for particles on top of the sample.

Using inter-particle spacing and mortar to aggregate ratio it is possible to determine the potential of segregation in low slump concrete with high vibration rate. With high vibration rate over 7000 VPM, It is possible for low slump concrete to segregate, and the tendency of this segregation is that coarse aggregate will go up while fine aggregates go down.

6.3.2.3. Fabric tensor

Coarse aggregate orientation is presented in Table 3. Intensity of each orientation is in Figures 21 and Figure 22. Difference between top and bottom in intensity was negligible for rodding or vibration at frequency below 7000 VPM for both mixtures. The difference between top and bottom became larger when vibration frequency went over 7000 VPM. Lower intensity means that fewer aggregates are in the same orientation, and higher intensity means more aggregates are parallel to each other. With proper consolidation, it is expected that intensity of orientation for both top and bottom of the sample would be similar, as seen in rodded samples and 4000 samples. This distinction between top and bottom was expected, since there was vertical movement in these samples due to vortex formation and larger radius of action. When a parcel is floating, it would float in an orientation with highest capillary force, at the same time, it would maintain a stable center of gravity (Daniello et al. 2014). This explains the tendency of aggregate movements under each vibration rate. If there is no tendency of movement under vibration, intensity of orientation within sample should be similar to samples consolidated with rodding. On the other hand, intensity would decrease when aggregates are moving (or at least have a tendency for moving), since each aggregate would find its own stable center of gravity,

which is depending on its own properties and not parallel to each other. As a result, particles are in different orientations and the intensity would be low. Lower intensity indicates more aggregates tend to move during vibration. As can be seen in Figure 19 and Figure 20, samples vibrated with frequency over 7000 RPM have quite distinguished intensity between top and bottom of the sample. This proves that the injection depth of internal vibrator affects movement of coarse aggregates. Coarse aggregates in higher frequency and closer to vibrator have higher tendency to move.

Table 6.7. Coarse aggregate orientation for Mix 1 and Mix 2

Mix 1										
Vibration Rate(VPM)	Rod		4000		8000		10000		12000	
Position	Bot	Top	Bot	Top	Bot	Top	Bot	Top	Bot	Top
Orientation °	85.37	75.90	179.80	173.70	179.06	79.93	5.78	84.60	167.40	69.08
Mix 2										
Position	Bot	Top	Bot	Top	Bot	Top	Bot	Top	Bot	Top
Orientation °	87.74	91.02	4.26	123.03	2.31	23.91	11.32	74.04	173.81	68.18

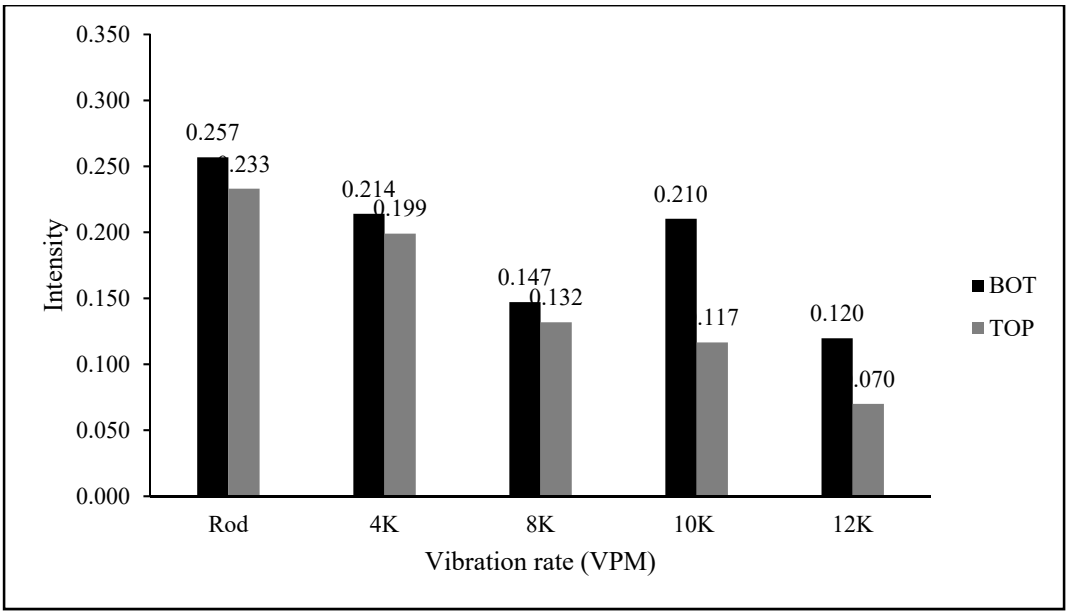

Figure 6.16. Intensity of aggregate orientation for Mix 1

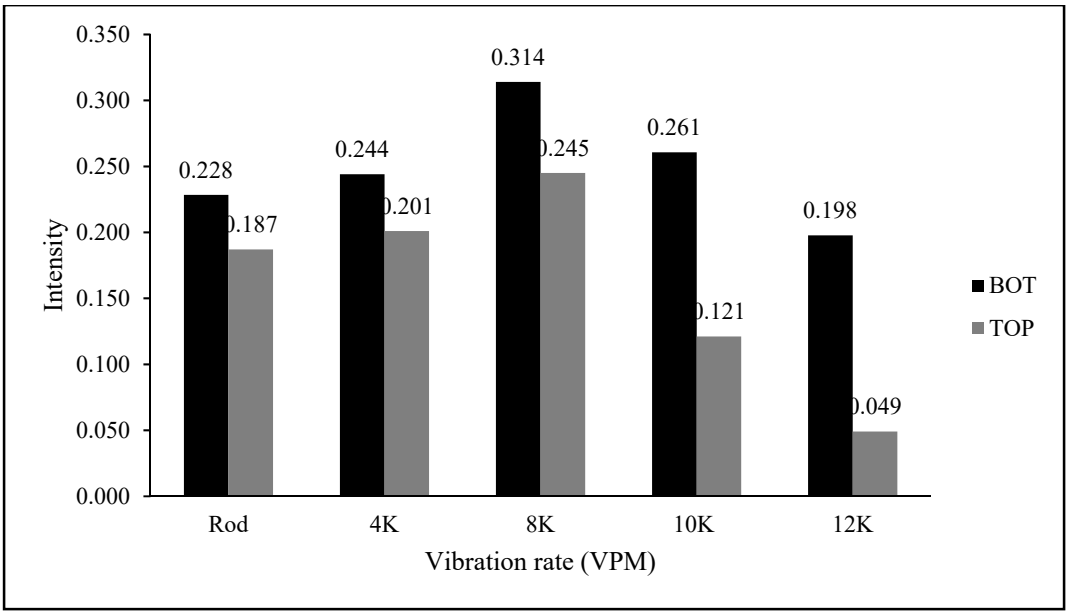

Figure 6.17. Intensity of aggregate orientation for Mix 2

6.4. Conclusion

In this study, stability of air void system for two types of AEA+WRA combination was evaluated using foam drainage test. These two combinations were used for concrete casting and then consolidated using internal vibrator with different vibration speeds. Average air content and contour map for hardened air content was calculated for both mixes. Digital image processing

was used for aggregate distribution analysis for these two mixes. Inter-particle spacing and mortar thickness index was calculated from the image, and fabric tensor was calculated as well. The following conclusions can be drawn based on the results of this research:

- Increasing of air content would occur in 30.5x15.2 cm cylinders vibrated with high vibration speed over 8000, regardless of AEA chemical base.
- The position (or depth) of air increment caused by internal vibration is depending on both depth of injection and stability of admixtures combination used in the system. For stable combination the air bubbles tend to stay close to the point of injection, while in unstable combination these bubbles tend to rise up to the surface
- Under high vibration rate over 7000 VPM, coarse aggregates tend to get close together on top of the sample, while aggregates on bottom of the sample were less affected. With the same amount of aggregates on top and bottom, closer aggregate spacing is indicating segregation.
- Inter-particle spacing and mortar to aggregate ratio were able to indicate the aggregate distribution in low slump concrete. They could be used to evaluate the segregation level of such concrete.
- Fabric tensor could be used to determine the tendency of movement for coarse aggregates during vibration. A low intensity of fabric tensor (comparing with samples consolidated with rodding) is indicating more aggregates tend to move during vibration, which could be a sign of segregation.

6.5. References

ACI 309-1R-09, "Report on behavior of fresh concrete during vibration," American Concrete Institute, 2008

Banfill, P.F.G; Teixeira, M.A.O.M; Craik, R.J.M.; "Rheology and vibration of fresh concrete: Predicting the radius of action of poker vibrators from wave propagation", Cement and Concrete Research, 2011.

Abrams, D.A., "Effect of vibration, Jigging, and pressure on fresh concrete," *Bulletin 3*, Structural Materials Research Laboratory, Lewis Institute, Chicago, IL

ASTM C125-18, "Standard Terminology Relating to Concrete and Concrete Aggregates," ASTM International, West Conshohocken, PA, 2018

Power, T.C., "Void Spacing as a Basis for Producing Air-entrained concrete," *Research Bulletin,* 49, Portland Cement Association, Journal of the American Concrete Institute, 1954, pp. 741-760

Cross, W., Duke, E., Kellar, J., and Johnston, D., *Investigation of Low Compressive Strengths of Concrete Paving, Precast and Structural Concrete*. South Dakota Department of Transportation, Office of Research, Pierre, SD, 2000

Gutmann, P. F., Bubble Characteristics as they Pertain to Compressive Strength and Freeze-thaw Durability. ACI Materials Journal, 1988, pp. 361-366

Taylor P.C., Johansen V.C., Graf L.A., Kozikowski, R.L., Zemajtis J.Z., and Ferraris C.F, *Identifying Incompatible Combinations of Concrete Materials, Volume II—Test Protocol*. Federal Highway Administration, Research, Development, and Technology, Turner-Fairbank Highway Research Center, McLean, VA, 2006

ACI Committee 237R-07, "Self-Consolidating Concrete," American Concrete Institute, 2007

ACI Committee 238, "Report on measurements of workability and rheology of fresh concrete," Farmington Hills, 2008

Ahmad K., Smalley, I.J., "Observation of particle segregation in vibrated granular systems," *Powder Technology*, Vol. 8, 1973, pp.69-75

Legg, F.E., “Efficiency of Vibrators in Consolidating Paving Concrete,” Final Report, DRDA Project 320351, 1974

Kosmatka, S.H., Wilson, M.L., *Design and Control of Concrete Mixtures*, 16th edition, 2016

Petrou, M.F, Wan, B.L., Gadala-Maria, F., Kolli, V.G., and Harries, K.A, Influence of mortar Rheology on Aggregate Settlement,” *ACI Materials Journal*, Vol. 97, No.4, 2000

Banfill. P.F.G., Xu, Y.M, and Domone, P.L.J., “Relationship between the rheology of unliberated fresh concrete and its flow under fibration in a vertical pipe apparatus,” *Magazine of Concrete Research*, Vol. 51, 1999, pp. 181-190

Navarrete, I., Lopez, M., “Understanding the relationship between the segregation of concrete and coarse density and size,” 2017, Construction and Building Materials, Vol. 149, 2017, pp.741-748

Kudrolli, A., “Size segregation in vibrated granular matter”, *Reports on Progress in Physics*, Vol. 67, 2004

Tang, P., Puri, V.M., “Methods for minimizing segregation: A Review, *Particulate Science and Technology*, Vol 22, 2004, pp.321-337

Bui, V.K., Montgomery, D., Hinczak, I., Turner, K., “Rapid testing method for segregation resistance of self-compacting concrete,” *Cement and Concrete Research*, Vol. 32, 2002, pp. 1489-1496

Association Francaise de Genie Civil, “Betons Auto-Placants– recommandations Provisoires ,” France, 2000

Wang, X.H., Wang, K.J, Han, J.G., Taylor, P., “Image analysis applications on assessing static stability and flowability of self-consolidating concrete,” Cement & Concrete Composites, Vol. 62, 2015

Han. J.G., Wang, K.J, Wang, X.H, Monteiro, P.J.M., “2D image analysis method for evaluating coarse aggregate characteristic and distribution in concrete,” Construction and Building Materials, Vol. 127, 2016, pp.30-42

MATLAB®, The MathWorks Inc., 2013

JMP®, Version <Pro13>. SAS Institute Inc., Cary, NC

Oda, M., Nakayama, H., Yield function for soil with anisotropic fabric, *Journal of Engineering Mechanics*, Vol. 115, 1989

CHAPTER 7 GENERAL CONCLUSIONS

7.1. Summary

The objective of this dissertation was to investigate variation of air void system in fresh and post-fresh concrete. The investigation of such topic will improve the current understanding of formation and variation of air void systems in both fresh and hardened concrete.

Discussions on air void system usually focus on either fresh air content or hardened air void system analysis. This dissertation started from the origin of air void formation, which is interaction between water, cement, and admixtures. By modifying foam drainage test, an existing test that can evaluate compatibility of admixtures, this work proposed a more detailed method to evaluate the compatibility between ingredients mentioned above, and provided a pass/fail limit to evaluate the potential stability of air void system in concrete. Then the focus change to air void system during fresh air content testing. By measuring air void system for concrete and mortar in various pressure stages, this dissertation calculated volume changes of air bubbles during pressure stages and found the correlations between fresh air void data and hardened air void analysis results. Lastly this dissertation investigated the changes happened to both air void system and aggregate system for concrete subjected to vibration. By analyzing air void system and aggregate distribution, this dissertation was able to propose the mechanism to explain the behavior of air bubbles and aggregate particles during excessive vibration.

7.2. Conclusions

Conclusions from each paper in this dissertation are as follows:

A Modified Foam Drainage Test Protocol for Assessing Incompatibility of Admixture Combinations and Stability of Air Structure in Cementitious Systems:

- Temperature, speed of mixing, and dosage of admixtures will all affect the stability of air void system created by such conditions.
- Stability of air void system in concrete is a case-by-case property just like fresh air content and slump, which needs to be evaluate in every concrete mixture forehead.
- Using modified foam drainage test it is possible to predict the stability of air void system of concrete using the same cement-admixtures combination, and correlation between prediction and actual results from air void analysis for concrete is good.

Variations in Air Void System for Mortar and Concrete Tested with Pressure Method or Sequential Air Method:

- Bubbles with chord length of 20-30 μm, 80-100 μm, and 500-1000 μm are the main bubbles that are affected by pressure
- At 100-kpa bubbles in 20-30 μm lost air to 80-100 μm and vanished, then at 200-kpa bubbles in 80-100 μm also losses air becoming smaller bubbles, and at 300-kpa this tendency is the same. Bubbles in 500-1000 μm keep receiving air from smaller bubbles.
- During pressurization, bubbles are experiencing both compression and dissolution. Volume reduction caused by compression is growing with higher pressure while volume deduction due to dissolution is decreasing with higher pressure.
- Using pressures collected from Super Air Meter test, it is possible to calculate volume change ratio at each pressure stage at each round, and the difference between each round at same pressure stage correlates with spacing factor from hardened air void system analysis.

Increasing of Air Content in Concrete Molds Consolidated by Internal Vibrator:

- Concrete samples consolidated by internal vibrators may experience air content increasing in part of sample due to vortex created by vibration.
- The mechanism of air increment was that rotary movement caused by vibrator created a vortex inside of liquefied fresh concrete, and this vortex will suck air bubbles into concrete. And these air bubbles will be stabilized by left-over AEA in the system
- The degree of this incremental air content depend on duration of vibration, frequency of vibration, and the amount of AEA left in the system.

Air and Aggregate Distribution for Concrete Molds Consolidated by Internal Vibrator:

- Increment of air content would occur to 30.5×15.2 cm cylinders vibrated by internal vibrator with a speed up to 8000 RPM, regardless of AEA chemical base, possibly depending on compatibility of AEA.
- Position of increment of air content happening is depending on depth of injection of internal vibrator and compatibility of admixtures and cement used in the system.
- With high vibration rate over 8000 RPM, coarse aggregates tend to get close together on top of the sample, while aggregates on bottom of the sample were less affected. With the same amount of aggregates on top and bottom, closer aggregate spacing is indicating segregation.
- Inter-particle spacing and MTI were able to indicate the aggregate distribution in low slump concrete. They could be used to evaluate the segregation level of such concrete.
- Fabric tensor could be used to determine the tendency of movement for coarse aggregates during vibration. A low intensity of fabric tensor (comparing with samples consolidated with

rodding) is indicating more aggregates tend to move during vibration, which could be a sign of segregation.

7.3. Future work recommendations

Recommendations for foam drainage test and stability of air void system in concrete

- Using modified foam drainage test to test an comprehensive list of admixture combinations that may affect stability of air void system in concrete to build up an pass/fail line for common applications
- A definition and a test method for stability of air void system in concrete is needed.
- Find a more clear correlation between results from foam drainage test and stability of air void system in concrete

Recommendations for variations in air void system for mortar and concrete tested with pressure method or sequential air method

- Evaluate the changes of air void system for mortars with different air void system and different type of AEAs.
- Find a possible method to observe the volume change of bubbles contacting with cement paste and test the volume change rate for different bubble size.
- One or more equations is needed to predict the hardened air void properties using fresh air void testing results.

Recommendations for aggregate and air voids distribution for concrete using internal vibrator

- Investigate this issue in field condition, for instance any type of construction using internal vibrator, to see if there is large air variation in such application.
- Simulate the vibrator used in concrete pavement in lab and evaluate the air void system and aggregate distribution consolidated by this type of vibration.
- A test method to measure the amount of remaining AEA in the system is needed.